3- ARTÍCULOS

Effects of photoperiod on rat motor activity rhythm at the lower limit of entrainment

Artículo publicado en *Journal of Biological Rhythms*

Indice de Impacto: 2,979
Área: Fisiología
Posición: 21/74

Effects of Photoperiod on Rat Motor Activity Rhythm at the Lower Limit of Entrainment

Trinitat Cambras,[*,1] Juan Chiesa,[*] John Araujo,[†] and Antoni Díez-Noguera[*]

[*]*Departament de Fisiologia, Facultat de Farmacia, Universitat de Barcelona;*
Departamento de Fisiologia, Universidade federal do Rio Grande do Norte, Natal-RN, Brazil

Abstract   The experiment described here studied the rat motor activity pattern as a function of the photoperiod of circadian light-dark cycles in the limits of entrainment (22- and 23-h periods). In most cases, the overt rhythm showed 2 circadian components: 1 that followed the external LD cycle and a 2nd rhythm that was free run. The expression of these components was directly dependent on the photoperiod, and there was a gradual transition in the manifestation of 1 or the other. The component with a period equal to that of the external cycle was more manifested under long photoperiods, while the other 1 was more expressed during short photoperiods. Also, the period of the free-running component was longer under T22 than T23. For each period, the free-running component was longer under a longer photoperiod. At first sight, the presence of these 2 components in most of the rats might appear to be due to the fact that in the limits of entrainment, some rats do not entrain and thus show a free-running rhythm plus masking. However, the gradation observed in the different patterns of the overt motor activity rhythm, especially those patterns related to the different balance between the 2 components and the length of the period of the free-running component under LD as a function of the photoperiod, suggests that the circadian system can be functionally dissociated.

Key words   photoperiod, circadian rhythms, masking, entrainment

The circadian system is formed by a set of structures that generates circadian rhythms in the organisms. The main structure involved in this process is the SCN of the hypothalamus, but the retina also contributes to the regulation of the rhythmicity, as it sends the SCN photic information that modulates the expression of the endogenous rhythm. The light-dark (LD) cycle is the most crucial zeitgeber in mammals, as it entrains practically all their rhythms. However, light also has a masking effect on the animals' activity, such that in a nocturnal animal, the activity tends to be suppressed by light. This indicates that the overt rhythm of an animal under LD cycles is affected by 2 light-dependent mechanisms: (1) entrainment of a circadian clock by light, resulting in endogenously clock-controlled events at specific times, and (2) direct masking effects of light on clock-controlled variables and/or nonclock-controlled variables (Redlin and Mrosovsky, 1999). It is difficult to differentiate the masking and entraining effect of an LD cycle. Consequently, most studies address the intrinsic nature of the circadian clock under constant conditions, or else they mention entrainment without considering the accompanying and unavoidable effect of masking.

At the limits of entrainment, under LD cycles whose period is not close enough to the endogenous rhythm to allow entrainment, animals manifest a number of phenomena such as relative coordination or partial entrainment (Aschoff, 1981). These rhythmic patterns are sometimes difficult to interpret and analyze. In particular, it is difficult to differentiate whether the patterns are due to "masking" or to the entrainment effect of the LD cycle. We consider that the analysis of these patterns provides a good opportunity to study the functional structure of the circadian pacemaker.

In previous experiments, we studied the pattern of rat motor activity rhythm under different T cycles at the lower limit of entrainment. Under LD cycles of 22 and 23 h, rats show 2 simultaneous circadian rhythms, 1 of which has the same period as the external rhythm while the other free runs with a period close to 24.5 h (Vilaplana et al., 1997; Campuzano et al., 1998). The expression of these 2 components depended on light intensity and on physical exercise (Cambras et al., 2000). Thus, we interpreted that their expression may be linked to the degree of coupling between the oscillators that drive the circadian system. As light may affect the degree of coupling (Aschoff, 1981), we hypothesized that the photoperiod could influence the adaptation of the circadian system to external cycles at the limits of entrainment, modifying, in consequence, the expression of the 2 circadian components.

MATERIAL AND METHODS

A total of 50 female and 50 male 2-month-old Wistar rats were used for the experiment. Rats were purchased from CRIFFA (France). When they reached our laboratory, they were kept in transparent cages measuring $22 \times 22 \times 15$ cm. Half of the rats were submitted to an LD cycle of a 22-h period (T22) and the other half to an LD cycle of a 23-h period (T23). For each period, 5 groups were established on the basis of the distinct photoperiods to which they were exposed. The groups, which were named according to the percentage of light hours in the whole cycle, were made up of 5 males and 5 females as follows:

Group 23L: Rats submitted to 23% of light in the LD cycle. This corresponded to rats maintained under 5L:17D under T22 and 5.2L:17.8D under T23.

Group 36L: Rats submitted to 36% of light in the LD cycle. This corresponded to rats maintained under 8L:14D under T22 and 8.4L:14.6D under T23.

Group 50L: Rats submitted to 50% of light in the LD cycle. This corresponded to rats maintained under 11L:11D under T22 and 11.5L:11.5D under T23.

Group 63L: Rats submitted to 63% of light in the LD cycle. This corresponded to rats maintained under 14L:8D under T22 and 14.6L:8.4D under T23.

Group 77L: Rats submitted to 77% of light in the LD cycle. This corresponded to rats maintained under 17L:5D under T22 and 17.8L:5.2D under T23.

Light for the experiment was provided by 2 fluorescent lamps at an intensity of 300 lux at the level of the cages. Darkness was attained using a dim red light with an intensity of less than 0.1 lux. Each group was maintained in a soundproof room, with independent lighting conditions. The experiment was carried out in 2 parts, each done in the same season of the year (fall). The first part studied the groups under T22, the second, those under T23. Animals were maintained under these LD conditions for 1 month, after which they were transferred to constant darkness for 30 days to observe the free-running rhythm and to calculate its phase relationship with respect to the previous LD cycle. Motor activity was detected throughout the experiment by means of an activity meter with 2 crossed infrared beams. The number of movements was cumulated and recorded every 15 min. During the experiment, the rats had free access to food and water.

Mathematical and Statistical Analysis

Motor activity data were analyzed in 2 parts separately, under exposure to the LD cycle (LD stage) and under constant darkness (DD stage).

In both stages, the periodogram of Sokolove and Bushell (1978) was used to detect the rhythm. This method provided information about the significant periods as well as the percentage of variance (PV) explained by the rhythm. The PV is an indicator of the importance (amplitude) of the rhythm. For the LD stage, the periodogram was calculated between days 10 to 30, to avoid the first days of adaptation to the new environment. For the DD stage, the periodogram was calculated for the whole stage and also for the 2 halves (days 1-15 and days 15-30). In most cases, the LD stage showed 2 statistically significant periods, thereby reflecting the presence of 2 rhythms. As 1 of these periods always had the same length as the external LD cycle (T22 or T23), we named it the light-dependent component (LDC) since it does not necessarily imply *entrainment* or *masking* but only a reflection of the external cycle. The other component free ran with a period that was distinct from T, and this will be men-

tioned as the free-running component under LD. The PVs explained by the LDC (PV LDC) and by the free-running component (PV free running) were used as indicators of the expression of the 2 rhythms, respectively. Moreover, the PV LDC/(PV free-running + PV LDC) variable, which expresses the balance between the 2 components and thus is referred to as the LDC ratio, was considered an indicator of the adjustment of the overt rhythm to the LD cycle. In this way, if the animal only shows the LDC, the index would have a value of 1, and if the animal only has the free-running component, the value would be 0.

A mean daily waveform for each animal was constructed on the basis of the external period T. From this waveform, we calculated the mean motor activity per cycle and also the cumulative motor activity in the dark and light phases. To obtain a common index for all the groups, we calculated the amount of activity per hour in light (A_l) and the amount of activity per hour in darkness (A_d). The variable A_d/A_l indicates the effect of the external cycle (adaptation or reactivity) on the rat's motor activity. It also indicates the extent to which the motor activity is confined in the dark phase.

In the DD stage, the phase relationship between the onset of activity and the last LD cycle was also calculated. For this purpose, we visually extrapolated the onset of activity for the first 10 days under DD to the last LD cycle. To test the statistical significance of the grouping of these phases, we used a Rayleigh z-test (Batschelet, 1981). In the LD stage, 2 components can be observed in most of the animals; thus, we also tested the phase relationship between the rhythm under DD and each 1 of the 2 components separately. To calculate the relationship between the rhythm under DD and the LDC, we used the following procedure: (a) the mean waveform was calculated according to T for the LD stage. (b) The onset of alpha was determined taking into account that there were mainly 2 types of waveform: when motor activity was coincident with the dark onset (this was practically only the groups with long photoperiod) and when there was no such coincidence. In this last case, we considered that the beginning of alpha coincides with the point at which the activity crosses up the median, after the reactive bout of activity due to the beginning of darkness. (c) The onset of alpha determined in (b) was placed in the LD cycle. (d) We extrapolated the phase of the onset of the rhythm under DD to the last LD cycle. (e) We calculated for each animal the differences among these 2 phases, that of the onset of alpha

and that of the extrapolation of the onset of the rhythm under DD. (f) The dispersion of the phase differences of the animals of each group was tested by means of the Rayleigh z-test.

To calculate the relationship of the rhythm under DD with the free-running component under LD, we visually extrapolated the middle of the free-running component to the last day under LD and the onset of activity of the first 10 days under DD to the last LD cycle. The phase relationship between these 2 components was calculated, and the dispersion of the phase differences of the animals of each group was also tested by a Rayleigh z-test.

Statistical analysis was carried out by an ANOVA of a general linear model, considering the period T, the photoperiod, and the sex as independent variables. As dependent variables, we used PV LDC, PV free-running component, PV explained by the rhythm under DD, LDC ratio, mean motor activity per cycle, A_d, A_1, A_d/A_1, and the values of the period of the free-running component under LD and that under DD. Linear correlations among some of these variables were also studied.

Calculations were carried out by means of an integrated package for chronobiology "El Temps" (A. Díez-Noguera, Universitat de Barcelona, 1999), and statistical analysis was performed with the SPSS® package.

RESULTS

In the double-plotted actograms (Fig. 1), 2 components of the motor activity rhythm were observed: 1 is the reflection of the external LD cycle, while the other has a period longer than 24 h. The periodogram analysis also detected 2 significant peaks in most of the rats: 1 had the period of the external cycle, 22 or 23 h (LDC), while the other was longer than 24 h (free-running component). The number of animals that showed 1 or 2 significant peaks differed depending on the photoperiod: most of the rats showed 2 peaks (Fig. 2), except some that only showed the peak corresponding to the LDC period: for T22, 2 rats from the group 77L, and for T23, 7 rats from the group 77L, 6 rats from the group 63L, 2 rats from the group 50L, and 2 rats from the group 36L.

There was a gradual transition in the expression of the 2 components depending on the number of hours of light of the cycle (Fig. 1). For T22 and T23, when the photoperiod was long, the LDC was the most visible
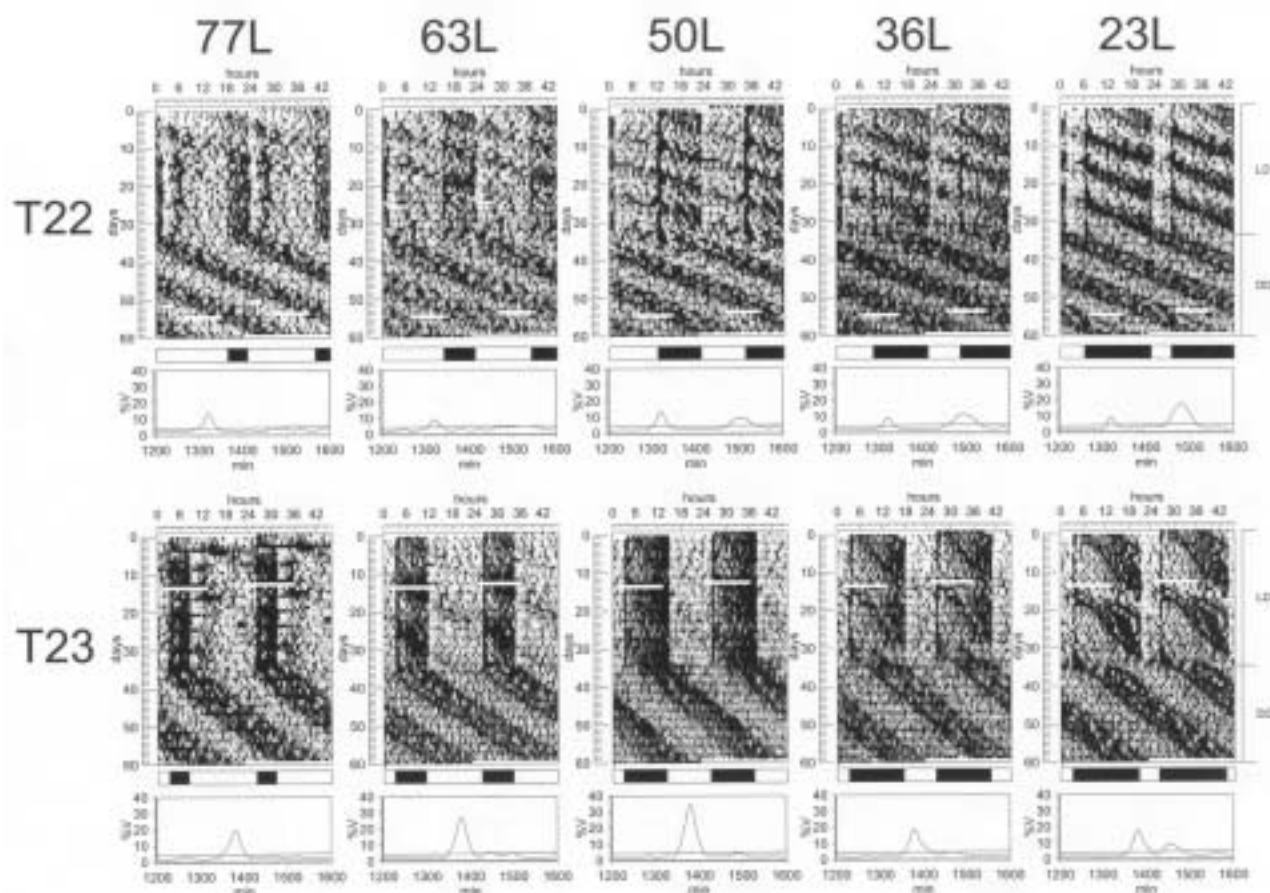
Figure 1. Actograms, plotted at modulo T, and periodograms of 1 representative animal from each group of rats. Labels indicate the group according to the period of the external cycle (T22 or T23) and the photoperiod (77L, 63L, 50L, 36L, or 23L). Black and white bars indicate the light-dark cycle. Periodograms correspond to the LD stage data: the horizontal axis shows the periods assayed, and the vertical axis corresponds to the percentage of variance explained by the rhythm.

component (i.e., 77L or 63L), while the free-running component was most clear when the photoperiod was short. We note that in some examples, such as T23-23L, the free-running component shows relative coordination. In those rats with 2 significant peaks, the period of the free-running component differed depending on the groups (Fig. 3E): it lengthened when the photoperiod increased ($p < 0.001$) and was longer in T22 than in T23 rats ($p < 0.01$).

To quantify the importance of 1 or the other of the 2 components during the LD stage, we calculated, for each animal, the PV explained by each component. In calculation, when 1 of the 2 components was not statistically significant, we still used the value of the highest peak in the periodogram as PV of this component. We consider that the percentage of variance explained by the free-running rhythm cannot be 0 since all the rhythms (any period) can explain a small, even if not significant, amount of data variance. An
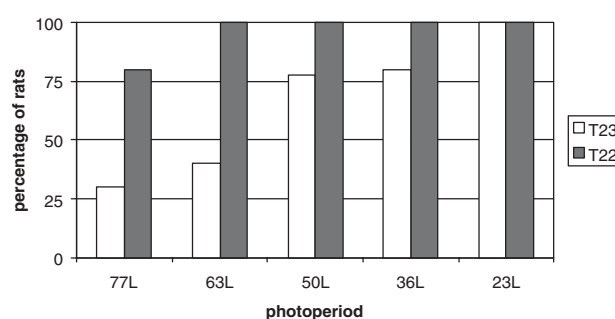

Figure 2. Percentage of rats for each group showing 2 significant circadian peaks in the periodogram.

ANOVA with the PV LDC confirmed that this value depended on the period ($p < 0.001$) and on the photoperiod ($p < 0.001$) (Fig. 3A). The PV free-running component also depended on the period ($p < 0.001$)
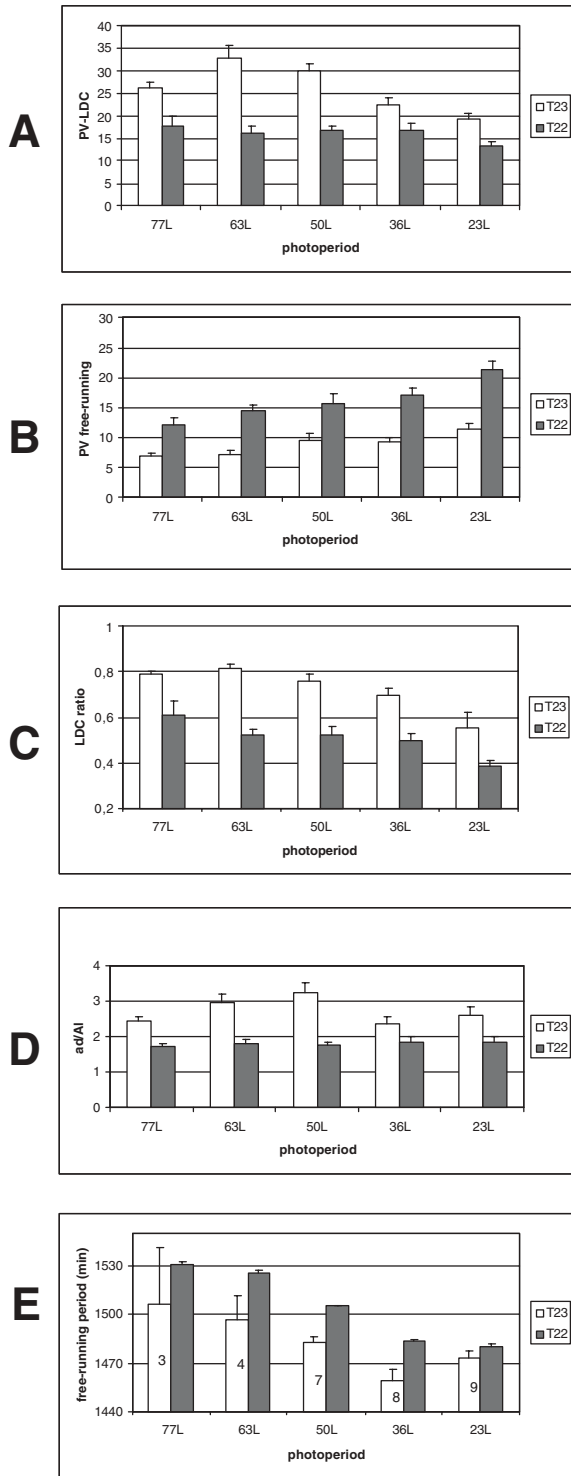
Figure 3. Mean and standard error of a number of variables for each group of rats: (A) percentage of variance explained by the light-dependent component (LDC), (B) percentage of variance explained by the free-running component, (C) LDC ratio (see text), (D) motor activity per hour of darkness/motor activity per hour of light, and (E) period of the free-running component. For each graph, the mean values are obtained from all the individuals of the group, except group T23 in E, in which the number of individuals is indicated.
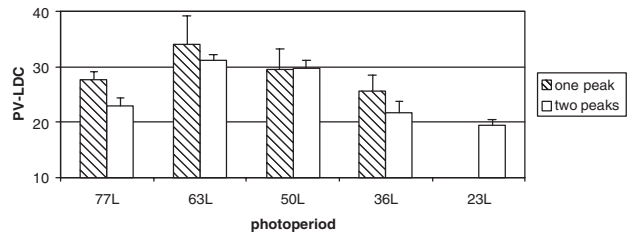

Figure 4. Percentage of variance explained by the light-dependent component (LDC) of T23 rats, separated into 2 groups: 1 peak (those that show only 1 significant peak in the periodogram) and 2 peaks (those that show 2 significant peaks).

and the photoperiod ($p < 0.001$), but in this case, sex was also a significant factor ($p < 0.001$). The PV free-running component decreased in inverse proportion with the photoperiod but was always higher under T22 than T23 (Fig. 3B). T22 females showed higher PV free-running values than males. The value of the LDC ratio (Fig. 3C) increased with the photoperiod ($p < 0.0001$) and was always higher in T23 than in T22 rats ($p < 0.0001$). This variable also depended on the sex of the rats ($p < 0.01$).

Since under T23, the periodogram of the motor activity data of some rats only shows 1 significant peak and others 2 significant peaks, we analyzed (ANOVA) the PV LDC as a function of the photoperiod by considering the rats of these 2 groups separately. The results show (Fig. 4) that the tendency was the same in each of the groups as when considering all the rats. The photoperiod was a statistically significant factor in determining the value of PV LDC in the rats with 2 components ($p < 0.001$) but not in rats with 1 peak due to the lower number of animals. Thus, for further calculations and interpretation of the results, we used the values of all the rats together except when studying the value of the period of the free-running rhythm under LD, which is only present in rats with 2 peaks.

An ANOVA of the mean motor activity per cycle as the dependent variable shows that both the photoperiod ($p < 0.05$) and the period ($p < 0.05$) are statistically significant factors, with the highest values of this variable being found under T22 and short photoperiods. A linear regression showed that the mean motor activity per cycle decreased as the photoperiod increased ($p < 0.01$). However, the activity per hour of light and the activity per hour of darkness depended on the T ($p < 0.001$) and on the photoperiod ($p < 0.005$). A_d / A_l was higher in T23 than in T22 rats ($p < 0.001$). This variable did not change
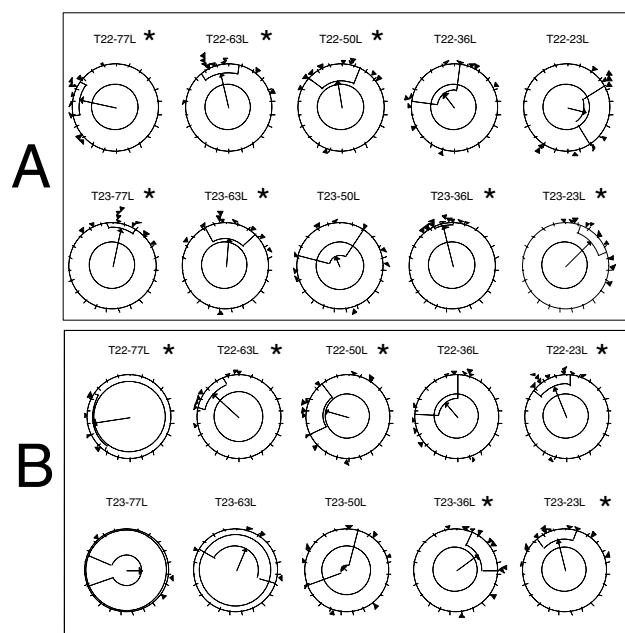
Figure 5. The Rayleigh *z*-test for the clustering of the phase relationships between the onset of the endogenous rhythm under DD and (A) the onset of the activity phase of the light-dependent component at the end of the LD stage and (B) the activity phase of the free-running component under LD at the end of the LD stage. The interior dashed circle indicates the threshold of significance at *p* < 0.05. Asterisks indicate significant clustering.

with the photoperiod in T22 rats but did change in T23 ($p < 0.005$), being highest in the 50L group (Fig. 3D).

Significant and positive correlations were found for the number of light hours versus the period of the endogenous component ($p < 0.0001$) and versus the LDC ratio ($p < 0.001$). Negative correlation was obtained between the PV of the LDC and the PV of the free-running component under LD ($p < 0.005$).

When the rats were transferred to DD, all showed a circadian component with a mean tau of 24 h, 23 min (SE = 1.08 min) for T22 and 24 h, 17 min (SE = 1.33 min) for T23. The differences between the 2 groups were statistically significant ($p < 0.005$), although no significant differences were found because of the previous photoperiod. The tau under DD was also calculated for 2 parts of the DD stage, with tau1 corresponding to days 1 to 15 and tau2 to days 16 to 30 under DD. The former was longer in T22 rats than in T23 ($p < 0.05$), but there were no differences caused by the photoperiod. Tau2 did not differ between the groups. A Student's *t*-test for paired data between tau1 and tau2 for each of the groups revealed that the latter was longer in all the T23 groups except for 50L but in none of the T22

groups. Moreover, when we studied separately those rats in T23 groups that showed 1 or 2 components, we found that those rats with 1 component showed a shorter tau than those with 2 components ($p < 0.05$).

A Rayleigh *z*-test showed that the onset of the rhythm under DD with respect to the phase of the last LD cycle is significantly clustered in all T23 groups except 50L, but only in 77L and 63L of the T22 groups. Similar results were obtained when the phase relationship between the onset of the rhythm under DD and the LDC was calculated (Fig. 5A). However, in some groups, there is clustering between the onset of the rhythm under DD and the free-running component under LD (Fig. 5B).

DISCUSSION

In the lower limits of the range of entrainment to the LD cycle, rats show several patterns in their overt motor activity rhythm. We believe that the study of these patterns may reveal some functional characteristics of the circadian system. The clearest results are that in most of the rats, 2 components can be detected: 1 following the LD cycle (which can be due to entrainment or masking) and the other free running. In an initial analysis, we can suggest that the 2 components are due to the fact that some rats do not entrain, and thus they show the free-running component plus masking. However, a more careful analysis indicates that there is a gradation, according to the period and photoperiod, in the expression of the 2 components; furthermore, this might indicate a functional dissociation of the circadian system.

In the analysis of the overt motor activity rhythm, we found a wide variety of patterns, from clear entrainment (only the light-dependent component) to the free-running rhythm (practically only the endogenous component). In between, we found different patterns showing 2 components, 1 of which was more intense than the other, and, in some rats, the typical pattern of relative coordination. Therefore, we decided to analyze the overt rhythms, not by classifying the animals into groups (i.e., rats that entrain and those whose rhythm is free run and masked by the LD cycle) but by using a single objective method for all of the animals. The method chosen was the analysis of the 2 peaks obtained in the periodogram, whose balance seems a clear indicator of the patterns we observe. Otherwise, the imposed dichotomy between entrainment and free running plus masking may

induce information loss in regard to motor activity data and thus constrain interpretation of the underlying process.

In the analysis of the overt rhythms of motor behavior, we must take into account that there are 2 light-dependent mechanisms. The 1st is the entrainment of a circadian clock by light, which in turn directs the animal to be active in the day or at night. The 2nd process involves an acute response to light, which, given that the rat is nocturnal, inhibits activity and is known as masking (Redlin and Mrosovsky, 1999). Masking and entrainment may be distinct responses to light in terms of behavior and physiology (Redlin and Mrosovsky, 1999; Vitaterna et al., 1999). However, at the receptor level, masking and entrainment may have considerable common features since they are both spared in retinally degenerate mutant mice (Mrosovsky, 2003; Mrosovsky et al., 1999). Under normal synchronization (i.e., $T = 24$ h), the entraining and masking effect of light is supplementary since masking may influence the amplitude of overt rhythms. In the case of the rat, the activity concentrates in the darkness because of the action of the circadian pacemaker and also because of the inhibition of activity during light. Thus, in our case, the manifestation of the LDC can be due to a "pure" masking, a "pure" entrainment, or a mixture of the 2 processes. It is difficult to discern between these possibilities in the case of our study since the animals in question are intact rats submitted to a complete LD cycle (not skeleton), and the effect of masking of the LD cycle cannot be separated from the effect of entrainment. Moreover, masking also depends on the phase of the circadian rhythms (Mrosovsky, 1999) and can contribute to the appearance of circadian rhythmicity.

Hence, we considered that the different patterns observed in the overt rhythm are explainable on the basis of a common process that involves the functionality of the circadian pacemaker. Therefore, we decided to analyze the patterns of motor activity only by quantifying the expression of the 2 components without considering whether these are due to entrainment or masking. Our analysis examines the percentage of variance explained by the significant peaks obtained in the periodogram of Sokolove and Bushell (1978). In this way, an objective variable was obtained, one that reflects the degree of adjustment of the activity pattern to the light-dark cycle.

One of the most critical points of this experiment involves knowing whether the LDC is really due to entrainment, apart from masking. In regard to the characteristics of entrainment—specifically, period control, stable phase relationship, and phase control of the rhythm under DD (Moore-ede et al., 1982)—it seems that the patterns of the actograms of T23 and those of some rats of the T22 group (especially T22-77L) are not only due to masking because entrainment also appears to be present. There is period control (since motor activity follows the external period T22 or T23), stable phase relationship of the LDC even with the presence of the free-running rhythm (i.e., T22-50L in Fig. 1), and, in some cases, phase control of the rhythm under DD in the presence of the 2 components (i.e., T22-36L, T23-63L in Fig. 1). Thus, we think that different patterns can be observed, apparently gradual, between complete entrainment of the LDC (T23 and long photoperiods) to a free-running rhythm plus masking (T22 and short photoperiods), and this indicates that interpretation of all the results should be found in a process that could also be gradual. When we analyze the results of the Rayleigh z-test, we can see that the phase differences between the rhythm under DD and the onset of the activity of LDC were significantly close in all T23 groups (except 50L) and in T22 (except 36L and 23L). However, we must also take into account that the free-running rhythm can also drive the phase of the rhythm under DD in some of the groups. Although it is important to notice that this last analysis cannot be done in those rats that only show only a single peak in the periodogram, the conclusion is that LDC can drive the phase of the rhythm under DD in most of the T23 rats and under long photoperiods, while the free running drives the phase in most of the T22 and short photoperiods. Thus, in some rats, the rhythm is driven by 1 component and in others by the other component, and in some cases, the 2 rhythms coincide. This, as well as the fact that the mean waveform shows us that the alpha phase does not coincide with dark onset in most of the rats, suggests that the expression of the LDC is not only masking but also entrainment (or at least part of the system entrained). Masking is visible as the reactive peak at the beginning of darkness and the reactive decrease at the beginning of light, and these are not continued under DD. Moreover, in T23, there are aftereffects since tau under DD lengthens. The differences between tau2 and tau1 were statistically significant only in L77 and L36 groups. The presence of a free-running component together with another component, which in some cases can be entrained, suggests to us the existence of a functional dissociation of the circadian system.

Other important results of this experiment were the dependence (and gradation) of the period of the free-running component under LD on the period and the photoperiod, as well as the dependence of the percentage of variance explained by both the light-dependent and free-running components. Several interpretations may account for them. For instance, there may be changes in the period of the free-running component under LD according to the photoperiod that can be attributed to the parametric effect of light on the circadian system. The parametric effect of light has been studied under continuous light, as described in Aschoff's rules, and also under high-frequency cycles that produce "demasking" (Aschoff, 1999). We studied it under T cycles in the circadian range, which produce a free-running rhythm that really seems to act as free running. Thus, the period lengthened and the amplitude (or PV) of the rhythm decreased when the number of hours of the photoperiod increased, which is similar to what happens under constant lighting conditions with increasing light intensity. In nocturnal animals such as the rat, it has been proposed that light decelerates the velocity of the circadian pacemaker since the period of the free-running rhythm increases according to light intensity (Aschoff, 1981). Thus, the observation that the period of the free-running component increased with a lengthened photoperiod is compatible with a parametric model and can be easily explained by surmising that the oscillators ran more slowly for a longer time, which made the duration of a whole revolution (period of the free-running component) longer than under shorter photoperiods.

However, the free-running period not only changes due to the photoperiod but also due to T. The distinct velocity of the oscillators during light or darkness does not explain why the period of the free-running rhythm under T22 is longer than under T23 since the total amount of light at the end of the experiment was the same for both periods. The distinct value of the free-running period according to T has also been demonstrated in previous experiments covering a wider range of periods (Campuzano et al., 1998). Nonlinearity in the response to light can be posed as an explanation for these differences, but it can be demonstrated mathematically that this effect would account for a very low (less than 0.1%) variation in the resulting T (unpublished results). Another interpretation for the changes in the period of the free-running component could be done by considering that when there is relative coordination, the period of free-running rhythm changes depending on the phase relationship

with the light. Although this explanation may fit for the changes due to the different T, it does not explain the differences obtained in the values of the percentage of variance of the 2 components. Moreover, this would produce a paradoxical situation since the animals whose endogenous period was closer to T were those rats that entrain less and show a lower percentage of variance of the LDC component. In addition, because relative coordination was not observed in most of the rats, we do not consider this explanation viable.

Finally, other results to be interpreted are the percentage of the variance shown by each of the 2 components. We have taken these values to be representative of the importance of the rhythm. However, prior to interpretation, some of the problems concerning these variables must be taken into account since the variables do not distinguish between masking or entrainment in the case of the LDC, and the PV LDC can be increased by both processes. Given that what we want to measure is the expression of the different patterns in a quantitative way, this analysis proved itself very useful. The value of PV explained by a determined component increases in direct proportion with amplitude and constancy of the rhythm. PV value is also a useful analytical tool because it provides the quantification of the period and PV of the 2 rhythms independently of each other. Moreover, a quantification of the balance between the 2 components fits with the pattern observed in the LD stage. Simulations carried out in our laboratory with data following simultaneous rhythms with different amplitudes indicate that the periodogram of Sokolove and Bushell (1978) reflects much better than other periodograms (Lomb and Scargle periodogram, regressive periodogram) the ratio between the amplitude of the 2 components.

The percentage of variance explained by the LDC was higher under a long photoperiod than under a short one, while the percentage of variance of the free-running component showed the opposite relationship. This balance between the 2 components could be explained in terms of energy balance in such a way that if an animal has only a certain number of calories to expend, it must divide its activity among a given number of activity bouts. Thus, in a particular photoperiod, if fewer calories are expended in the free-running component, there will be more calories available for the LDC and vice versa.

To arrive at a single interpretation that could fit all the results of this experiment (presence of 2 simultaneous components, balance in the expression of the 2

components depending on T and the photo-period, and period of the free-running period increasing with the photoperiod and decreasing with the period), we consider it necessary to think of a flexible functional structure of the circadian pacemaker. Thus, 2 populations of oscillators can work with distinct degrees of coupling.

At present, there is some evidence that the circadian pacemaker is a multioscillatory system (Díez-Noguera, 1994; Miller, 1998) formed by at least 2 functional populations of oscillators (Lee et al., 2003; Moore et al., 2002; Daan and Pittendrigh, 1976a, 1976b), with 1 of them being mainly sensitive to light (Moore et al., 2002). Recent studies reveal multiple-phase grouping of SCN oscillators, suggesting that light regulation of oscillator interactions within the SCN underlies entrainment to the photoperiod (Quintero et al., 2003). Moreover, there are different conditions under which the circadian rhythmicity is distinctly organized, and consequently, the clock genes in the SCN show different patterns (de la Iglesia et al., 2000; Edelstein et al., 2003). Taking all this into account, we believe that our results could be best explained by considering 2 subpopulations in the SCN whose intracoupling and intercoupling changes according to the period and the photoperiod. In this way, assuming that the 2 populations of oscillators could have different spontaneous frequencies, the oscillators that generate the LDC could be more entrainable than the others, oscillating with the external cycle while the rest of oscillators, coupled among them, would free run and thus generate the free-running rhythm. Since completely entrained and completely free-running rhythms are poles of a continuum, we can suppose that the minimum expression of the PV LDC is due to masking of the LDC, and when the action of different oscillators is added on, this value will increase. Thus, under T22, most of the oscillators that form the circadian pacemaker will be involved in the expression of the free-running component and only a few in the LDC. The contrary will occur under T23. Furthermore, in both cases, the quantity of light produces a gradual transition from 1 component to the other. This difference in the functional structure of the circadian system, based on the number of functional oscillators that may constitute each of the populations, may explain all the results of this experiment (changes in the period of the endogenous component, the importance [PV] of each of the 2 components, and the gradation in the overt motor activity patterns according to T in the photoperiod).

This could imply a flexible organization for the adjustment to the external cycles. Further research will decide the anatomical basis of this interpretation.

ACKNOWLEDGMENTS

REFERENCES

Aschoff J (1981) Freerunning and entrained circadian rhythms. In *Handbook of Behavioral Neurobiology: Biological Rhythms*, J Aschoff, ed, p 82, Plenum, New York.

Aschoff J (1999) Masking and parametric effects of high-frequency light-dark cycles. Jpn J Physiol 49:11-18.

Batschelet E (1981) *Circular Statistics in Biology.* Academic Press, London.

Cambras T, Vilaplana J, Campuzano A, Canal-Corretger MM, Carulla M, and Díez-Noguera A (2000) Entrainment of the rat motor activity rhythm: Effects of the light-dark cycle and physical exercise. Physiol Behav 70:227-232.

Campuzano A, Vilaplana J, Cambras T, and Díez-Noguera A (1998) Dissociation of the rat motor activity rhythm under T cycles shorter than 24 h. Physiol Behav 63:171-176.

Daan S and Pittendrigh CS (1976a) A functional analysis of circadian pacemakers in nocturnal rodents: I. The stability and lability of spontaneous frequency. J Comp Physiol 106:223-252.

Daan S and Pittendrigh CS (1976b) A functional analysis of circadian pacemakers in nocturnal rodents: II. The variability of phase response curves. J Comp Physiol 106:253-266.

de la Iglesia HO, Meyer J, Carpino A, and Schwartz WJ (2000) Antiphase oscillation of the left and right suprachiasmatic nuclei. Science 290:799-801.

Díez-Noguera A (1994) A functional model of the circadian system based on the degree of intercommunication in a complex system. Am J Physiol 267:R1118-R1135.

Edelstein K, de la Iglesia HO, and Mrosovsky N (2003) Period gene expression in the suprachiasmatic nucleus of behaviorally decoupled hamsters. Mol. Brain Res 114:40-45.

Lee HS, Nelms JL, Nguyen M, Silver R, and Lehman MN (2003) The eye is necessary for a circadian rhythm in the suprachiasmatic nucleus. Nat Neurosci 6:111-112.

Miller JD (1998) The SCN is comprised of a population of coupled oscillators. Chronobiol Int 15:489-451.

Moore RY, Speh JC, and Leak RK (2002) Suprachiasmatic nucleus organization. Cell Tissue Res 309:89-98.

Moore-ede MC, Sulzman FM, and Fuller CA (1982) *The Clocks That Time Us.* Harvard University Press, Cambridge, MA.

Mrosovsky N (1999) Masking: History, definitions and measurement. Chronobiol Int 16:415-429.

Mrosovsky N (2003) Contribution of classic photoreceptors to entrainment. J Comp Physiol A 189:69-73.

Mrosovsky N, Foster RG, and Salmon PA (1999) Thresholds for masking responses to light in three strains of retinally degenerated mice. J Comp Physiol A 184:423-428.

Quintero JE, Kuhman SJ, and McMahon DG (2003) The biological clock nucleus: A multiphasic oscillator network regulated by light J Neurosci 23:8070-8076.

Redlin U and Mrosovsky N (1999) Masking by light in hamsters with SCN lesions. J Comp Physiol A 184:439-448.

Sokolove PG and Bushell WN (1978) A chi square periodogram: Its utility for the analysis of circadian rhythms. J Theor Biol 72:131-160.

Vilaplana J, Cambras T, Campuzano A, and Diez-Noguera A (1997) Simultaneous manifestation of free-running and entrained rhythms in the rat motor activity explained by a multioscillatory system. Chronobiol Int 14:9-18.

Vitaterna MH, Selby CP, Todo T, Niwa H, Thompson C, Fruechte EM, Hitomi K, Thresher RJ, Ishikawa T, Miyazaki J, et al. (1999) Differential regulation of mammalian period genes and circadian rhythmicity by cryptochromes 1 and 2. Proc Natl Acad Sci USA 96:12114-12119.

Activity rhythm of golden hamster (Mesocricetus auratus) can be entrained to a 19-h light-dark cycle

Artículo publicado en *American Journal of Physiology (Regulatory Integrative and Comparative Physiology)*

Indice de Impacto: 3,405
Área: Fisiología
Posición: 15/74

Activity rhythm of golden hamster (*Mesocricetus auratus*) can be entrained to a 19-h light-dark cycle

Juan J. Chiesa, Montserrat Anglès-Pujolràs, Antoni Díez-Noguera, and Trinitat Cambras

Department of Physiology, Faculty of Pharmacy, University of Barcelona, Barcelona, Spain

Submitted 24 February 2005; accepted in final form 18 May 2005

Chiesa, Juan J., Montserrat Anglès-Pujolràs, Antoni Díez-Noguera, and Trinitat Cambras. Activity rhythm of golden hamster (*Mesocricetus auratus*) can be entrained to a 19-h light-dark cycle. *Am J Physiol Regul Integr Comp Physiol* 289: R998–R1005, 2005; doi:10.1152/ajpregu.00139.2005.—Both temporary access to a running wheel and temporary exposure to light systematically influence the phase producing entrainment of the circadian activity rhythm in the golden hamster (*Mesocricetus auratus*). However, precise determination of entrainment limits remains methodologically difficult, because such calculations may be influenced by varying experimental paradigms. In this study, effects on the entrainment of the activity pattern during successive light-dark (LD) cycles of stepwise decreasing periods, as well as wheel running activity, were investigated. In particular, the hamster activity rhythm under LD cycles with a period (T) shorter than 22 h was studied, i.e., when the LD cycle itself had been shown to be an insufficiently strong zeitgeber to synchronize activity rhythms. Indeed, it was confirmed that animals without a wheel do not entrain under 11:11-h LD cycles (T = 22 h). Subsequently providing hamsters continuous access to a running wheel established entrainment to T = 22 h. Moreover, this paradigm underwent further reductions of the T period to T = 19.6 h without loss of entrainment. Furthermore, restricting access to the wheel did not result in loss of entrainment, while even entrainment to T = 19 h was observed. To explain this observed shift in the lower entrainment limit, our speculation centers on changes in pacemaker response facilitated by stepwise changes of T spaced very far apart, thus allowing time for adaptation.

entrainment limits; wheel running; circadian rhythms

ENTRAINMENT OF CIRCADIAN OSCILLATORS produces synchronization between inner and outer temporal programs and involves cyclic environmental cues (zeitgeber) within the species' ecologic niche. Self-sustained endogenous oscillators with a free-running period (τ) can be entrained to zeitgeber cycles whose period lengths (T) differ from τ. Entrainment is achieved when *1*) τ progressively changes until it equals T, *2*) a stable phase relationship is reached between the oscillator and the zeitgeber, and *3*) the rhythm oscillates once in constant darkness from the initial phase attained when the zeitgeber was present. However, entrainment can only be produced within a limited range of periods T that encompass the range of entrainment (2). This range varies depending on the animal species (3), age (21), and the strength of the zeitgeber (2). Outside the range of entrainment, the oscillator free-runs with a period close to that measured in constant conditions (1) or with an intermediate one, when its frequency is periodically modulated by the zeitgeber, the so-called relative coordination phenomenon (2).

The study of entrainment range, as well as the precise determination of its limits, presents some difficulties, such as observation of unstable or "relative entrainment" toward the limits of the range, resulting in periodic fluctuations of τ (65). Moreover, exposure of organisms to a given zeitgeber at the limits of entrainment might lead to a situation in which various rhythms have different ranges of entrainment (1), as has been observed in humans as fractional desynchronization (23, 64) or in rats as dissociation patterns (17). Indeed, some studies have suggested that a circadian system submitted to extreme short or long T periods might become arrhythmic and would then entrain to an unlimited range of T cycles (2).

Consequently, the different methodological approaches might produce different results. To date, the limits of photic entrainment of the hamster activity rhythm to a given zeitgeber have been studied using one of the following procedures: *1*) exposure of animals to distinct T cycle periods across the studied range (3); *2*) exposure during progressively increasing (8), or both increasing and decreasing (9, 10), T cycle periods starting from T = 24 h until loss of entrainment; and *3*) by prediction, using the known τ and the respective phase-response curve for the hamster in such a manner that both the lower and upper limits are defined by τ minus the maximum phase advance or τ plus the maximum phase delay, respectively (44). In each of these scenarios, there remains a short time of "adaptation" before the exposure to the newly introduced condition: in *1*, the animals are transferred to the new T cycle directly from T = 24 h, so adaptation time is zero; in *2*, the new condition is changed gradually (daily), and adaptation time depends on the derivative of the change in T per day. However, it has not been established whether stepwise changes, with a longer time for adaptation, facilitate entrainment to a new T cycle.

Although daily light-dark transitions are the dominant zeitgeber for epigeous organisms, a wide array of nonphotic stimuli may prove effective entraining agents in rodents. Therefore, cycles of food availability (7, 37), ambient temperature (24), social interactions (27), and the induction of wheel running activity (20, 26, 30, 51, 61) may entrain or modify the phase of free-running rhythm when experimentally manipulated. In addition, activity induced by behavioral manipulations has been shown to accelerate the rate of reentrainment in hamsters (41, 52). It is known that nonphotic events induce the behavioral activation (arousal) in animals with concomitantly increased activity levels. Janik and Mrosovsky (29) showed that larger phase advances occurred accompanied by higher wheel running activity.

In addition, the periodicity of free-running rhythm appears to be inversely related to the amount of wheel running activity in some rodent species, such as in hamsters (40, 62) and rats (68, 69). However, several studies in mice suggest that the strength of this correlation is species and strain dependent (6, 20). Behavioral activity or vigilance state has been shown to modify the spontaneous firing activity rhythm of the hypothalamic suprachiasmatic nucleus cells of freely moving animals (15, 55), thereby suggesting a direct feedback of the behavioral state on the circadian clock. However, the function of activity feedback on the circadian clock as found in nature, when such arousing events most likely occur at night, remains unclear. Because of the powerful resetting effects of light, the role of nonphotic stimuli such as wheel running during light-dark (LD) cycles remains difficult to assess in the laboratory. In addition, the interaction between wheel running and light is not well understood, and activity feedback on the circadian clock may become more apparent when studied near the limits of photic entrainment.

The aims of this study were twofold: *1*) to investigate the influence of wheel running activity on entrainment, and *2*) to study entrainment of the activity rhythm at various LD cycles, stepwise decreasing period T further below the known lower limit of entrainment.

MATERIALS AND METHODS

Animals and experimental paradigm. Eight 2-mo-old male golden hamsters (*Mesocricetus auratus*) arrived at the laboratory directly from the provider (Harlan France, Gannat, France). The animals were housed isolated in individual transparent metacrylate cages measuring 22 × 22 × 15 cm (Panlab, Barcelona, Spain) and covered with a stainless steel grid, with wood shaving bedding (Souralit, La Rioja, Spain). Cages were maintained in sound-proof humidity- and temperature-controlled chambers (room temperature and humidity were between 18 and 22°C and 50 and 80%, respectively) with time-adjustable illumination cycles. Illuminance during the light phase was supplied by two 36-W Mazdafluor fluorescent tubes, producing ~300 lux of reflected cool white light at cage level and a dim red light of ~0.1 lux during the dark phase (Mavolux 5032B digital luxmeter; Gossen-Metrawatt-Camille Bauer). After 30 cycles, the animals were transferred to transparent metacrylate cages measuring 48 × 22 × 15 cm, equipped with running wheels (diameter = 30 cm), where they remained until the end of the experiment. During the entire experiment, the animals received food (Harlan Teklad 2040 Global Diets) and tap water ad libitum. Cage cleaning, as well as food and water supply, was conducted once a week at irregular daylight hours.

The animals were subjected to symmetrical LD cycles whose period (T) was changed sequentially from T = 22 h (T22) to T = 19 h (T19). At the end of the experiment, the animals were transferred to constant darkness (DD), with lights off maintained from the last scotophase in LD. The sequence of LD cycles with their respective extensions and wheel availability was as shown in Table 1. As at LD T20, the lower limit of entrainment was greatly exceeded; *stage 4* lasted twice the duration, attaining a stable rhythmic pattern before a further shortening of LD.

Motor activity and wheel running measurement. In *stage 0*, spontaneous motor activity (MA) of the animals was measured by means of an activity meter with two perpendicular infrared light beams crossing the cage at a height of 7 cm. From *stage 1* until the end of the experiment, MA was measured with an activity meter consisting of one infrared light beam crossing the cage at a height of 7 cm and placed in a manner to avoid wheel-related movement. Each beam interruption represented an activity count that was measured and compiled in bins of 15 min, obtaining regularly sampled time series.

Table 1. *Sequence of LD cycles*

Stage	Illuminance Conditions	No. of Cycles	Wheel Availability
0	T22 (11:11 h)	30	−
1	T22 (11:11 h)	28	+
2	T21 (10.5:10.5 h)	24	+
3	T20.4 (10.2:10.2 h)	30	+
4	T20 (10:10 h)	64	+
5	T19.6 (9.8:9.8 h)	26	+
6	T19.6 (9.8:9.8 h)	32	−
7	T19 (9.5:9.5 h)	12	−
8	DD	16	−

LD, light-dark; DD, dark-dark; T, period length of cycle (i.e., T22, T = 22 h).

When the running wheel was available for animals, wheel running activity (WR) was acquired by means of magnetic switches activated by a magnet placed on the wheel axis. Wheel revolutions were compiled in bins of 15 min, and two independent types of animal activity, MA and WR, were recorded simultaneously. All data samples were acquired through parallel channels and stored in a computer for further analysis. LD cycles were recorded simultaneously with activity in a separate channel connected to a photocell pulse generator.

Time-series and statistical analysis. Time-series analysis and statistical comparisons were carried out separately for each data set of MA and WR signals. Detection of MA and WR rhythms at each LD stage was conducted with a χ^2 periodogram (58), obtaining both the percentage of variance (PV) explained by the rhythm (11) and its period estimation. The period range examined was from 16 to 26 h. *P* level for significant periodicities was set at 0.05.

Daily phases of WR rhythm during each LD stage were calculated using least-squares data fitting to a cosine function with a period equal to T. Each set of daily phases was studied with circular statistics to assess the directedness of phase distribution along respective T cycles, using a Rayleigh *z*-test (4). This test obtains an **r** vector with its origin at the center of a circumference of radius one, where the daily estimated phases of the WR rhythm are distributed. The direction and length of the **r** vector was calculated as the vectorial mean of the unitary vectors associated with daily phases. Thus the length of **r** (between 0 and 1) is proportional to the degree of phase homogeneity during the respective T cycles and may be considered a measure of the rhythm's phase stability during successive days. Therefore, higher **r** values indicate a greater constancy of rhythm phase as a consequence of the pacemaker's stable response to the LD cycles (because the rhythm starts at similar phases during successive zeitgeber cycles), and lower **r** values correlate to unstable entrainment, when most spontaneous oscillation prevails during LD cycles.

The daily mean waveform was calculated at each stage for WR activity. The phase angle was calculated on waveforms as the phase difference between the lights off, at zeitgeber time = 12 (ZT 12), and the onset of activity. Onset of activity for the entire analysis was defined as the intersection of the mean WR activity with waveform. This definition was deemed reliable because the waveform for WR exhibits smooth variations during the α (activity) phase.

In addition, waveform analysis permitted the inclusion of *1*) the mean WR activity, calculated as the total WR per T cycle divided by the number of bins of corresponding T cycle length; *2*) the distribution of WR activity over the α phase, dividing α into two parts: α_i, from onset to time of maximum activity value (t_{max}), and α_f, from t_{max} to the offset of α. Because of the smoothness of waveforms, t_{max} was visually estimated without ambiguity in all cases. Distribution of activity was calculated as the percentage of activity at α_i with respect to total activity at α phase (%WR α_i). To better understand the changes occurring in the waveform, the time span for α, α_i, and α_f were calculated at the different stages.

Double-plot graphic analysis was used to observe changes in the rhythm during the different stages and to evaluate the temporal

relationship between the rhythm under T19 and under DD. In addition, the onset of the MA rhythm during the first five cycles in DD was calculated by projecting an eye-fitted vertical line in actograms plotted at modulo τ. This line was projected through the last cycle in T19 to estimate the phase of the rhythm in LD. Individually obtained phases were evaluated to discriminate between randomness or one-sided distribution along the T19 cycle by means of a Rayleigh z-test.

MA rhythm in DD was analyzed with a regressive periodogram by using four harmonics to avoid waveform interference (32). The period range examined was from 20 to 26 h, and P level for significant periodicities was set at 0.05. Analysis was done by dividing the entire DD stage into two consecutive parts of 8 days (S_1 and S_2). Aftereffects of previous entrainment were studied by comparing the τ values obtained between S_1 and S_2. Only significant periodicities were included for this comparison.

Statistical analysis of variance (ANOVA) was carried out to perform comparisons. Normal distributions and homogeneity of variances for categories (the stages) of the previously defined variables were found, except for the phase angle, which was log-transformed to achieve homogeneity (Kolmogorov-Smirnoff test, $P > 0.1$, and Levene test, $P > 0.05$) (57). Regression analysis was performed to assess stage differences for the phase angle, mean WR activity per cycle, %WR α_i, and the time span of α, α_i, and α_f. Correlation analysis was done to study the relationship between the PV of the rhythm and phase stability, and a t-test for dependent samples to compare the τ between S_1 and S_2. Heterogeneity of variances was found for phase stability and, because mathematical transformation did not attain homogeneity, nonparametric Kruskal-Wallis ANOVA and Mann-Whitney U-test were utilized for this variable. The level of statistical significance for all tests was defined at $P = 0.05$. Obtained P values lower than 0.01 are reported as 0.01.

Graphs and calculations were made using the integrated package for analysis in chronobiology "El Temps" (http://www.ub.es/dpfisiv/ soft/ElTemps/). For statistical analysis and comparisons, STATISTICA software was utilized (StatSoft).

RESULTS

Running wheel transference. The entire MA record of a representative animal is displayed in Fig. 1A on a double-plotted actogram at modulo T20. During the first 30 cycles at T22, all animals exhibited nonentrained MA rhythms with relative coordination patterns (mean $\pm$ SE of rhythm period: 22.5 ± 0.24). On the 30th cycle, hamsters were transferred to cages with running wheels. Providing a running wheel led to entrainment for both MA and WR rhythms, with the activity phase confined to the scotophase. Further reductions of the LD cycle period to T19.6 were conducted without loss of entrainment. However, subsequent blocking of the wheel did not result in loss of entrainment during the study period of 32 cycles, nor did it result in loss of entrainment during a further 12 cycles at T19. Only periods equal to T were detected significantly in periodograms calculated for each LD part, for both MA and WR rhythms. An actogram for one representative animal at modulo T22 displays the MA rhythm during the first 52 cycles of the study both at *stage 0* and *stage 1* (Fig. 1B). Similar patterns of MA were observed on actograms for all the animals in the experiment.

Phase stability. The phase changes of WR rhythms are clearly visible in single-plotted actograms at modulo T (Fig. 2A). Daily phase of the overt WR rhythms shows day-to-day instabilities that increased with the shortening of the T cycle. However, the rhythm generally remains confined to the scoto-
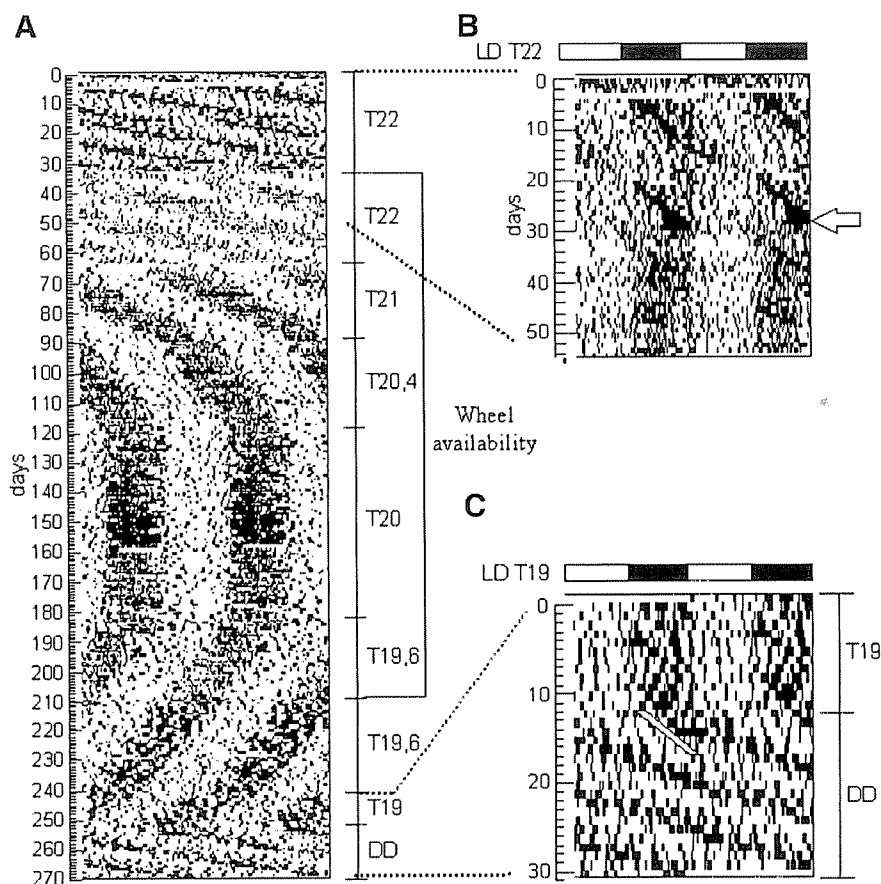

Fig. 1. Actogram of a representative hamster from the experiment. A: double-plotted actogram at modulo T20 (period length T = 20 h) showing the complete record of general motor activity (MA). The succession of the different T cycles are indicated on bar at *right*. Wheel availability is also indicated. B: double-plotted actogram at modulo T22 showing MA record of the corresponding section indicated in A. Solid and open bars at *top* indicate dark and light phases of the light-dark (LD) cycle, respectively. The arrow indicates the day of transference to a cage provided with a running wheel. C: double-plotted actogram at modulo T19 exhibiting specific features of the MA rhythm during both the entire T19 and constant darkness (DD) sections, which are indicated on bar at *right*. Solid and open bars at *top* indicate dark and light phases of the LD cycle, respectively. Open bar in actogram indicates the predicted onset of activity during the last cycle at LD, projected by eye fitting from the first 5 cycles at DD.
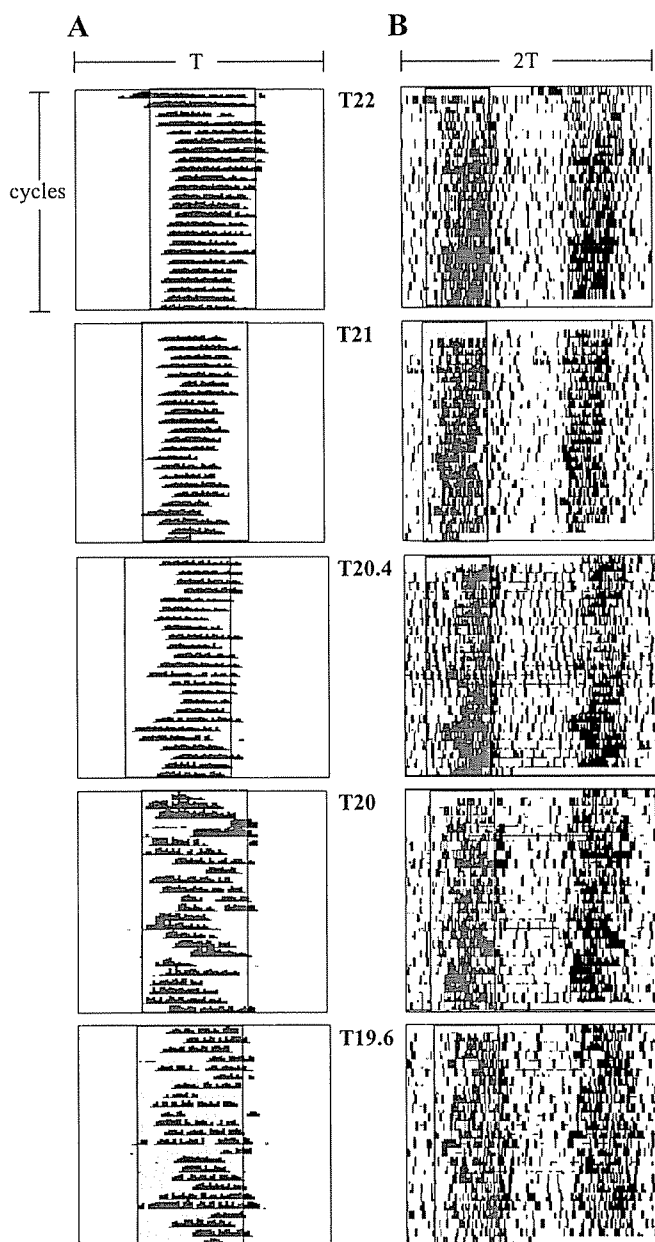
A

B

Fig. 2. *A*: representative single-plotted actograms at modulo T showing wheel running (WR) activity rhythm for each consecutive stage of the experiment. Histograms of 15-min intervals with between 0 and 500 compiled wheel revolutions during 24 cycles are shown. Shaded areas indicate the dark phase of the LD cycle. Phase instabilities are more pronounced at the lower T cycles, but overt rhythm remains synchronized with the T cycle. *B*: double-plotted actograms of general MA rhythm corresponding to the same animals as in *A*. Because of the different amounts of activity for the animals, the scale was adjusted individually to achieve a better view. Single-plotted shaded areas indicate the dark phase of the LD cycle.

phase when considered as a whole. Also, this can be observed in the general MA rhythm (Fig. 2*B*). Note that these patterns are different from relative coordination, where angular frequency decelerates and accelerates together with α decompression and compression. Comparable patterns were observed for all animals. In addition, variations of the **r** vector (Fig. 3*A*) manifested a higher phase stability at T22 and T21, whereas they diminished from T20.4 to T19.6 (Kruskal-Wallis ANOVA, $P < 0.01$; Mann-

Whitney *U*-test, T22 and T21 higher than T20.4, T20, and T19.6, $P < 0.01$). This relationship could be interpreted as an objective measure of that described in the actograms of Fig. 2. Furthermore, the percentage of variance explained by the rhythm (Fig. 3*B*) exhibits this same tendency (correlation: $r = 0.85$, $P < 0.01$), suggesting that the robustness of rhythm is related to phase stability as a feature of entrainment.

Phase angle. Figure 4 exhibits the phase angle variation as a response to T cycle changes calculated for the WR rhythm. The phase angle value was positive, increasing from ~1.5 h ZT at T22 to 3 h ZT at T19.6, when the WR onset progressively phase-lagged light offset as the period of the T cycle decreased. A significant linear regression was found for the phase angle vs. T cycle relationship (regression: $r = 0.35$, $P < 0.05$). Therefore, these modifications of the phase relationship between T cycle and the rhythm might indicate active changes in the pacemaker activity.

Changes in WR activity. Calculations on WR activity derived from waveforms were performed to study the amount and distribution of activity at α phase. Figure 3*C* shows mean wheel revolutions related to T cycle. Lowering the T cycle caused a decrease in mean WR activity (regression: $r = 0.63$, $P < 0.01$). However, the distribution of WR activity at α phase also changed in relation to T cycle. Figure 3*D* shows variations in the percentage of running activity at the α_i interval. Percentage of WR at α_i increased significantly as the T cycle shortened (regression: $r = 0.68$, $P < 0.01$). Moreover, duration for α_f decreased significantly in relation to T cycle shortening (regression: $r = 0.7$, $P < 0.01$), but no changes on α_i were detected (regression: $P > 0.1$) (Fig. 3*E*). Changes in duration of α were found to be proportional to changes on T (data not shown). These results indicate that the incremented percentages of WR at α_i, found at the beginning of α in relation to T cycle shortening, may be associated with changes in activity distribution during the α phase.

Phase control of rhythm. Temporal coincidence between the rhythm under LD and that under DD on the LD-DD transition suggests that the internal phase of the circadian clock was controlled by the LD zeitgeber. After the animals were transferred from LD T19 to DD, a significant phase grouping was found (Rayleigh *z*-test: **r** = 0.94, $P < 0.01$). Because constant darkness was initiated from the last scotophase in LD, no effects on the rhythm phase in constant darkness can be attributed to lights off. The phase control of rhythm also was evident in the actograms. Figure 1*C* displays a double-plotted actogram at modulo T19 for one representative animal during the transition from LD T19 to DD. MA rhythms began to exhibit free-run from the phase held during the preceding LD conditions.

Aftereffects. Free-running period changes in constant darkness were assessed to verify the presence of aftereffects of previous entrainment. A significant increment of τ was observed during the 16 days in DD, closely approximating the spontaneous value of 24 h (*t*-test for dependent samples: $P < 0.05$, S_1: τ = 23.1 ± 0.2 vs. S_2: τ = 23.8 ± 0.1). Two nonsignificant periods were detected at periodograms at both S_1 and S_2 and were excluded from this comparison.

DISCUSSION

In this study, entrainment of the circadian activity pattern in hamsters, subject to various stepwise decreasing T cycles, was assessed. Starting at T22, data confirmed that animals without

a wheel exhibited nonentrained activity rhythms with relative coordination patterns. Continuous access to a running wheel rapidly accelerated entrainment to T22 and may well have contributed to the maintenance of entrainment during further T cycle reductions to T19.6. However, when the access to the wheel was removed at T19.6, there was no loss of entrainment,
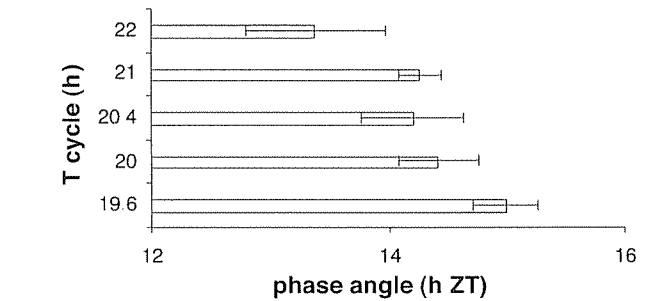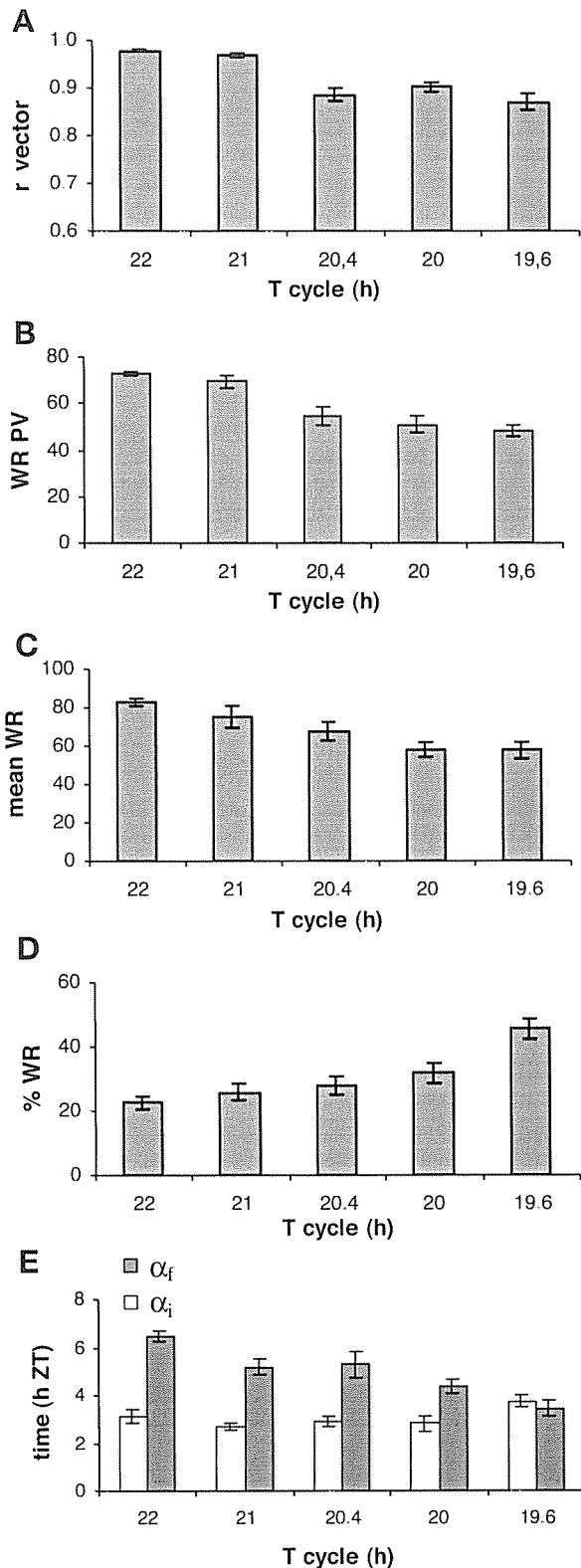

Fig. 4. Phase angle calculated as the phase difference between lights off and the onset of activity, expressed in ZT under the different T cycles experienced by the animals. The phase angle was always positive, being the onset of the WR rhythm progressively delayed in respect to lights off, and its value increased with T cycle shortening. ZT24 corresponds to lights on (linear regression: $r = 0.35$, $P < 0.05$).

nor when T was reduced to T19. Therefore, these data suggest that during T22 the spontaneous WR activity contributed to drive the phase of the pacemaker via feedback mechanisms and that once entrainment was acquired (during the following shortened T cycles), it became partially independent of WR.

Entrainment to short T cycles has already been described, but not entrainment to a T as short as T19. A study by Carmichael et al. (12) reported entrainment in hamster to T cycles close to T21.5. This paradigm was based on a stepwise decreases in T cycle of 15 min/day or less from 14:10-h LD, maintaining a 14-h fixed photophase and shortening the scotophase. Also, Boulos et al. (9) reported the lower entrainment limit for hamster activity rhythms in LD square cycles as being close to T22. In that study, the animals were exposed to LD cycles with a light intensity of 10 lux, with changes in T cycle of 5 min/day from T24 to T21.5, whereas the present data were obtained using a stepwise decreasing protocol, which could have allowed sufficient time for adaptation. This suggests that entrainment limits are not fixed but depend largely on the methods used to evaluate them. Furthermore, Boulos et al. (9) indicated that a precise estimation of the entrainment limits is possible "in a relatively short period of time" with a 5 min/day rate of change of T. However, this takes the implicit assumption that adaptation time determines the limits of entrainment. Usui et al. (60) studied the entrainment range of activity rhythms in rats, assessing stepwise changes in T every 30 cycles, and reported a value near 28.5 h for the upper limit and 23.5 h for the lower one, whereas Boulos et al. (9) reported

Fig. 3. A: variation of the r vector calculated for WR activity rhythm manifested higher phase stability at T22 and T21, whereas it diminished from T20.4 to T19.6. Kruskal-Wallis ANOVA, $P < 0.01$; Mann-Whitney U-test, T22 and T21 higher than T20.4, T20, and T19.6, $P < 0.01$. B: the percentage of variance (PV) explained by the WR activity rhythm exhibits the same relationship as the phase stability with respect to T cycle ($r = 0.85$, $P < 0.01$). C: mean WR activity calculated from waveforms for each T cycle, calculated as total WR activity divided by the number of bins of the corresponding T cycle, expressed as wheel revolutions per 15 min. Lowering the T cycle caused a decrease in the mean WR activity ($r = 0.63$, $P < 0.01$). D: %WR activity at α_i in respect to total WR activity at the α phase, calculated after dividing α into two parts: α_i, from onset to time of maximum activity value (t_{max}), and α_f, from t_{max} to the offset of α. %WR activity at α_i increased significantly as the T cycle shortened ($r = 0.68$, $P < 0.01$). E: time span for α_f significantly diminished in relation to T cycle shortening ($r = 0.7$, $P < 0.01$), but no changes on α_i were detected ($P > 0.1$). ZT, zeitgeber time. Values are means ± SE of the different variables described in MATERIALS AND METHODS.

values that were close to 25.5 and 22 h, respectively. More-over, it has been reported in rats that the upper entrainment limit of feeding activity rhythm occurs at 28 h if the animals are exposed directly to T cycles from T24, and only at 26 h 44 min with a 10 min/day increase in T cycle from T24 to T30 (36). These studies suggest that pacemaker function is differentially affected depending on previous environmental history or on the time required to adapt to changing conditions.

According to the present results, adaptation time for a T cycle could be considered an important aspect of the experimental paradigm in assessing the entrainment limits of hamster activity rhythm to LD square cycles, at least for the lower one. This suggests that the range of entrainment is more a dynamic than a static property of the system. If the period of circadian rhythm is inversely related to the intrinsic velocity of the endogenous oscillator, ω, the upper and lower limits of entrainment can be associated with velocities ω_U and ω_L, respectively. In Fig. 5, we have represented the expected changes in these values from the theoretical point of view. According to the graph in Fig. 5, both a stable free-running and an entrained rhythm will be represented as horizontal lines, because the angular velocity remains constant over time. Change in velocity, when T cycle is imposed, is represented as a vertical displacement on the graph. Under these conditions, the system exhibits a sort of inertia in modifying its internal velocity. Entrainment beyond a certain limit is not possible because the system is unable to maintain the acceleration (change of velocity over time) imposed by the zeitgeber. In light of this experimental evidence, a border separating the regions where entrainment is and is not possible can be drawn. Furthermore, it can be assumed that this border must have a horizontal asymptote, representing the real limits for entrainment, adopt-
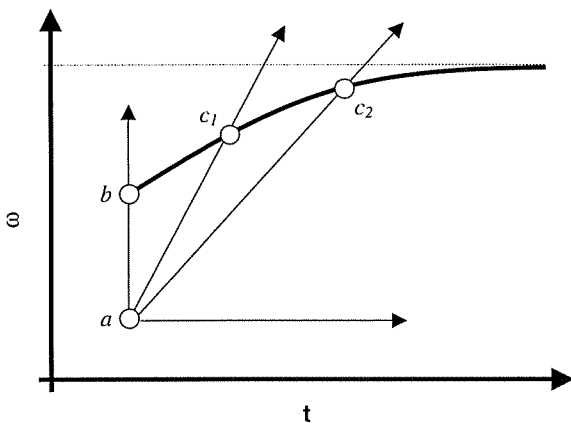
ing the concept of "dynamic range of entrainment" instead of that currently used (static).

The mechanism by which these differences are produced cannot be determined with the present data. However, it is known that in most physiological processes, sufficient adaptation time is necessary for setting compensation mechanisms, particularly when response to a new environmental condition is nearing the limits of the system adaptability.

Although the adaptation time to a T cycle seems to be an important factor to improve entrainment, the systematic changes found in the amount of WR activity also suggest the role of a possible activity feedback. Mean WR activity diminished when the T cycle was shortened, when shorter τ or larger phase advances are typically required to entrain. However, distribution of WR activity, as a percentage of running during the initial part of the α phase, increased significantly from T22 to T19.6. Thus it is possible that not only the amount of volitional WR activity but also its distribution in the α phase should be considered as a feedback-related variable. Edgar et al. (20) reported that a shorter τ was observed in mice when intense activity was performed during early subjective night, whereas a longer τ occurred when activity was concentrated at its end. In addition, Mistlberger and Holmes (38) reported that the activity feedback over the phase angle of entrainment in mice that had been exposed to different LD cycles less than T24 occurred mainly during the first 2 h at α phase. These findings suggest that the feedback contribution of WR activity on entrainment could depend on the activity levels that occur at certain circadian phases. The ecologic function of this mechanism may be related to instances of entrainment reinforcement, whereby occurrences of behavioral significance may concentrate the animal's temporal perception of its environment (e.g., encounters with mating opportunities, food sources, or a predator's presence) (27). However, because entrainment was achieved at T19.6 and T19 without running wheel access, the contribution to entrainment of continuous wheel running, once the circadian system has been already entrained, is not so important as expected. Gorman et al. (25) reported that the presence or absence of a running wheel had only minor effects on entrainment to lengthening T cycles. Although the shortening of τ by activity feedback could be accounted to explain entrainment, at least to T22, we observed in the laboratory (unpublished observations) that hamsters did not entrain to T27, but they did when the wheel was available. Therefore, the precise role of activity feedback on entrainment remains to be established.

Control of the overt rhythm's period was observed during the entire experiment, because the same period as the external LD was acquired by both WR and MA rhythms. In addition, phase angle was positive, increasing systematically from ~1.5 h ZT at T22 to 3 h ZT at T19.6. With the use of a single discrete phase reference, these results are in agreement with the expected phase relationship on steady-state entrainment of a rhythm by a high-frequency zeitgeber (2). However, the temporal structure of hamster WR activity throughout the day seems to be more complex than a single and continuous α phase and would be regulated by a coupled multioscillatory system. Pittendrigh and Daan (46) suggested that changes in activity peaks within α reflect the behavior of two coupled oscillators and the phase relationship between them. Moreover, the possibility that each component of a complex but regular activity pattern may be under the control of a separate circadian

Fig. 5. Graphic representation of the concept of dynamic limits of entrainment. On the ordinates, the intrinsic angular velocity of the oscillator (ω) is represented, and on the abscissas, time (t), to show how ω evolves through time as a consequence of changes in the period (T) of zeitgeber. The horizontal arrow starting at a represents a system running at constant velocity (entrained or free running). The vertical arrow represents a theoretically instantaneous increase in ω as a consequence of a direct transition to a new T. b is the maximum velocity that the system can assume after such a transition (conventional limit of entrainment). Gradual modifications of T constitute an intermediate situation that can be graphically represented as inclined lines, with slopes proportional to the rates of change of T. The thick curve indicates the maximum velocity that the system can assume under these different conditions (c_i), defining the "dynamic limit of entrainment." Considering all the possible rates of change, the dotted line represents the asymptote at which tends the real absolute limit of entrainment.

oscillator was suggested (22). Furthermore, it has been proposed that activity time appears as a "window" controlled by the pacemaker during which expression of different WR activity components, controlled by additional circadian oscillators, is permitted (14). Within this framework, daily WR activity patterns can be considered a function of the phase relationship between the window pacemaker and the activity components. A comparable scenario is illustrated in Fig. 2A at T20 and T19.6 stages, where the overt WR rhythm remains entrained but also seems to present rhythmic components that tend to free-run. Although the overt rhythm observed at T20 and T19.6 appeared to be partially driven by light, this influence was sufficient to drive the pacemaker's phase, as can be shown when the phase of free-running rhythm is observed after being released in constant darkness.

Despite entrainment, it is clear that hamsters do not exhibit the same phase stability under the different T cycle. This suggests that the temporal pattern of WR activity is regulated by a coupled multioscillatory circadian system, a hypothesis that has been studied using different theoretical (18, 45, 54, 59, 66) and empirical approaches (28, 34, 35, 43, 63, 70). Moreover, this coupling strength seems to be modulated mainly by light intensity, which under specific conditions can prompt a functional reorganization of the oscillatory components of circadian system (17, 33, 42, 49). Therefore, cycle-to-cycle phase stability of the overt rhythm with respect to the zeitgeber phase could be interpreted as the "degree of entrainment" of the system, allowing one to imagine the entrainment process as a continuous or gradual one. Indeed, the phase stability of the overt rhythm could indicate the entrainment degree of the system as a measure of the temporal organization of the phases of the different oscillators. T cycles shorter than that of the spontaneous frequency of the system produce phase instability and a "low entrained" system with more free-running components. However, because the amount of light per cycle remains the same at different T cycles, the incremental phase instability that occurs at lower T cycles must depend on the τ/T relationship. In addition, the present results suggest a relationship between entrainment degree and the robustness of the output signal. This suggests an interesting hypothesis, namely, that rhythm variability may be a quantitative function of the coupling level, as well as a measure of the system's functional coherence (67).

At the end of the experiment, changes in the free-running period from 23.1 to 23.8 h were observed under DD. It has been shown that the continuous effects of the LD cycle can modify the pacemaker period to compensate for differences with the T period (5, 16, 47). Remarkably, detecting values below 24 h, specifically 23.1 h over eight cycles at DD after release from LD, proved strong evidence in demonstrating how pacemaker period is affected by the LD cycle.

Although the present study cannot demonstrate the existence of discrete entrainment, it does suggest that the history of entrainment may affect the phase-resetting mechanism of the pacemaker. Reebs and Doucet (50) reported that T cycle frequency may influence the responsiveness of the pacemaker to both light and induced wheel running: whereas shorter T cycles produced shorter τ when free-run under DD, large phase advances were induced after light and activity pulses, contrary to the expected relationship between τ and phase shifts (13, 48, 56). This evidence makes it clear that the sensitivity and/or responsiveness of the pacemaker to resetting stimuli (the resetting contour in a state plane; see Ref. 31 for revision) are not solely characteristics of a "phase only

system," which always responds with the same phase-response curve (53), but they may been affected by previous illuminance and entrainment history.

In conclusion, as far as we know, this is the first time that the activity rhythm of the hamster has been entrained to a T19 cycle. We believe that once entrainment has been established (a process in which access to the running wheel may have an important role), the time of adaptation before a new change of the T cycle may be considered an important factor to evaluate the "real" dynamic entrainment limits, whose values depend not only on the sum of $\tau \pm$ the maximum phase shift observed at the phase-response curve but also on the rate of change of the imposed T cycle.

REFERENCES

1. **Aschoff J.** Circadian rhythms within and outside their ranges of entrainment. In: *Environmental Endocrinology*, edited by Assenmacher I and Farner D. New York: Springer-Verlag, 1978, p. 172–181.
2. **Aschoff J.** Freerunning and entrained circadian rhythms. In: *Handbook of Behavioural Neurobiology: Biological Rhythms*, edited by Aschoff J. New York: Plenum, 1981, p. 81–93.
3. **Aschoff J and Pohl H.** Phase relations between a circadian rhythm and its zeitgeber within the range of entrainment. *Naturwissenschaften* 65: 80–84, 1978.
4. **Batschelet E.** *Circular Statistics in Biology.* London: Academic, 1981.
5. **Beersma DGM, Daan S, and Hut RA.** Accuracy of circadian entrainment under fluctuating light conditions: contributions of phase and period responses. *J Biol Rhythms* 14: 320–329, 1999.
6. **Benus RF, Koolhaas JM, and Van Oortmerseen GA.** Aggression and adaptation to the light-dark cycle: role of intrinsic and extrinsic control. *Physiol Behav* 43: 131–137, 1988.
7. **Boulos Z and Terman M.** Food availability and daily biological rhythms. *Neurosci Biobehav Rev* 4: 119–131, 1980.
8. **Boulos Z, Macchi M, and Terman M.** Twilight transitions promote circadian entrainment to lengthening light-dark cycles. *Am J Physiol Regul Integr Comp Physiol* 271: R813–R818, 1996.
9. **Boulos Z, Macchi MM, and Terman M.** Twilights widen the range of photic entrainment in hamsters. *J Biol Rhythms* 17: 353–363, 2002.
10. **Bruce VG.** Environmental entrainment of circadian rhythms. *Cold Spring Harb Symp Quant Biol* 25: 29–48, 1960.
11. **Canal-Corretger MM, Vilaplana J, Cambras T, and Díez-Noguera A.** Functioning of the rat circadian system is modified by light applied in critical postnatal days. *Am J Physiol Regul Integr Comp Physiol* 280: R1023–R1030, 2001.
12. **Carmichael MS, Nelson RJ, and Zucker I.** Hamster activity and estrous cycles: control by a single versus multiple circadian oscillator(s). *Proc Natl Acad Sci USA* 78: 7830–7834, 1981.
13. **Daan S and Pittendrigh CS.** A functional analysis of circadian pacemakers in nocturnal rodents. II. The variability of phase response curves. *J Comp Physiol [A]* 106: 253–266, 1976.
14. **Davis FC and Menaker M.** Hamsters through time's window: temporal structure of hamster locomotor rhythmicity. *Am J Physiol Regul Integr Comp Physiol* 239: R149–R155, 1980.
15. **Deboer T, Vansteensel MJ, Detari L, and Meijer JH.** Sleep states alter activity of suprachiasmatic nucleus neurons. *Nat Neurosci* 6: 1086–1090, 2003.
16. **De Coursey P.** Photoentrainment of circadian rhythms: An ecologist's viewpoint. In: *Circadian Clocks and Ecology*, edited by Hiroshige T and Honma K. Sapporo, Japan: Hokkaido University Press, 1989, p. 187–206.
17. **De la Iglesia HO, Cambras T, Schwartz WJ, and Díez-Noguera A.** Forced desynchronization of dual circadian oscillators within the rat suprachiasmatic nucleus. *Curr Biol* 14: 796–800, 2004.

18. Diez-Noguera A. A functional model of the circadian system based on the degree of intercommunication in a complex system. *Am J Physiol Regul Integr Comp Physiol* 267: R1118–R1135, 1994.

19. Edgar DM and Dement WC. Regularly scheduled voluntary exercise synchronizes the mouse circadian clock. *Am J Physiol Regul Integr Comp Physiol* 261: R928–R933, 1991.

20. Edgar DM, Martin CE, and Dement WC. Activity feedback to the mammalian circadian pacemaker: influence on observed measures of rhythm period length. *J Biol Rhythms* 6: 185–199, 1991.

21. Ehret CF, Groh KR, and Meinert JC. Circadian dyschronism and chronotypic ecophilia as factors in aging and longevity. In: *Aging and Biological Rhythms*, edited by Samis HV and Campobianco S. New York: Plenum, 1978, p. 185–213.

22. Enright JT. The circadian tape recorder and its entrainment. In: *Physiological Adaptation to the Environment*, edited by Vernberg J. New York: Educational, 1975, p. 465–476.

23. Folkard S, Minors DS, and Waterhouse JM. Is there more than one circadian clock in humans? Evidence from fractional desynchronization studies. *J Physiol* 357: 341–356, 1984.

24. Francis AJ and Coleman GJ. The effect of ambient temperature cycles upon circadian running and drinking activity in male and female laboratory rats. *Physiol Behav* 43: 471–477, 1988.

25. Gorman MR, Kendall M, and Elliott JA. Scotopic illumination enhances entrainment of circadian rhythms to lengthening light:dark cycles. *J Biol Rhythms* 20: 38–48, 2005.

26. Hastings MH, Mead SM, Vindlacheruvu RR, Ebling FJP, Maywood ES, and Grosse J. Non-photic phase shifting of the circadian activity rhythm of Syrian hamster: the relative potency of arousal and melatonin. *Brain Res* 591: 20–26, 1992.

27. Honrado GI and Mrosovsky N. Interaction between periodic sociosexual cues and light-dark cycles in controlling the phasing of activity rhythms in golden hamsters. *Ethol Ecol Evol* 3: 221–232, 1991.

28. Jagota A, de la Iglesia HO, and Schwartz WJ. Morning and evening circadian oscillations in the suprachiasmatic nucleus in vitro. *Nat Neurosci* 3: 372–376, 2000.

29. Janik D and Mrosovsky N. Nonphotically induced phase shifts of circadian rhythms in the golden hamster: activity-response curves at different ambient temperatures. *Physiol Behav* 53: 431–436, 1993.

30. Janik D, Goodfrey M, and Mrosovsky N. Phase angle changes of photically entrained circadian rhythms following a single nonphotic stimulus. *Physiol Behav* 55: 103–107, 1994.

31. Johnson CH, Elliott JA, and Foster R. Entrainment of circadian programs. *Chronobiol Int* 20: 741–774, 2003.

32. Klemfuss H and Clopton P. Seeking tau: a comparison of six methods. *J Interdiscip Cycle Res* 24: 1–16, 1993.

33. Kuhlman S, Silver R, Le Sauter J, Bult-Ito A, and McMahon D. Phase resetting light pulses induce Perl and persistent spike activity in a subpopulation of biological clock neurons. *J Neurosci* 23: 1441–1450, 2003.

34. Liu C, Weaver DR, Strogatz SH, and Reppert SM. Cellular construction of a circadian clock: period determination in the suprachiasmatic nuclei. *Cell* 91: 855–860, 1997.

35. Low-Zeddies SS and Takahashi JS. Chimera analysis of the Clock mutation in mice shows that complex cellular integration determines circadian behavior. *Cell* 105: 25–42, 2001.

36. Madrid JA, Sanchez-Vazquez FJ, Lax P, Matas P, Cuenca EM, and Zamora S. Feeding behavior and entrainment limits in the circadian system of the rat. *Am J Physiol Regul Integr Comp Physiol* 275: R372–R383, 1998.

37. Mistlberger RE. Scheduled daily exercise or feeding alters the phase of photic entrainment in Syrian hamsters. *Physiol Behav* 50: 1257–1260, 1991.

38. Mistlberger RE and Holmes MM. Behavioral feedback regulation of circadian rhythm phase angle in light-dark entrained mice. *Am J Physiol Regul Integr Comp Physiol* 279: R813–R821, 2000.

39. Mistlberger RE, Bossert JM, Holmes MM, and Marchant EG. Serotonin and feedback effects of behavioral activity on circadian rhythms in mice. *Behav Brain Res* 96: 93–99, 1998.

40. Mrosovsky N. Further experiments on the relationship between the period of circadian rhythms and locomotor activity levels in hamsters. *Physiol Behav* 66: 797–801, 1999.

41. Mrosovsky N and Salmon PA. A behavioural method for accelerating re-entrainment of rhythms to new light-dark cycles. *Nature* 330: 372–373, 1987.

42. Nagano M, Adachi A, Nakahama K, Nakamura T, Tamada M, Meyer-Bernstein E, Sehgal A, and Shigeyoshi Y. An abrupt shift in the day/night cycle causes desynchrony in the mammalian circadian center. *J Neurosci* 23: 6141–6151, 2003.

43. Nakamura W, Honma S, Shirakawa T, and Honma K. Regional pacemakers composed of multiple oscillator neurons in the rat suprachiasmatic nucleus. *Eur J Neurosci* 14: 666–674, 2001.

44. Pittendrigh CS. Circadian systems: entrainment. In: *Handbook of Behavioral Neurobiology: Biological Rhythms*, edited by Aschoff J. New York: Plenum, 1981, p. 95–124.

45. Pittendrigh CS. Circadian systems: general perspective. In: *Handbook of Behavioral Neurobiology: Biological Rhythms*, edited by Aschoff J. New York: Plenum, 1981, p. 57–80.

46. Pittendrigh CS and Daan S. A functional analysis of circadian pacemakers in nocturnal rodents. V. Pacemaker structure: a clock for all seasons. *J Comp Physiol [A]* 106: 333–355, 1976.

47. Pittendrigh CS and Daan S. A functional analysis of circadian pacemakers in nocturnal rodents. I. The stability and lability of spontaneous frequency. *J Comp Physiol [A]* 106: 223–252, 1976.

48. Puchalski W and Lynch GR. Relationship between phase resetting and the free-running period in Djungarian hamsters. *J Biol Rhythms* 7: 75–83, 1992.

49. Quinteros J, Kuhlman SJ, and McMahon DG. The biological clock nucleus: a multiphasic oscillator network regulated by light. *J Neurosci* 23: 8070–8076, 2003.

50. Reebs SG and Doucet P. Relationship between circadian period and size of phase shifts in Syrian hamsters. *Physiol Behav* 61: 661–667, 1997.

51. Reebs SG and Mrosovsky N. Effects of induced wheel running on the circadian activity rhythms of Syrian hamsters: entrainment and phase-response curve. *J Biol Rhythms* 4: 39–48, 1989.

52. Reebs SG and Mrosovsky N. Large phase-shifts of circadian rhythms caused by induced running in a re-entrainment paradigm: the role of pulse duration and light. *J Comp Physiol [A]* 165: 819–825, 1989.

53. Roenneberg T, Daan S, and Merrow M. The art of entrainment. *J Biol Rhythms* 18: 183–194, 2003.

54. Rosenwasser AM and Adler AT. Structure and function in circadian timing systems: evidence for multiple coupling circadian oscillators. *Neurosci Biobehav Rev* 10: 431–448, 1986.

55. Schaap J and Meijer JH. Opposing effects of behavioural activity and light on neurons of the suprachiasmatic nucleus. *Eur J Neurosci* 13: 1955–1962, 2001.

56. Schwartz WJ and Zimmerman P. Circadian timekeeping in BALB/c and C57BL/6 inbred mouse strains. *J Neurosci* 10: 3685–3694, 1990.

57. Sokal RR and Rohlf FJ. *Biometría. Principios y métodos estadísticos en la investigación biológica*. Madrid: Blume, 1979.

58. Sokolove PG and Bushell WN. A chi square periodogram: its utility for the analysis of circadian rhythms. *J Theor Biol* 72: 131–160, 1978.

59. Strogatz SH. Human circadian rhythms: a simple model based on two coupled oscillators. *J Math Biol* 25: 327–347, 1987.

60. Usui S, Takahashi Y, and Okazaki T. Range of entrainment of rat circadian rhythms to sinusoidal light-intensity cycles. *Am J Physiol Regul Integr Comp Physiol* 278: R1148–R1156, 2000.

61. Van Reeth O and Turek FW. Stimulated activity mediates phase shifts in the hamster circadian clock induced by dark pulses or benzodiazepines. *Nature* 339: 49–51, 1989.

62. Weisgerber D, Redlin U, and Mrosovsky N. Lengthening of circadian period in hamsters by novelty-induced wheel running. *Physiol Behav* 62: 759–765, 1997.

63. Welsh DK, Logothetis DE, Meister M, and Reppert SM. Individual neurons dissociated from rat suprachiasmatic nucleus express independently phased circadian firing rhythms. *Neuron* 14: 697–706, 1995.

64. Wever RA. Fractional desynchronization of human circadian rhythms: a method for evaluating entrainment limits and functional interdependencies. *Pflügers Arch* 396: 128–137, 1983.

65. Wever R. Virtual synchronization towards the limits of the range of entrainment. *J Theor Biol* 36: 119–132, 1972.

66. Winfree A. Biological rhythms and the behavior of populations of coupled oscillators. *J Theor Biol* 16: 15–42, 1967.

67. Winfree AT. On emerging coherence. *Science* 298: 2336–2337, 2002.

68. Yamada N, Shimoda K, Ohi K, Takahashi S, and Takahashi K. Free-access to a running wheel shortens the period of free-running rhythm in blinded rats. *Physiol Behav* 42: 87–91, 1988.

69. Yamada N, Shimoda K, Takahashi K, and Takahashi S. Relationship between free-running period and motor activity in blinded rats. *Brain Res Bull* 25: 115–119, 1990.

70. Yamaguchi S, Isejima H, Matsuo T, Okura R, Yagita K, Kobayashi M, and Okamura H. Synchronization of cellular clocks in the suprachiasmatic nucleus. *Science* 302: 1408–1412, 2003.

History-dependent changes on entrainment of the activity rhythm in the Syrian hamster (Mesocricetus auratus)

Artículo aceptado para su publicación en *Journal of Biological Rhythms*

Indice de Impacto: 2,979
Área: Fisiología
Posición: 21/74

PMB 336
4938 Hampden Lane
Bethesda, MD 20814-2914
USA
phone: (301) -656 -4655
e-mail: edjbr@earthlink.net

October 11, 2005

Dr. Juan J. Chiesa.
Departament de Fisiologia
Facultat de Farmacia
Universitat de Barcelona
Av Joan XXIII s/n
08028 Barcelona
Spain

MS#:   05-056
TITLE: **History-dependent changes on entrainment of the activity rhythm
                  in the Syrian hamster (Mesocricetus auratus)**
AUTHOR(S):   *Juan J. Chiesa, Montserrat Anglès-Pujolràs, Antoni Díez-Noguera,
                  and Trinitat Cambras*

Dear Dr. Chiesa:

I have received the revised version of your manuscript cited above. I consider that you have adequately addressed the reviewers' concerns and am pleased to inform you that your paper has now been accepted for publication in the *Journal of Biological Rhythms.*

Future communications regarding your paper will come from Sage, the publisher. Your paper will appear in February or April, 2006.

Thank you for submitting your work to the JBR.

Sincerely,

Martin Zatz
Editor

History-dependent changes on entrainment of the activity rhythm in the Syrian hamster (*Mesocricetus auratus*)

JUAN J. CHIESA[1], MONTSERRAT ANGLÈS-PUJOLRÀS, ANTONI DÍEZ-NOGUERA, AND TRINITAT CAMBRAS.

Departament de Fisiologia, Facultat de Farmacia, Universitat de Barcelona, 08028 Barcelona, Spain.

RUNNING TITLE: hamster activity pattern and lighting history.

[1]CORRESPONDING AUTHOR: Juan J. Chiesa. Departament de Fisiologia, Facultat de Farmacia, Universitat de Barcelona. Av Joan XXIII s/n, 08028 Barcelona, Spain. Phone: (0034) 93 402 4505, Fax: (0034) 93 403 5901; e-mail 1: jchiesa@ub.edu, e-mail 2: cambras@ub.edu

ABSTRACT

We have studied the activity rhythm of Syrian hamsters exposed to square LD cycles with a 22-h period (T22) with the aim of testing the effects of the previous history on the rhythmic pattern. To do so, sequential changes of different lighting environments were established followed by the same LD condition. Also, our protocol included T22 cycles with varying lighting contrasts, to test the extent to which a computational model predicts experimental outcomes. At the beginning of the experiment, exposure to T22 with 300 lux and dim red light occurring respectively at photophase and scotophase ($LD_{300 / dim\ red}$) mainly generated relative coordination. Subsequent transfer to cycles with ~ 0.1-lux dim light during the scotophase ($LD_{300 / 0.1}$) promoted entrainment to T22. However, a further reduction in light intensity to 10 lux during the photophase ($LD_{10 / 0.1}$), generated weak and unstable T22 rhythms. When, after that, animals were transferred again to the initial $LD_{300 / dim\ red}$ cycles, the amplitude of the rhythm still remained very low and the phases were very unstable. Exposure to constant darkness partially restored the activity rhythm, and when afterwards the animals were submitted again to $LD_{300 / dim\ red}$ cycles, a robust T22 rhythm appeared. Our results demonstrate history-dependent changes in the hamster circadian system, since the locomotor activity pattern under the same T22 cycle can show relative coordination or unstable or robust entrainment depending on the prior lighting condition. This suggests that the circadian system responds to environmental stimuli depending on its previous history. Moreover, computer simulations let us predict entrainment under $LD_{300 / 0.1}$ cycles, and indicate that most of the patterns observed in the animals due to the light in the scotophase can be explained by different degrees of coupling among the oscillators of the circadian system.

Keywords: entrainment, hamster, T cycle, coupling, multioscillatory model.

INTRODUCTION

The temporal adaptation of organisms to their environment depends on the ability of the circadian pacemaker to entrain, using daily environmental information provided primarily by the light-dark (LD) transitions imposed by the solar day. Photic information is processed by the pacemaker, which is located in the suprachiasmatic nucleus of the hypothalamus (SCN). Entrainment involves adjustments in the phase and period of pacemaker activity, and hence their rhythmic outputs synchronize with the environmental cycle (Daan and Aschoff, 2001). These fine-tuning entrainment mechanisms can be modelled within the laboratory, utilizing either continuous or discrete light action. The continuous model is based on the assumption that the free-running period (τ) of the pacemaker continuously decreases or increases by daily changes in light intensity (Aschoff, 1981). In the discrete model, τ is considered a constant of the pacemaker, and its adjustment to the zeitgeber period (T) occurs solely via phase shifts elicited by discrete LD (or DL) transitions (Pittendrigh, 1981a). The direction and magnitude of the phase shift depends on the phase response curve (PRC), which has been regarded as a functional characteristic of the pacemaker that rigidly defines the T cycle range into which it will be entrained; as $T = \tau \pm$ maximum phase-shift at PRC (Pittendrigh, 1981a).

The hamster circadian system appears to be more complex than a single pacemaker that invariably responds with the same PRC to environmental stimuli. Of course, a flexible phase angle becomes important for the hamster, a photoperiodic species which is seasonally entrained to a varying day length. The photoperiod modulates entrainment, generating behavioural and physiological rhythms appropriate for each phase of the year (Pittendrigh and Daan, 1976b; Elliott and Tamarkin, 1994; Schwartz et al., 2001). Even under constant darkness, the circadian pacemaker retains the influence of the previous entraining photoperiod, as reflected in the rhythm's τ, waveform, and photic PRC (Pittendrigh and Daan, 1976a; Pittendrigh et al., 1984), and this influence is also reflected in the SCN activity (Mrugala et al., 2000; Schaap et al., 2003).

Pittendrigh and Daan (1976b) considered that the hamster circadian clock is made up of a complex pacemaker consisting of two mutually coupled oscillators, morning (M), accelerated by light and synchronized to dawn, and evening (E), decelerated by

light and synchronized to dusk. These oscillators may adopt a range of variable phase angles to regulate the overt rhythm, the α phase duration reflecting the phase relationship between them (Ψ_{EM}). The period of the coupled system depends on the interaction of these two components, while the strength of this interaction depends on Ψ_{EM}. Distinct phase relationships for both E and M oscillators with respect to the zeitgeber have been considered to explain the effects of light intensity changes on motor activity (Gorman et al., 1997) and pineal melatonin rhythms (Elliott and Tamarkin, 1994). However, the historical dependence of the pacemaker state, reflected in the form of aftereffects on both τ and α (Aschoff, 1981; Pittendrigh and Daan, 1976a), suggests that the actual state is not solely dependent on a given lighting condition. The Ψ_{EM} is also established historically by the previous environmental conditions, namely hysteresis phenomena, initially described by Hoffman (1971).

It has been demonstrated that dual circadian oscillation are present in the SCN tissue in vitro, that correspond to M and E oscillators underlying photoperiodic phenomena (Jagota et al., 2000). However, it is not known whether they are a property of individual SCN cells or instead emerge from an intercellular network interaction. The principal functional bases of mammalian pacemakers were also modelled from a multioscillatory standpoint (Winfree, 1967; Díez-Noguera, 1994; Achermann and Kunz, 1999). These models take the central assumption that many pacemaker characteristics may arise at the level of intercellular interactions. It is well known that single circadian oscillators are arranged in individual cultured neuronal clocks (Welsh et al., 1995) with spontaneously dispersed periods (Herzog et al., 1998; Honma et al., 2004). Neuronal clocks synchronize among them within the integrated SCN tissue by their network interactions, attaining stable phase relationships and generating the circadian output (Yamaguchi et al., 2003). Indeed, the circadian period of both pacemaker and behavioral rhythms may be determined by the mean period arising from such interactions between clock cells (Liu et al., 1997; Low-Zeddies and Takahashi, 2001). Neural communication via both electrical (Long et al., 2005), Na^{+}-dependent action potential (Honma et al., 2000; Yamaguchi et al., 2003) and chemical synapses (Aton et al., 2005), participate in both synchrony and rhythmicity maintenance among SCN cells. Remarkably, Long et al. (2005) demonstrated that impaired coupling at the SCN produced a less coherent behavioral output with reduced precision.

Rat shows arrhythmic or ultradian behavioral patterns in prolonged exposure to constant light (LL) (Eastman and Rechtschaffen, 1983; Depres-Brummer et al., 1995). Furthermore, it was suggested that light could prompt such behavioral reorganization by inhibiting internal coupling at pacemaker (Vilaplana et al., 1997). Importantly, recent data has shown that LL generated desynchronization of SCN cultured neurons dissected from behaviorally arrhythmic mice (Ohta et al., 2005). Also, some evidence indicated that entrainment of the SCN pacemaker to LD cycles (Quintero et al., 2003) or to light pulses (Kuhlman et al., 2003) involved changes effecting SCN internal coupling, and that light intensity may participate in such changes.

In our own laboratory, we employed a computational model to simulate the functioning of the circadian system (Díez-Noguera, 1994). Built on possible physiological correlates, it can be used as an inductive tool, potentially identifying unknown elements of the system (Helfrich-Förster and Díez-Noguera, 1993). The model's two main assumptions are: 1) that a multioscillatory structure is at work; and 2) that its functioning, and thus its output pattern, depends on the coupling strength between oscillators. The purpose of the present experiment is to determine whether changes in entrainment of activity rhythm elicited by modifying illuminance contrast of the LD cycle, can be explained by coupling changes in our model simulations. Moreover, we tested the effect of prior lighting conditions on entrainment to the same LD cycle in order to study a possible plasticity in the response of the system. A comparison of the results obtained with behavioral and simulation experiments would allow further insight into the mechanisms underlying the circadian system.

MATERIALS AND METHODS

Animals and housing

Twenty male golden hamsters (*Mesocricetus auratus*) arrived at the laboratory directly from the provider (Harlan France SARL). These two month-old animals were housed individually in transparent metacrylate cages measuring 22x22x15 cm (Panlab, Spain) and covered with a stainless steel grid, with wood shaving bedding. Cages were maintained in a sound-proof, temperature-controlled chamber (18-22 ºC, humidity 40-

80 %) with time-adjustable illumination cycles. Throughout the entire experiment, the animals received food (Harlan Teklad 2040 global diets®) and tap water *ad libitum*. Cage cleaning, along with food and water replenishment, was done once a week at irregular time intervals, taking care to avoid performing maintenance tasks on the days close to stage transitions.

Procedures

Once they had arrived at our laboratory, the animals were submitted to light-dark cycles with a 22-h period (T22). T cycles initially comprised an 11-h photophase of 300 lux, and an 11-h scotophase of 0.1-lux dim red light ($LD_{300 / \text{dim red}}$, LD_1, stage duration: 19 cycles). From the initial group of 20 animals, 8 clearly exhibiting a relative coordination pattern throughout this stage were selected for the present experiment (see the process of selection in "Results" section). Subsequently, T22 cycles that differed in their illuminance contrast were used to verify two predictions generated by model simulations (see "Simulations" below). Hence, a second stage of T22 cycles with a 300 lux photophase, and a 0.1-lux dim illuminance at scotophase was imposed ($LD_{300 / 0.1}$, stage duration: 77 cycles). As rhythms became unstable, this stage was prolonged for more than a month, and then for an additional month to achieve stable entrainment. Then a next stage of T22 cycles reducing illuminance to 10 lux at the photophase, and maintaining the same previous 0.1-lux dim light at scotophase was imposed ($LD_{10 / 0.1}$, stage duration: 27 cycles). $LD_{300 / \text{dim red}}$ condition was reinstated to test the different entrainability of rhythm (LD_2, stage duration: 31 cycles). Afterwards, the animals were transferred to constant darkness, maintaining lights-off from the last scotophase (DD, stage duration: 25 cycles). Finally, $LD_{300 / \text{dim red}}$ cycles were reinstated to thereby compare the resulting rhythm with previous LD_1 and LD_2 (LD_3, stage duration: 55 cycles). A scheme in Figure 1 outlines the entire experimental paradigm, and light sources had the following characteristics:

- for $LD_{300 / \text{dim red}}$: two 36 W Mazdafluor fluorescent tubes that yielded ~ 300 lux of indirect lighting at photophase. The spectral composition featured two major irradiance peaks at 440 and 540 nm wavelength, as well as a bandwidth measuring between 550-600 nm. Lighting at scotophase was delivered by indirect dim red light ~ 0.1 lux, with a major band from 650 nm extending to the infrared region.

- for $LD_{300/0.1}$: lighting at photophase was the same as for $LD_{300/\text{dim red}}$, and scotophase consisted of illuminance level supplied by light emitting diodes (LEDs) producing ~ 0.1 lux of indirect dim light. LEDs provided a major irradiance bandwidth of 450-470 nm, as well as a secondary one measuring 530-620 nm.

- for $LD_{10/0.1}$: lighting at photophase was delivered by two 18 W Philips fluorescent tubes laterally covered by opaque wooden badges, producing ~ 10 lux of reflected light with a spectra similar to 300 lux lighting. Scotophase used the same LEDs as $LD_{300/0.1}$.

Illuminance and irradiance were measured at cage level with a Gossen Metrawatt Camille Bauer, Mavolux 5032B digital luxmeter, GMC-Instruments Schweiz SA, Zurich, Switzerland, and with a Handheld FieldSpec® spectroradiometer, Analytical Spectral Devices, Inc., Boulder, USA, respectively.

Data collection - Time-series analysis

Animal motor activity was measured by means of an activity-meter consisting of two perpendicular infrared light beams crossing the cage at a height of 7 cm above the floor, coupled to a suitable electronic device. Each beam interruption due to animal movement represented an activity count that was recorded and compiled at 15-min intervals. Individual data samples were acquired in parallel channels and stored in a computer for further analysis. Lighting cycles were recorded simultaneously with activity in a separate channel connected to a photocell pulse generator.

Time-series analysis was carried out separately for data series corresponding to each stage. Time-series were smoothed by 30-min step moving average, to enhance circadian tendency viewing, and data segments of 19 cycles (LD_1 stage length) were averaged to obtain the mean daily activity profile at each stage at T22. $LD_{300/0.1}$ profiles comprised three consecutive segments of 19 cycles, the first beginning at the 20th cycle of the stage when the rhythm phase appeared generally stabilized on the actograms. For the remaining stages, data from the first 19 cycles of each one were used. χ_2 periodograms (Sokolove and Bushell, 1978) were calculated by taking raw data corresponding to each of the previously defined 19-cycle segments, together with all of the data at LD_1 and the first 19 cycles at DD. The highest significant peak ($p<0.05$), scanned within a range from 20 to 26 h, was considered for period estimation, hence

obtaining the percentage of variance explained by the dominant rhythm. When a non-significant peak occurred on the periodogram, we still used the value of percentage of variance explained by the expected periodicity at 22 h, as it was previously described (Cambras et al., 2004).

The rhythm phase control exerted by the previous LD cycle was examined at DD stage. First, an eye-fitted line was drawn on the actograms by taking the tendency of the rhythm's onset during the first 10 days in DD. This line was projected backwards to the last day of the LD_2 stage. Then the projected activity onsets of the individuals were studied with the Rayleigh z-test (Batschelet, 1981), which calculates the temporal distribution of individual phases across the T cycle. Hence, a sidedness distribution suggests that, due to entrainment, the rhythm free-runs from the phase held by the zeitgeber when it was present.

Graph and calculations were made using the integrated package for analysis in chronobiology, "El Temps" (©Antoni Díez-Noguera, University of Barcelona, Spain, 1998-2005, http://www.ub.es/dpfisiv/soft/ElTemps/).

Computer simulations

Model description

The model we used for simulations assumes that, functionally, the pacemaker consists of a population of coupled limit-cycle oscillators with a distribution of angular velocities (Díez-Noguera, 1994). Each individual oscillator is mathematically described by two differential equations for two state variables. In the model, the state variables of a single oscillator are continuously modified by the effect of the state variables of the other oscillators. These interactions act in such a way that oscillators tend to approach to the average value of the whole system, and linearly depend on a global coupling factor. In such a model, coupling changes generate phase-shifts of the rhythmic output of the system.

Simulations were done just by varying coupling strength, which was cyclically imposed as a square wave, by alternating a part of high coupling values (Hc) with another of lower ones (Lc), emulating an LD cycle with abrupt transitions. To verify

model predictions in the experiment, scotophase of the LD cycle was assumed to be analogous to Hc in model simulations, whereas photophase corresponded to Lc.

Although different pairs of equations that fulfil the formal requirements needed for the model may be used, for this study we used Selkov (Selkov, 1968) equations. This oscillator had produced good simulations in previous experiments (Díez-Noguera, 1994; Díez-Noguera et al., 2003). Importantly, the Selkov model provides a PRC to coupling interactions that has a shape similar to the photic PRC of rodents, and is adequate for present simulation aims. In previous studies conducted in our laboratory (Díez-Noguera et al., 2003) we demonstrated that the PRC amplitude is not greatly affected by the number of oscillators (between 2 and 64). Although a more realistic model should include the ~ 10.000 neurons that make up the SCN tissue, a small percentage of these cells may participate through coupling interactions in the rhythmic output of the pacemaker (Long et al., 2004; Aton et al., 2005). Also, as in other assayed models of the circadian system (Oda et al., 2000), the single mathematical oscillator may represent a subset of pacemaker cells. Thus for this study we used 32 oscillators, enough to ensure a high number of stable and short-termed simulations.

Simulations

A- First of all, we carried out a set of simulations conducted to gauge a range of coupling strength values for both Hc and Lc parts. To do so, the coupling cycle was composed of 88 calculation steps (44 Hc/44 Lc) in such a way that it paralleled a 22 h cycle with intervals of 15 min defined for motor activity data collection (15 min x 88=1320 min = 22 h). 100 cycles were defined for all simulation lengths. The mean velocity of the system was fine-tuned to obtain a stable free-running period near 24 h, when Hc=Lc. Subsequently, the Hc/Lc ratio was varied in a systematic study encompassing a wide range of values. Thus, a parametric region where output patterns changed from stable entrainment to relative coordination was selected (Hc range=0.5 – 0.6; Lc range=0.1 – 0.2). Then both Hc and Lc were varied on a logarithmic scale to improve graphic representation.

B- The second set of simulations was carried out to model the transitions between the first two stages of the paradigm used for animal experiments. LD_1 and $LD_{300 / 0.1}$ were simulated by dividing 100 coupling cycles into two parts: In the first part Hc and

Lc were defined according to A, in such a way that relative coordination would appear; and in the second part the value of Lc was fixed, but that of Hc was reduced in a linear manner, to simulate the light increase during the scotophase.

RESULTS

Animal experiments

In the first T22 stage (LD_1) when $LD_{300 / \text{dim red}}$ cycles were imposed, the initial group of 20 hamsters showed different activity patterns. Since one of the purposes of the experiment was to verify model simulations (see "Simulations" below), by exposing the animals to T22 cycles that differed in their illuminance contrast, we selected a group with a homogeneous activity pattern. Since relative coordination was the most common pattern of overt rhythm at LD_1 stage (n=11), we selected 8 of them for the experiment (8 hamsters was the optimal number allowed by animal facilities at that time). The rest of the animals were used for other experiments. Relative coordination was established by the observation of the actograms on the basis of the following criteria (Aschoff, 1981): a) a free-running rhythm whose phase changes periodically with the zeitgeber; b) the rhythm has a different period depending on whether it coincides with light or with darkness; and c) there is an α phase modulation, with a compression during light and decompression during darkness.

An actogram in a 22-h double-plotted format with data on a representative hamster throughout the entire experimental period is shown in Fig. 1. The 22-h activity profile obtained by averaging data of the 8 individuals is also displayed. During LD_1, the relative coordination pattern of the selected animals featured a period value between the endogenous τ and external T (mean ± SD: 23.5 ± 0.06 h). The subsequent exposure of hamsters to cycles with 0.1-lux dim light at the scotophase during the $LD_{300 / 0.1}$ stage gradually promoted the period adjustment of the rhythm to T22. However, different rhythmic patterns were observed during the initial days of this stage (Fig. 2). Two animals still tended to free-running, and this continued for several days (panels B and C). In two other hamsters, a great phase jump was observed during the first day under $LD_{300 / 0.1}$, which was indistinguishable in terms of advance or delay (panels D and E).

In the remaining four animals, the α phase was rapidly confined to the scotophase (panels A, F, G and H), but presented some onset fluctuations. Generally, after major phase stabilization occurred, activity rhythm synchronized to T22 acquiring a stable phase relationship during the following days (8 of 8 animals with significant 22-h rhythm in both the first and middle 19-cycle segments). Afterwards, the α duration gradually increased, with the rhythm displaying a dampened amplitude towards the last part of the stage (5 of 8 animals with significant 22-h rhythm in the last 19 cycles). These changes can be observed at mean daily activity profile obtained after major period stabilization at T22 (Fig. 1). During the first and intermediate days at $LD_{300 / 0.1}$, it can be seen that a clear bimodal pattern remained confined to scotophase. After that the rhythm amplitude appeared dampened and the α phase tended to be enlarged during the last days, with certain loss of bimodality.

When the animals were transferred to the $LD_{10 / 0.1}$ stage, by changing photophase illuminance from 300-lux to 10 lux, an unstable pattern was still observed in most hamsters (4 of 8 animals with significant rhythm). Also, the mean pattern of the 22-h profile revealed a very low amplitude of rhythm with an almost indiscernible   phase (Fig. 1). During further re-exposure to $LD_{300 / dim\ red}$ cycles for a month (LD_2 stage), the activity rhythm did not recover, and a flattened low amplitude rhythm remained (5 of 8 animals with significant rhythm). In spite of this unstable pattern, the control of the rhythm phase by the zeitgeber was verified by significant clustering of the activity onsets (Rayleigh z-test: $r = 0.98$, $p < 0.01$).

During continuous exposure for nearly a month to constant darkness (DD stage), χ_2 periodogram detected 5 of 8 animals with significant free-running rhythms (mean $\pm$ SD, $\tau = 23.4 \pm 0.1$). After DD, reinstating of LD cycles (LD_3 stage) was accompanied by a stable circadian rhythm synchronized to T22 (8 of 8 animals with significant rhythms). A clear 22-h rhythm can be observed in the daily activity profile including a major onset peak (Fig. 1).

In addition, the percentage of variance explained by the rhythm quantifies the entrainability of the activity pattern to the different T22 and DD stages (Fig. 3). Starting from stable circadian rhythmicity with high values at baseline at LD_1, a decrease elicited by $LD_{300 / 0.1}$ cycles was sustained throughout this stage, maintaining minimal values at $LD_{10 / 0.1}$, LD_2, and DD. An increase of the percentage of variance was

registered when reinstating the $LD_{300 / dim\ red}$ condition during the last LD_3 stage, after exposure to DD.

Thus, three different patterns appeared under the same LD illuminance (LD_1, LD_2 and LD_3), though with different prior conditions: 1) direct transfer of naive animals to T22 (LD_1 stage) produced a large homogeneous group showing relative coordination; 2) a rhythm with a dampened amplitude and unstable daily pattern revealed by a low percentage of variance was obtained during LD_2; and 3) a stable rhythm with a great percentage of variance, synchronized better to T22 during LD_3 following previous exposure to DD.

Model simulations

Model simulations were conducted to predict the response of the hamster circadian system, observed under different illuminance contrasts of T22 cycles. The functioning of the system for different degrees of coupling strength for both Hc and Lc parts is shown in Fig. 4A. One can see that the system output changes from free-running, relative coordination or entrainment depending on the ratio between Hc and Lc. Moreover, a reduction in the coupling strength in both Hc and Lc parts drives the system period toward entrainment. Thus, from these simulations two predictions can be obtained: 1) a reduction in the coupling strength during Hc part (analogous to the LD_1 - $LD_{300\ /\ 0.1}$ change) tends toward entrainment; and 2) an increment in the coupling strength during Lc part (analogous to the $LD_{300\ /\ 0.1}$ - $LD_{10\ /\ 0.1}$ change in the animal experiment) tends toward relative coordination.

Figure 4B displays the simulations that successfully predict the experimental results obtained after transfer from LD_1 to $LD_{300 / 0.1}$. An initial part with a fixed Hc/Lc ratio (selected from Fig. 4A) corresponds to LD_1 and is followed by another part with varying values for Hc, which corresponds to $LD_{300\ /\ 0.1}$. A linear augmentation of the coupling strength in the Hc part is shown in each of the 10 successive actograms displayed in the two rows. One can see that depending on the value of Hc in the second part of the simulation, intermediate transitions between relative coordination and entrainment are obtained. Some of these patterns resemble those of the animals during the initial part of the $LD_{300 / 0.1}$ stage (see Fig. 2).

The second model prediction failed since instead of detecting relative coordination, as the model predicts for an increment of Lc values, the activity pattern of

animals in the transfer from $LD_{300/0.1}$ - $LD_{10/0.1}$ tended to a decrease in the rhythm manifestation.

DISCUSSION

This experiment provides evidence about two points: 1) that changes in the motor activity rhythm due to light intensity may be parallel to those produced in the output of a multioscillatory system, by changes of coupling among the oscillators; and more important, 2) that the overt rhythm can be very changeable depending on the previous lighting conditions.

The starting point of our work was the selection of hamsters for this experiment. The simulations with the computer system revealed transitions between stable entrainment, relative coordination, and free-running, induced by very small changes in internal coupling. These changes only affect the ratio between Hc and Lc, which can be defined as the degree of coupling of the whole circadian system. When hamsters were exposed to initial T22 cycles, several patterns were also observed, although the most common was relative coordination. According to the model, these patterns could be interpreted to mean that each hamster may also have a different coupling degree in its circadian system (compare Fig. 2A vs. 5B). At present it is not known what coupling is, but it is probably a multifactorial outcome (see Miche and Colwell, 2001 for review). In any case, any of these factors can accept different degrees, which could explain the individual differences under a single lighting condition. This suggests the importance of studying coupling from both experimental and simulation points of view. With this idea, we selected 8 hamsters with a similar activity pattern for the experiments, assuming that they corresponded to the same internal coupling degree as the model, and thus a more homogeneous response was to be expected when light conditions were changed. Actually, the general response to light was similar for the selected hamsters under all the lighting conditions.

The model simulations indicate that, from a specific coupling degree of the system that produces relative coordination in its output, a decrease of the coupling degree in the scotophase induces entrainment. This is corroborated *in vivo*, since hamsters submitted to T22 cycles (LD_1 stage) changed from an initial relative

coordination to entrainment when dim nocturnal illumination was applied ($LD_{300 / 0.1}$ stage). We cannot definitively confirm that entrainment occurs during $LD_{300 / 0.1}$, since both the adoption of a unique and stable phase relationship, as well as the free-running of rhythm under constant conditions from the phase predicted by the zeitgeber, must be demonstrated (Daan and Aschoff, 2001). We do believe, however, that active changes in pacemaker activity certainly did occur at this stage. Activity onset gradually advanced, chiefly during the initial part of the $LD_{300 / 0.1}$ stage with a consequent α expansion, which implies active modifications in the circadian system (i.e. Fig. 1, 2). Evidence from various experiments employing dim nocturnal light that induced splitting (Gorman et al., 2003), short photoperiod re-entrainment (Gorman and Elliott, 2004), and entrainment to lengthening T-cycles (Gorman et al., 2005), suggests that scotopic light may alter the phase relationship between oscillators. Since we do not have more conclusive data, we are still puzzled as to why entrainment occurred with such an illuminance change. A possible explanation for the observed change from relative coordination to entrainment could also be arrived at by considering the efficiency of light related to its action spectra. Although a 2-h pulse of red light can modify the phase of the free-running rhythm in rats (McCormack and Sontag, 1980), scotopic light used in the present work featured an adequate spectral composition for irradiance detection in the circadian system (Berson et al., 2002; Foster, 2005). Considering Aschoff's rules (Aschoff, 1981), increasing light intensity produces τ lengthening; thus, entrainment to a 22 h T-cycle should be prevented. However, this is not the case in our hamsters, but fits with other experiments involving rats in which we found that entrainment to T22 cycles improved when the photoperiod was augmented (Cambras et al., 2004).

Model simulations predicted a change from relative coordination to entrainment, if light intensity increased at scotophase. This was based on the central assumption that the coupling strength would diminish proportionally with light intensity. Light has been proposed to act on the circadian system by inhibiting the pacemaker coupling in several rodent species (Vilaplana et al., 1997; Honma and Honma, 1999; Ohta et al., 2005). It is known that prolonged constant light (LL) disrupts behavioral rhythms by disrupting the cellular synchronization within the SCN pacemaker, without stopping the core molecular clocks of individual cells (Ohta et al., 2005). Arrhythmicity induced by LL in hamsters was also explained as the uncoupling of multiple oscillators (Pittendrigh, 1981b). However, the LL effects appeared to be more complex than arrhythmicity

alone. Indeed, some animals show splitting of activity rhythms into two components that remained coupled with a stable phase relationship of 180º or an unstable one (Pittendrigh and Daan, 1976b; Pittendrigh, 1981b). Moreover, based on the E and M composed pacemaker, simulations with a dual oscillator model explain experimental data in the hamster with the assumption that prolonged exposure to constant darkness gradually reduces the coupling strength (Oda et al., 2000). Models for circadian pacemakers have to contribute to understanding their mechanism and/or function (i.e. Oda et al., 2000), as well as predict the outcome of new experiments. In this sense, there are no "correct" models to represent the reality of the circadian pacemaker, but there are some that can be useful for achieving these aims (Beersma, 2005). Our model seems useful for predicting changes in the activity pattern by assuming that coupling strength diminishes with light intensity, when the daily action of light may affect the coupling mechanisms.

The model also predicted that if there were entrainment, then incremental changes in the coupling strength during the Lc part would drive the system from entrainment to relative coordination. To verify this, our experiment involved a further reduction in illuminance intensity from 300 to 10 lux during the photophase. Contrary to this prediction, not only was relative coordination not recorded as expected from simulations, but a very low amplitude circadian rhythm was generated. Although we cannot explain these changes with the data available in the present work, the possible saturation of the entrainment pathways (Nelson and Takahashi, 1999) could be considered in terms of the incremental instability of rhythm throughout $LD_{300 / 0.1}$. Thus, despite the fact that 10 lux illuminance is above the response threshold for SCN electrical activity (Meijer et al., 1986), a virtual "constant light" setting during the $LD_{10 / 0.1}$ stage rapidly drove the system towards instability. $LD_{10 / 0.1}$ conditions may also provide weak photic input to visual detection systems, which may merge with the circadian system at the receptor level (Berson et al., 2002; Hattar et al., 2003) disrupting the output pathways due to possible ambiguities in the light information between the photophase and scotophase. In addition, overt rhythm manifestation is due to the functioning of the circadian system together with other structures mediating possible masking processes (Mrosovsky, 1999) that could be modulated by lower light contrast, hence producing a lower amplitude rhythm. However we must take into account that under the previous stage, $LD_{300 / 0.1}$, the system was continually changing, as observed in

the evolution of the rhythm profile in this stage. Thus, one can suppose that under $LD_{10/0.1}$ the contrast between the two light phases is not strong enough to stabilize the rhythm, and hence it maintains with the same dynamics as in the previous stage.

While our model successfully simulates functional features of the circadian pacemaker (i.e. entrainment, PRC, dependence of period on light intensity, splitting) by controlling the coupling strength between oscillatory elements (Helfrich-Förster and Díez-Noguera, 1993; Díez-Noguera, 1994; Díez-Noguera et al., 2003), it is unable to generate dynamic changes. Since the functional state of a given oscillator is directly modified by those of the rest, and no mnesic imprints are acquired, none of the effects from the previous history are exerted. Therefore, the model should be more effective in predicting rhythm changes over the short-term, as occurs from LD_1 to $LD_{300/0.1}$. This suggests that models cannot be thought of as systems that produce a specific response (circadian pattern) for a specific stimulus (a particular LD cycle), since the internal structure of the system can change throughout the time. This was even more evident when we observed that the rhythm was strongly dependent on the activity rhythm pattern under previous conditions. Thus, a "memory component" of the system can be hypothesized, in which the pacemaker's response is a contextual interaction between its previous history and present conditions.

The system's progress throughout the different stages of the experiment was primarily influenced by previous experience, producing a hysteresis in the circadian system response (Hoffman, 1971). Notably, we found important differences in rhythm manifestation among three identical LD conditions that had been preceded by different illuminance environments (see Fig. 1 for LD_1, LD_2 and LD_3). First, relative coordination during LD_1 was found in naive animals moved directly to a 22 h T cycle. Second, after the $LD_{300/0.1}$ - $LD_{10/0.1}$ stage sequence, a condition that generated instability of rhythm, it could not be re-established under LD_2. And finally, a stable rhythmic pattern during LD_3 occurred following DD that synchronized better to the T cycle. Similar effects under prior constant darkness were observed in the Siberian hamster, facilitating re-entrainment to a phase-delayed LD cycle (Ruby et al., 2002). Therefore, if the circadian system properties are also modified, such plasticity may involve history-dependent changes in the coupling strength between pacemaker oscillators, as may happen during classical aftereffects.

Although on the basis of observed longitudinal changes our experimental protocol revealed novel history-dependent changes on entrainment of activity rhythm, the possible effects of aging should be taken into account. Age-related changes in circadian system properties are not yet well established, since evidence both for (Pittendrigh and Daan, 1974; Morin, 1988) and against (Davis and Viswanathan, 1998) τ changes has been published, and the same has occurred with regard to entrainment (Morin, 1988 *vs.* Aton et al., 2004). In any case, ageing is associated with an overall increase in the lability of circadian phase and a reduction in amplitude of endocrine, metabolic and behavioral rhythms in various animal species (see Turek et al., 1995 for review). Specifically for the Syrian hamster, it was shown that animals 12.25 months old submitted to LD 14:10, exhibited a more greatly reduced amplitude than 5.5 month old ones (Labyak et al., 1998). When comparing present changes in amplitude, our hamsters were ~ 6 months old at the beginning of LD_2, whereas ~ 8-month old animals at LD_3, exhibited changes in amplitude opposite to those associated with ageing. Also, old hamsters re-entrain better to phase-advanced LD 14:10 cycles (Zee et al., 1992). This was attributed to the shortening of activity rhythm τ with age. Although this could account for the better entrainment observed in LD_3 when compared with LD_2, hamsters show no important differences in age between these two stages. Thus, we assume that the effect of ageing did not account for the observed differences reported here. Also the reproductive state, which we did not test, could have changed due to illuminance modifications (Ferraro and McCormack, 1985), and affected the entrainment pattern. Because effects of entrainment history must be evidenced by the animal experience itself, the definition of present sequential design excludes the use of a control group. However, additional experiments with the same light-dark schedules in a different sequence could definitely demonstrate whether such observed longitudinal changes in entrainment depend solely on previous history, or other factors are involved.

In summary, two main conclusions can be drawn from the present study: 1) the assumption of both a coupled multioscillatory system, and that light may act by inhibiting coupling, explains entrainment under a T22 cycle; and 2) importantly, the actual state of the circadian system is established by its prior light (entrainment) history, perhaps by a memory component. Although the principle of coupling was conceived nearly four decades ago (Winfree, 1967), its physiological correlates remain elusive. Meanwhile, the present work offers a novel combination of two experimental strategies

that allow us to observe intriguing changes in the output of the circadian multioscillator system, employing animal experiments in tandem with computational model simulations. They have permitted us to conclude that changes in hamster activity patterns, including entrainment to T22 cycles, are partially related to modulations exerted by light intensity on the coupling strength between oscillators. Unfortunately there is still a lack of physiological evidence for coupling in the circadian pacemaker, and plasticity is lacking in most of the computational models of the pacemaker.
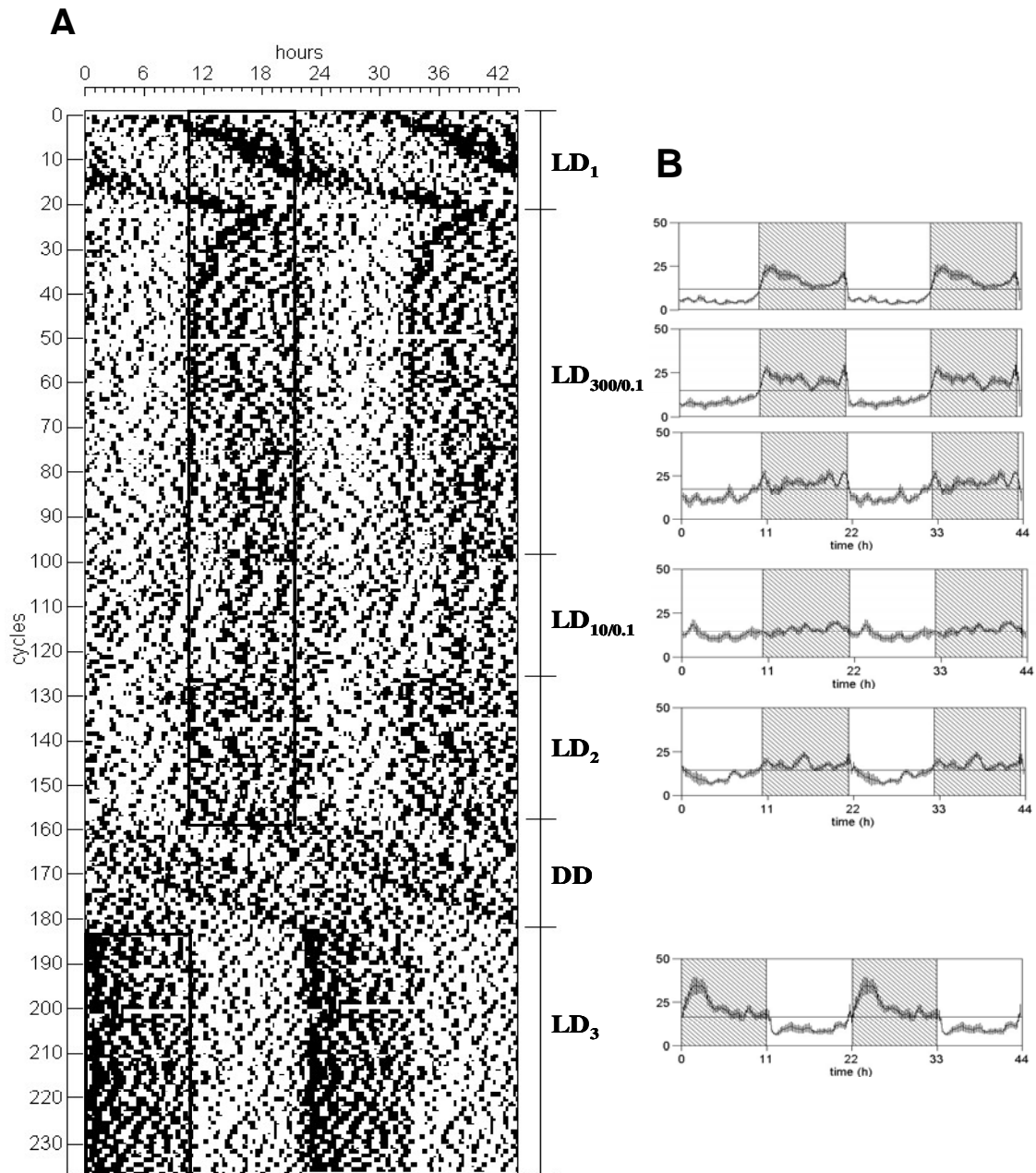
ACKNOWLEDGMENTS

Figure 1. A- Double-plotted actogram of a 22 h module for a representative hamster's motor activity. Single-plotted black rectangle represents scotophase timing of the T22 cycle. Subdivisions of the bar on the right indicate the corresponding stages with the various lighting regimes utilized (see text). B- Panels on the righ are the mean rhythm profiles double-plotted at T22, obtained from the 8 individuals at the corresponding stages indicated on the actogram. Data at the $LD_{300/0.1}$ stage was subdivided into three consecutive segments, the first beginning at the 40th cycle, when stable T22 rhythm
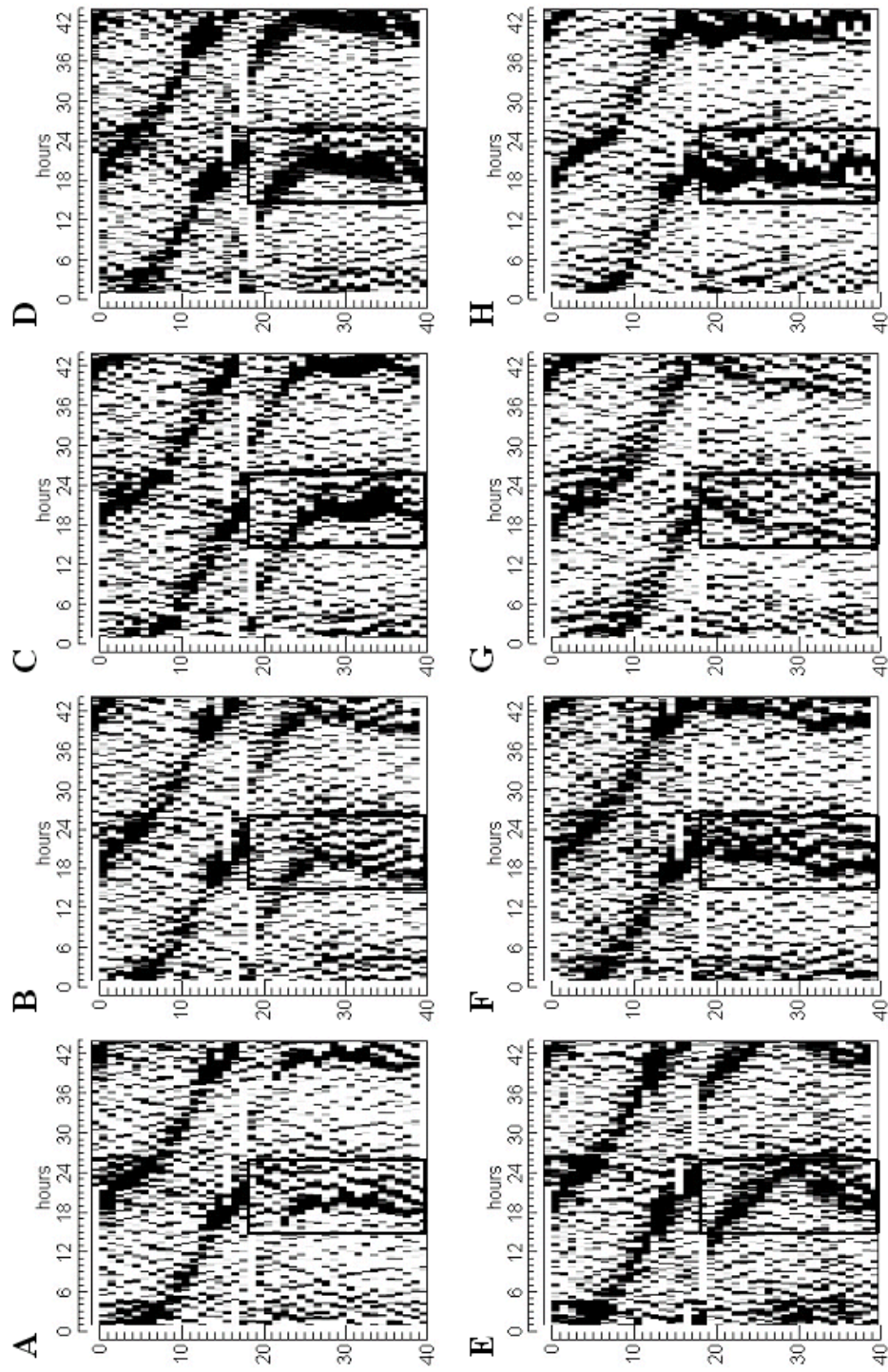
Figure 2. Double-plotted actograms in a 22 h module for each individual during LD_1 and the following 20 cycles in $LD_{300 / 0.1}$. The black rectangle within each panel indicates the $LD_{300 / 0.1}$ scotophase. Differences between individual responses during the initial cycles in $LD_{300 / 0.1}$ are shown (see text).
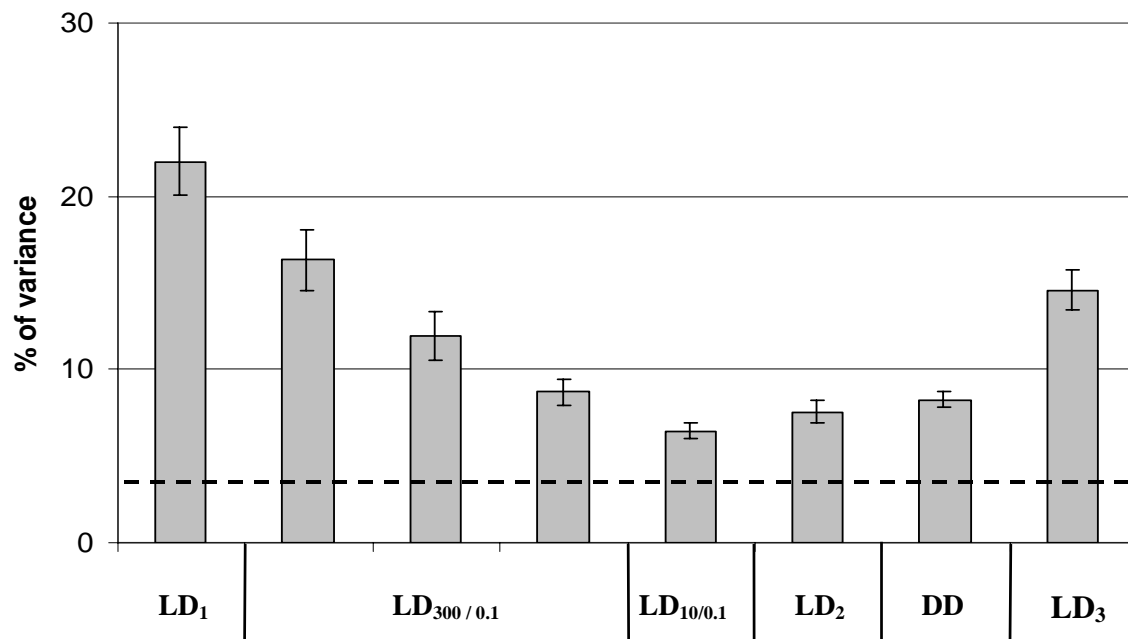
Figure 3. Mean and standard deviation of the percentage of variance calculated using the χ_2 periodogram on equal 19-cycle raw data segments corresponding to the stages of the experiment. Values were obtained from relative coordination patterns at LD_1, from free-running periodicities at DD, and from the 22 h rhythm for the rest of the stages. Data corresponding to the $LD_{300/0.1}$ stage were subdivided into three sequential segments. The dotted line indicates the percentage of variance value for the defined significance level, p=0.05.
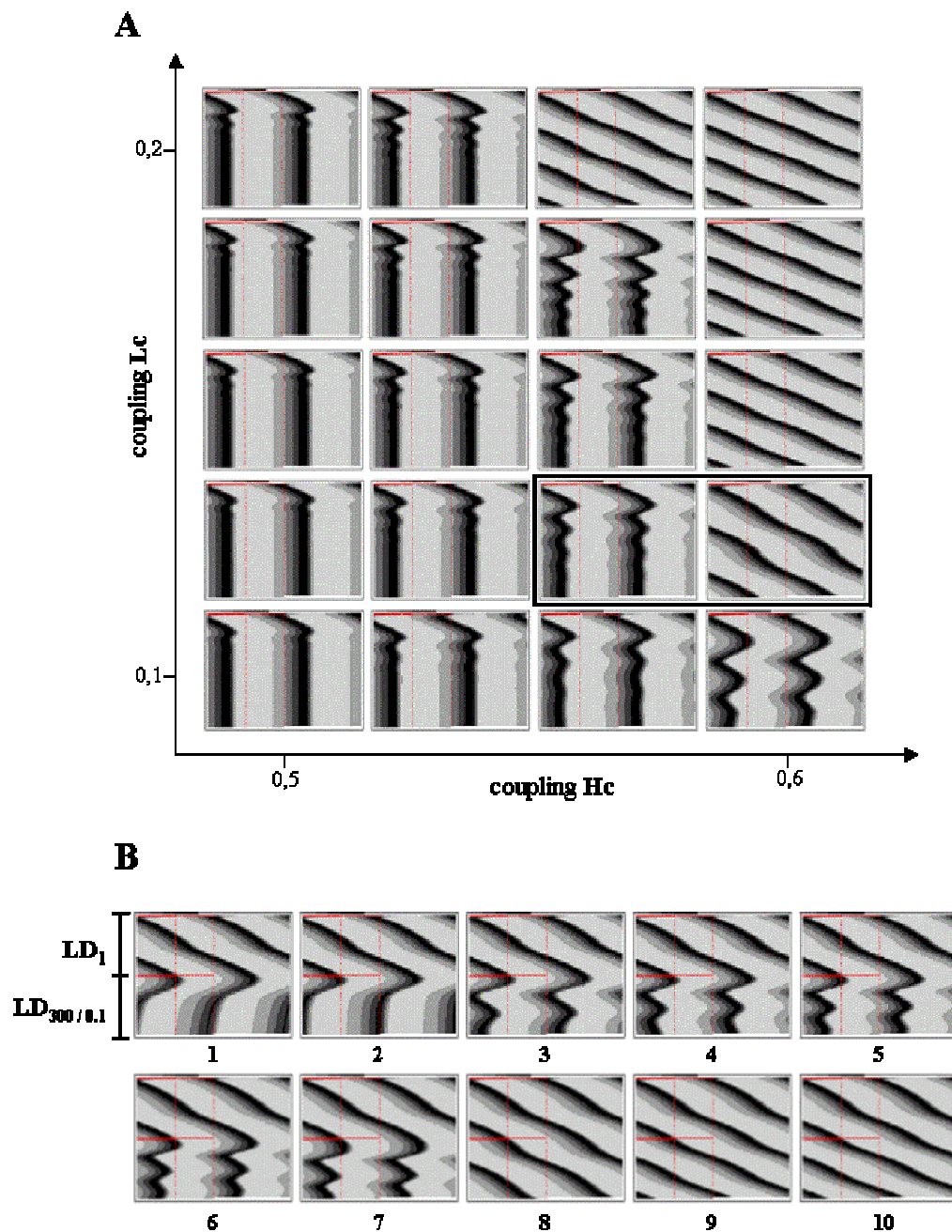
Figure 4. A- Matrix of double-plotted actograms for model's periodic outputs from 100-cycle simulation for a different Hc/Lc ratio. The black rectangle indicates the selected transition from relative coordination to entrainment, for simulations detailed in B. B- Model prediction for the experimental outcome. Selected values from the Hc/Lc ratio in A were fixed during the first 50 cycles in the simulation (LD_1). In the second 50 cycles ($LD_{300 / 0.1}$) Hc was variable by linear increments of 0.05, that correspond to double-plotted actograms numbered from 1 to 10 (Hc range=0.25 – 0.7). Hc in the model simulation was assumed to be analogous to the scotophase in the animal experiment, whereas Lc represented the photophase of a LD cycle.

REFERENCES

Achermann P, Kunz H (1999) Modeling circadian rhythm generation in the suprachiasmatic nucleus with locally coupled self-sustained oscillators: phase shifts and phase response curves. J Biol Rhythms 14(6):460-8.

Aschoff J (1981) Freerunning and entrained circadian rhythms. In: *Handbook of behavioural neurobiology: Biological rhythms*, J Aschoff, ed, pp 81-93, Plenum Press, New York.

Aton SJ, Block GD, Tei H, Yamazaki S, Herzog ED (2004) Plasticity of circadian behavior and the suprachiamatic nucleus following exposure to non-24-hour light cycles. J Biol Rhythms 19(3)198-207.

Aton SJ, Colwell CS, Harmar AJ, Waschek J, Herzog ED (2005) Vasoactive intestinal polypeptide mediates circadian rhythmicity and synchrony in mammalian clock neurons. Nat Neurosci 8(4):476-83.

Batschelet E (1981) Circular Statistics in Biology. London: Academic Press.

Beersma DG (2005) Why and how do we model circadian rhythms? J Biol Rhythms 20(4):304-13.

Berson DM, Dunn FA, Takao M (2002) Phototransduction by retinal ganglion cells that set the circadian clock. Science 295(5557):1070-3.

Cambras T, Chiesa J, Araujo J, Díez-Noguera A (2004) Effects of photoperiod on rat motor activity rhythm at the lower limit of entrainment. J Biol Rhythms (3):216-25.

Daan S, Aschoff J (2001) The entrainment of circadian systems. In: *Handbook of behavioural neurobiology: Circadian clocks*, JS Takahashi, FW Turek, RY Moore, eds, pp 7-43, Kluwer/Plenum, New York.

Davis FC, Viswanathan N (1998) Stability of circadian timing with age in Syrian hamsters. Am J Physiol Regul Integr Comp Physiol 275(4 Pt 2):R960-8.

Depres-Brummer P, Levi F, Metzger G, Touitou Y (1995) Light-induced suppression of the rat circadian system. Am J Physiol Regul Integr Comp Physiol 268:R1111-6.

Díez-Noguera A (1994) A functional model of the circadian system based on the degree of intercommunication in a complex system. Am J Physiol Regul Integr Comp Physiol 267:R1118-R1135.

Díez-Noguera A, Cambras T, Acosta O (2003) Properties of circadian system: are they just common properties of multioscillatory systems? VII Latin-American Symposium on Chronobiology, Tlaxcala, México.

Eastman C, Rechtschaffen A (1983) Circadian temperature and wake rhythms of rats exposed to prolonged continuous illumination. Physiol Behav 31(4):417-27.

Elliott JA, Tamarkin L (1994) Complex circadian regulation of pineal melatonin and wheel-running in Syrian hamsters. J Comp Physiol 174(4):469-84.

Ferraro JS, McCormack CE (1985) Gonadal regression despite light pulses coincident with locomotor activity in the Syrian hamster. Biol Reprod 33(1):93-102.

Foster, RG (2005) Neurobiology: bright blue times. Nature 433(7027):698-9.

Gorman MR, Elliott JA (2004) Dim nocturnal illumination alters coupling of circadian pacemakers in Siberian hamsters, Phodopus sungorus. J Comp Physiol A Neuroethol Sens Neural Behav Physiol 190(8):631-9.

Gorman MR, Elliott JA, Evans JA (2003) Plasticity of hamster circadian entrainment patterns depends on light intensity. Chronobiol Int 20(2):233-48.

Gorman MR, Freeman DA, Zucker I (1997) Photoperiodism in hamsters: abrupt versus gradual changes in day length differentially entrain morning and evening circadian oscillators. J Biol Rhythms 12(2):122-35.

Gorman MR, Kendall M, Elliott JA (2005) Scotopic illumination enhances entrainment of circadian rhythms to lengthening light:dark cycles. J Biol Rhythms 20(1):38-48.

Hattar S, Lucas RJ, Mrosovsky N, Thompson S, Douglas RH, Hankins MW, Lem J, Biel M, Hofmann F, Foster RG, Yau KW (2003) Melanopsin and rod-cone photoreceptive systems account for all major accessory visual functions in mice. Nature 424(6944):76-81.

Helfrich-Förster C, Díez-Noguera A (1993) Use of a multioscillatory system to simulate experimental results obtained for the *period-mutants* of *Drosophila melanogaster*. Proceedings of the 9th meeting ESC. J Interdiscipl Cycle Res 24(4):225-231.

Herzog ED, Takahashi JS, Block GD (1998) Clock controls circadian period in isolated suprachiasmatic nucleus neurons. Nat Neurosci 1(8):708-13.

Hoffmann K (1971) Splitting of the circadian rhythm as a function of light intensity. In: *Biochronometry*, M Menaker, ed, pp 134-150, Nat Acad Sci, Washington DC.

Honma S, Honma K (1999) Light-induced uncoupling of multioscillatory circadian system in a diurnal rodent, Asian chipmunk. Am J Physiol Regul Integr Comp Physiol 276:R1390-6.

Honma S, Nakamura W, Shirakawa T, Honma K (2004) Diversity in the circadian periods of single neurons of the rat suprachiasmatic nucleus depends on nuclear structure and intrinsic period. Neurosci Lett 358(3):173-6.

Honma S, Shirakawa T, Nakamura W, Honma K (2000) Synaptic communication of cellular oscillations in the rat suprachiasmatic neurons. Neurosci Lett 294(2):113-6.

Jagota A, de la Iglesia HO, Schwartz WJ (2000) Morning and evening circadian oscillations in the suprachiasmatic nucleus in vitro. Nat Neurosci 3(4):372-6.

Kuhlman S, Silver R, Le Sauter J, Bult-Ito A, McMahon D (2003) Phase resetting light pulses induce Per1 and persistent spike activity in a subpopulation of biological clock neurons. J Neurosci 23(4):1441-1450.

Labyak SE, Turek FW, Wallen EP, Zee PC (1998) Effects of bright light on age-related changes in the locomotor activity of Syrian hamsters. Am J Physiol Regul Integr Comp Physiol 274:R830-9.

Liu C, Weaver DR, Strogatz SH, Reppert SM (1997) Cellular construction of a circadian clock: period determination in the suprachiasmatic nuclei. Cell 91:855-860.

Long MA, Jutras MJ, Connors BW, Burwell RD (2005) Electrical synapses coordinate activity in the suprachiasmatic nucleus. Nat Neurosci 8(1):61-6.

Low-Zeddies SS, Takahashi JS (2001) Chimera analysis of the Clock mutation in mice shows that complex cellular integration determines circadian behavior. Cell 105:25-42.

McCormack CE, Sontag CR (1980) Entrainment by red light of running activity and ovulation rhythms of rats. Am J Physiol Regul Integr Comp Physiol 239(5):R450-3.

Meijer JH, Groos GA, Rusak B (1986) Luminance coding in a circadian pacemaker: the suprachiasmatic nucleus of the rat and the hamster. Brain Res 382(1):109-18.

Miche S, Colwell CS (2001) Cellular communication and coupling within the suprachiasmatic nucleus. Chronobiol Int 18(4):579-600.

Morin LP (1988) Age-related changes in hamster circadian period, entrainment, and rhythm splitting. J Biol Rhythms 3(3):237-248.

Mrosovsky N (1999) Masking: history, definitions, and measurement. Chronobiol Int 16(4):415-29.

Mrugala M, Zlomanczuk P, Jagota A, Schwartz WJ (2000) Rhythmic multiunit neural activity in slices of hamster suprachiamatic nucleus reflect prior photoperiod. Am J Physiol Regul Integr Comp Physiol 278(4):987-994.

Nelson DE, Takahashi JS (1999) Integration and saturation within the circadian photic entrainment pathway of hamsters. Am J Physiol Regul Integr Comp Physiol 277(5):R1351-61.

Oda GA, Menaker M, Friesen WO (2000) Modeling the dual pacemaker system of the tau mutant hamster. J Biol Rhythms 15(3):246-64.

Ohta H, Yamazaki S, McMahon DG (2005) Constant light desynchronizes mammalian clock neurons. Nat Neurosci 8(3):267-9.

Pittendrigh CS (1981a) Circadian systems: Entrainment. In: *Handbook of behavioural neurobiology: Biological rhythms*, J Aschoff, ed, pp 95-124, Plenum Press, New York.

Pittendrigh CS (1981b) Circadian systems: General Perspective. In: *Handbook of behavioural neurobiology: Biological rhythms*, J Aschoff, ed, pp 57-80, Plenum Press, New York.

Pittendrigh CS, Daan S (1974) Circadian oscillations in rodents: a systematic increase of their frequency with age. Science 186(4163):548-50.

Pittendrigh CS, Daan S (1976a) A functional analysis of circadian pacemakers in nocturnal rodents. IV. Entrainment: Pacemaker as clock. J Comp Physiol 106:291-351.

Pittendrigh CS, Daan S (1976b) A functional analysis of circadian pacemakers in nocturnal rodents. V. Pacemaker structure: A clock for all seasons. J Comp Physiol 106:333-355.

Pittendrigh CS, Elliott JA, Takamura T (1984) The circadian component in photoperiodic induction. Ciba Found Symp 104:26-47.

Quintero J, Kuhlman SJ, McMahon DG (2003) The biological clock nucleus: a multiphasic oscillator network regulated by light. J Neurosci 23(22):8070-8076.

Ruby NF, Joshi N, Heller HC (2002) Constant darkness restores entrainment to phase-delayed Siberian hamsters. Am J Physiol Regul Integr Comp Physiol 283:R1314-1320.

Schaap J, Albus H, Tjebbe VH, Eilers PH, Detari L, Meijer JH (2003) Heterogeneity of rhythmic suprachiasmatic nucleus neurons: Implications for circadian waveform and photoperiodic encoding. Proc Natl Acad Sci USA 100:15994-15999.

Schwartz WJ, de la Iglesia HO, Zlomanczuk P, Illnerova H (2001) Encoding le quattro stagioni within the mammalian brain: photoperiodic orchestration through the suprachiasmatic nucleus. J Biol Rhythms 16(4):302-11.

Selkov EE (1968) Self oscillations in glycolysis. Eur J Biochem 4:79-86.

Sokolove PG, Bushell WN (1978) A chi square periodogram: Its utility for the analysis of circadian rhythms. J Theor Biol 72:131-160.

Turek FW, Penev P, Zhang Y, Van Reeth O, Zee PC (1995) Effects of age on the circadian system. Neurosci Biobehav Rev 19:53-58.

Vilaplana J, Cambras T, Díez-Noguera A (1997) Dissociation of motor activity circadian rhythm in rats after exposure to LD cycles of 4-h period. Am J Physiol Regul Integr Comp Physiol 272:R95-102.

Yamaguchi S, Isejima H, Matsuo T, Okura R, Yagita K, Kobayashi M, Okamura H (2003) Synchronization of cellular clocks in the suprachiasmatic nucleus. Science 302(5649):1408-12.

Welsh DK, Logothetis DE, Meister M, Reppert SM (1995) Individual neurons dissociated from rat suprachiasmatic nucleus express independently phased circadian firing rhythms. Neuron 14:697-706.

Winfree A (1967) Biological rhythms and the behavior of populations of coupled oscillators. J Theor Biol 16:15-42.

Zee PC, Rosenberg RS, Turek FW (1992) Effects of aging on entrainment and rate of resynchronization of circadian locomotor activity. Am J Physiol Regul Integr Comp Physiol 263:R1099-103.

Different temporal structure of rat motor activity pattern between constant light-induced versus suprachiasmatic nucleus lesion-induced arrhythmicity.

Artículo pendiente de publicación.

Different temporal structure of rat motor activity pattern between constant light-induced versus suprachiasmatic nucleus lesion-induced arrhythmicity.

JUAN J. CHIESA[1], ÁGATA RITA CARPENTIERI, MONTSERRAT ANGLÈS-PUJOLRÀS, ANTONI DÍEZ-NOGUERA, AND TRINITAT CAMBRAS.

Departament de Fisiologia, Facultat de Farmacia, Universitat de Barcelona, 08028 Barcelona, Spain.

RUNNING TITLE: arrhythmicity due to LL or SCNx.

[1]CORRESPONDING AUTHOR: Juan J. Chiesa. Departament de Fisiologia, Facultat de Farmacia, Universitat de Barcelona. Av Joan XXIII s/n, 08028 Barcelona, Spain. Phone: (0034) 93 402 4505, Fax: (0034) 93 403 5901; e-mail 1: jchiesa@ub.edu, e-mail 2: cambras@ub.edu

ABSTRACT

In the rat, the suprachiasmatic nucleus of the hypothalamus (SCN) is the central pacemaker that regulates the phase and period of circadian rhythms by primarily encoding photic information. During constant darkness, motor activity rhythm spontaneously free-run with an endogenous stable period (τ). Also when a light-dark cycle with a period close to τ is imposed, a stable nocturnal activity distribution is performed due to the entrainment process. However, prolonged constant lighting (LL) induces gradual τ lenghtening in the rat, untill loss of rhythmicity occurs. A behavioral state of arrhythmicity can also be generated by lesion or ablation of the SCN pacemaker (SCNx). Here, we have comparatively studied the motor activity patterns of rats with behavioral arrhythmicity induced both by LL and by lesions of the SCN. Fourier analysis provided spectral decomposition into a set of harmonic components of time-series with such arrhythmicity. Mean serial analysis of individual spectra revealed ultradian components in LL-exposed animals, whereas no dominant harmonic appeared within SCNx. Also we have examined the highest frequency region allowed by data, with both a Power Spectral Density (PSD) and Autocorrelation analysis to study fractal measures of high frecuency variability (noise). The correlation structure of time-series revealed by fractal analysis was also different among groups. These findings suggest: 1) that the state of arrhythmicity induced by LL has a temporal structure, both at the ultradian and high frequency ranges, 2) that the interactions among the oscillatory elements can be modulated by light, effecting an ultradian pattern, that could be generated by the functional state of circadian oscillators at the SCN, 3) that such ultradian pattern is more than a simple apparent stochastic arrhythmicity, and involves possible underlying time-invariant regulatory mechanisms.

INTRODUCTION

The suprachiasmatic nucleus (SCN) of the hypothalamus is the pacemaker that drives the circadian rhythms in behavioral and physiological functions in mammals. In constant darkness (DD), rhythmicity spontaneously free-run with a stable period τ (Aschoff et al., 1981) (i.e. > 24 h for the rat). Also, the τ of free-running rhythm can be characterized under constant lighting (LL), and its value must depend on both whether the species are diurnal or nocturnal, and on the light intensity according to Aschoff's rules (Aschoff et al., 1981). Such period can be modified by imposing an environmental light-dark cycle (LD) with a period T close to τ, attaining entrainment (Aschoff et al., 1981). Thus, the pacemaking functions involve not only the rhythm maintenance, but also its active synchronization to the environment by encoding periodic lighting information. Moreover, it is well known that SCN pacemaker is composed of a population of oscillator neurons, each driven by a cell-autonomous circadian clock (Welsh et al., 1995). Furthermore, although a unique period equal to that of the overt rhythm is registered at the entire SCN tissue (Ralph et al., 1990), the individual cells dispersed at culture show distributed periods around 24 h in their electrical activity (Herzog et al., 1998). These individual oscillators are phase-organized by neural communication *via* both electrical (Long et al., 2005) and chemical synapses (Honma et al., 2000; Aton et al., 2005) among other factors. The maintenance of stable phase relationship among them generating a coherent rhythm depends on their network interactions (Yamaguchi et al., 2003). Indeed, the functional substrate for pacemaker entrainment may be underlying the regulation by light of such interactions (Quintero et al., 2003).

Prolonged exposure to LL disrupts the circadian activity and temperature rhythms in nocturnal rodents such as the rat (Eastman and Rechtschaffen, 1983; Depres-Brummer et al., 1995). Also, a study showed that arrhythmicity in the Siberian hamster can be generated by a single light pulse delivered at the subjective night (Steinlechner et al., 2002), as it was shown in *Drosophila* sp. in a previous study (Winfree, 1971). Two mechanistic hypotheses have been proposed to explain arrhythmicity: 1) that light stops the single pacemaker by displacing the system towards its singularity, the point at the phase plane where all circadian phases converge (Pittendrigh et al., 1981a); and 2) that several oscillators lose its mutual coupling gradually achieving distributed phases

(Pittendrigh et al., 1981b). A recent study in mice shows that prolonged LL that induced behavioral arrhythmicity also desynchronized celular clocks in the SCN (Ohta et al., 2005), pointing to the latter hypotheses. Another obvious way to generate arrhythmicity is by performing the complete lesion or ablation of the SCN. 24-h rhyhtms both in drinking and motor activity (Stephan and Zucker, 1972), as well as circadian control in body temperature and sleep (Eastman et al., 1984) are abolished after SCN lesion. However, it was shown that not all the temporal organization may be impaired by LL since ultradian rhythmicity remains (Depres-Brummer et al., 1995), even after complete lesions of the SCN (Ibuka et al., 1977; Baker et al., 2005), which may be related to homeostatic regulations.

The absence of any rhythm in the circadian range define the arrhythmicity state. However, from the standpoint of time-series and its temporal organization, other possibilities can be hypothesized: 1) lack of any periodicity within temporally uncorrelated data may reveal an underlying stochastic process, 2) non-circadian frequencies together with correlation, that the signal still has rhythmicity and structural complexity. The aim of this work is to study the motor activity of rats by comparing a group of animals submitted to prolonged LL, with another that holds lesions of the SCN. Although both conditions induce arrhythmicity, we will try to find differences by studying time-series not only with the classical spectral analysis, but also with fractal analysis in the frequency and time domains. Hence, the temporal organization of time-series was studied at the circadian, ultradian, and far beyond these ranges considering high frequency noise. The comparison among the two experimental groups may help to reveal the possible control scheme underlying the temporal regulation of motor activity.

MATERIAL AND METHODS

Animals and experimental procedure

4-month male rats that arrived from provider (Charles River Laboratories, Les Oncins, France) were isolated into transparent metacrilate cages of 25x25x12 cm with food pellets (Panlab® A04) and tap water *ad libitum*. Animals were confined in sound-proof, temperature and humidity conditioned chambers (room temperature ~ 20-22 ºC, humidity ~ 50-80 %). Lighting was supplied by two 36 W Mazdafluor fluorescent

tubes, that yielded ~ 300 lux of reflected cool white light at cage level (Gossen Metrawatt Camille Bauer, Mavolux 5032B digital luxmeter). 15 individuals were exposed to constant lighting (LL) conditions for about two months untill arrhythmicity was observed in motor activity data. Other group of 30 rats remained in dim 0.1-lux red lighting (DD). This latter group served to conduct lesions of the SCN, and hence animals remained in DD for a variable duration (from 1 to 2.5 months) depending on arrhythmicity and putative data obtention.

To conduct lesions, surgery was performed under ketamine ($\approx$ 0.12 g/kg) and xylazine ($\approx$ 0.01 g/kg) anesthesia. Animals were placed at a stereotaxic instrument (David Kopf®, model 900) to guide an electrode throughout the brain towards SCN tissue. A trepan made at skull with a drill at bregma point, allowed electrode pass nearly centered at SCN coordinates (-1.3 mm posterior to bregma; 9.2 mm down from the skull surface) obtained with stereotaxical atlas (Patxinos and Watson, 1998). Electrode supplied a radio-frequency from an electronic device (lesion generator system Radionics®, model RFG-4A), producing lesion by heating the tissue Temperature at tissue registered throughout a stimulation of 1-min was $\approx$ 90 ºC.

Data collection and analysis

General motor activity of the animals was monitored with infrared activity-meter provided with two perpendicular photobeams crossing the cage at 7 cm over de floor, coupled to electronic circuitry. Activity counts were sampled within 1-min interval generating time-series. Then, time-series were compiled within 15-min interval for basic analysis of rhythmicity: actogram, periodogram and Fourier analysis. Individual time-series of both LL and SCNx animals were monitored by means of actograms double-plotted at 24 h to visually determine loss of circadian rhythm. Then, χ^2 periodogram (Sokolove and Bushell, 1978) was calculated at each time-series on 10-day lenght data segments. Data meeting the criterion of a periodogram with any relevant peak revealing a major contribution of a given periodicity to the data variance, were selected for the rest of the analysis. Scanning range was defined from 8 h to 26 h, and level for significance was set at p=0.05.

To describe the ultradian frequency components, consecutive 24-h duration data segments were analysed by means of Fourier analysis by defining a cosenoidal function

of 24 h period as the fundamental harmonic. 24 entire submultiples of 24 h were added (harmonics, H_i) in order to cover a wide array of ultradian periodicities, from the 2nd harmonic (H_2) of 12-h period to the H_{25} of ~ 1-h. From the resulting spectral decomposition of time-series, the power content (PC) was obtained for each H_i as a measure of the presence of a given harmonic within the time-series. Hence, for each time-series, the set of PC values was averaged for each LL and SCNx group. A mean matrix of PC values for each harmonic (the columns) was therefore obtained over data segments of the selected 10 consecutive days (the rows). Each matrix was graphically represented by using a scale of greys: from black, representing the highest PC values, to white as the lowest ones. MANOVA tested which H_i variable significantly differ among the two groups.

Fractal analysis was conducted on data compiled at 1 min studying the degree of correlation within time-series in both the frequency (Power Spectral Density, PSD) and time (autocorrelation) domains. These methods were based on capturing the relationship between the logarithm of a given statistical feature of time-series, against the logarithm of both frequency or time scale (log-log plot) (Eke et al., 2002). PSD analysis calculated PC values of harmonics basing on Fourier analysis on the whole data segment of 10 days, by taking from the 240 h fundamental one through the Nyquist frequency at N/2 (the 7200th 2-min harmonic) the highest one allowed by data sampling. Graphic representation of PSD was done by averaging the individual spectra for each group. Afterwards, the relationship among PC and frequency was studied at individual time-series by the calculation of the miminum square fitting slope at log-log plot (spectral index, β) in the high frequency range, scaled from each 3, 2 and 1 h to the Nyquist frequency. Because a β of 0 denotes no interrelation among frequencies, incremental values of β indicates higher correlation. Autocorrelation analysis provided the correlational structure of time-series to determine to what extent the value of one given event depends on its past values separated by a number of time lags. The correlation coefficient (ρ) was calculated for consecutive lags (from 1 to N/2), and the slope from log-log plot for each individual time-serie was obtained within the interval from the 1st to the 8th lag. In this case, a slope of 0 indicates sustained correlation with lag revealing a deterministic process, whereas lack of correlation indicates a random one. The individual values of fractal measures, β and autocorrelation slope, were averaged to study differences among the two experimental groups. Two-way ANOVA tested

differences for β among the two groups for the three ranges evaluated. t-test for dependent samples was used to statistically compare the autocorrelation slope among groups. Previous to conduct parametric statistics, assumption for normal distributions and homogeneity of variances were tested.

RESULTS

Latency to arrhythmicity in LL showed variability among the animals. 13 of 15 within the group presented no aparent circadian rhythmicity in actograms at different days along the lighting history of the two months. Indeed, in some animals arrhythmicity was metaestable, and spontaneously reverted to an unstable circadian pattern. Since such heterogeneity was not important to the aims of the study, Fig. 1 shows two representative animals of the group with a different latency representing the process of selection of data. Double-plotted actograms at 24 h show that animal in panel A maintained circadian rhythm with period lenghtening for more days than the one in panel B. Also, periodogram analysis calculated by taking 10-day data segment (black rectangle) show similar contribution of periodicities to the variance of time-serie, with no dominant rhythmicity in the circadian range for both animals. On the other hand, 12 of 30 animals appeared with permanent loss of circadian rhythm from the immediate or the few days after the lesion. Fig. 1 shows two representative animals of the group, both with periodicities that contributed similarly to periodogram and with any major one in the circadian range.

Spectral decomposition in the circadian and ultradian range revealed great differences among the two groups. Fig. 2 shows mean daily PC spectra of each group plotted on the graphic matrix form, showing variability associated to harmonics from 24 h to 1 h. A marked ultradian band approximately from the 2nd to the 8th harmonic is observed in LL group, sustained throughout the 10 days. On the contrary, animals with SCNx lesion show flattened spectra without any dominant harmonic. The 24-h circadian harmonic appeared clearly diminished for both groups. MANOVA detected significant differences among groups for H_2 and H_9 ($p<0.01$), H_3, H_6, H_7 and H_8 ($p<0.001$), and H_4 and H_5 ($p<0.0001$).

PSD analysis was done to study the spectral composition of time-series in the high frequency range. Fig. 3 shows the mean PSD for each group, revealing a different

relationship between amplitude (PC) and frequency in the high frequency region. Expectedly, PC shows high values in the low frequency range starting at the H_1 (10 days) and PSD for SCNx group continuously decreased towards higher frequencies. Also a break in the tendency, with a more pronounced slope is observed approximately within H_{80} (3 h) to H_{240} (1 h) range. The groups maintain the same tendency in their amplitude - frequency relationships at frequencies higher than 1 h.

Fractal measures were used to study the correlational structure within time-series in both the frequency and time domains. β slope captured amplitude-frequency correlation from log-log plot obtained from PSD analysis for both LL and SCNx groups in the three ranges evaluated (Fig 4A). For the LL group, the β value was different if evaluated from 3, 2, or 1 h to 2 min ranges, whereas it does not change very much for the SCNx animals. Significant differences were obtained among the groups (ANOVA, $p<0.0001$), whereas the factor range does not show significant differences if considered taken the whole sum of squares. However, as range-group interaction was non-significant, principal group effects could be evaluated by fixing range and comparing among groups. Slope significantly differ among groups, appearing incremented for the LL one both in the 2 h – 2 min ($p<0.0001$) and the 3 h – 2 min ranges, while in the region of frequencies from 1 h to 2 min there were no significant differences. Moreover, the slope of autocorrelation function calculated from 1st to 8th sample lags evidences different degrees of correlation in the time domain between groups (Fig. 4B). This measure evidences to what extent the history of the process is relevant to determine the future state. Temporal correlation was also higher for the LL group, that shows a lower value (t-test for independent samples, $p<0.0001$).

DISCUSSION

In this work, we have studied the motor activity time-series of animals with behavioral arrhythmicity, to provide some heuristic description, at the system level, of the circadian regulation of motor activity. To this aim, the characterization of time-series near (circadian and ultradian range), and far beyond the daily rhythm regulation was conducted in animals whose circadian system was impeded by LL, or eliminated by lesion.

An evident distinct regulation in the range of ultradian frequencies appeared, with the LL animals having a prominent harmonic band within 12 and ~ 3 h. This suggests that, rather than be stopped by LL, the pacemaker components are probably still running but without maintaining a unique coherent phase. Two possibilities can explain such ultradian rhythmicities in motor activity data: 1) a single high frequency process with unstable phase (producing a frequency band in the spectra), 2) multiple circadian oscillators running with different periods, whose phases are distributed along the day.

Pointing to the latter, it is a claimed fact that coherent organization of neuronal population rhythms within the SCN is critical for driving robust circadian rhythms. Indeed, under forced dissociation conditions at T22, each nucleus of the SCN is able of independently driving a component of motor activity rhythm (de la Iglesia et al., 2004). However, it is likely that the organization of the SCN generates a more complex output (Antle and Silver, 2005). Recent findings shows that LL induces desynchronization among the individual oscillator neurons that phased along the day (Ohta et al., 2005) in correlation to the arrhythmic state of the animal, instead of stopping the pacemaker as it was early suggested (Pittendrigh et al., 1981). Remarkably, the maintenance of stable phase relationships among oscillators that make up a coherent rhythm, depend on their network interactions (Yamaguchi et al., 2003). Thus, rather than being a stochastic process, LL-induced arrhythmicity may involve an underlying temporal organization. Although syncronization or coupling mechanisms still lack its physiological correlates, a modulatory role of light on such phenomena was suggested (Honma and Honma, 1999; Quintero et al., 2003, Ohta et al., 2005). The pineal melatonin secretion supressed by light may also impede coupling among oscillators (Cassone et al., 1992). Hence, LL-induced arrhythmicity may rely on such oscillators uncoupling within the SCN.

SCNx animals maintained flattened spectra along the days which exhibited arrhythmicity. Some evidences shows that other circadian oscillators at brain areas as caudate-putamen and parietal cortex may participate in the daily phase setting of locomotor activity under dopaminergic stimulation (Masubuchi et al., 2000). However, a strong influence of the SCN does exist in normal rats in the regulation of daily rhythm, in which no other rhythmic control of motor activity output appeared downstreams the circadian system as it is shown by SCN lesion. In this case, a true arrhythmicity state with any dominant periodicity can be demonstrated in such animals.

The temporal structure of motor activity analysed both in the frequency and time domain, also reveals that possible time-invariant mechanisms may be involved even in the desynchronized system. The analysis of the high frequency variability revealed different degrees of correlation within time-series by fractal measures when comparing LL with SCNx. In the LL group, both measures revealed a certain degree of correlation, whereas arrhythmic state of SCNx animals was majorly uncorrelated noise. Time-series of the LL group presented scaling relationship pointing to a more complex regulation than SCNx ones. Far beyond the ultradian, aperiodic fluctuations are organized in time for LL animals, showing structural complexity. Also, it is important to note that such regulations appeared in the range from 3 h to higher frequencies, below the ultradian influences. Indeed, strong autocorrelation was revealed by studying the immediate history of time-series. Hence, if LL-induced pattern depend solely on the SCN output, it can be suggested that regulation mechanisms still remain due to labil network interactions among oscillators. A possible framework for such temporal structures underlying pattern regulation could involve the proper phase-adjustments of circadian oscillators. On the other hand, more random noise in motor activity organization prevailed in SCNx group as the read-out of a large number of weak influences coming from several central nervous system areas. Importantly, both lack of temporal correlation without the SCN, and its presence on a system impaired by light, suggest an important role for the SCN by imposing temporal structure at motor activity regulation.

In summary, in this study both the ultradian and the deep temporal distribution of motor activity characterising arrhythmicity, were analysed. The following conclusions can be drawn for the role of the SCN in the regulation of motor activity: 1) that the interactions among the oscillatory elements can be modulated by light, effecting an ultradian pattern, 2) that rather than been stochastic, such pattern maintains a temporal structure far beyond the ultradian range, 3) that the presence of the SCN is important for the fine temporal organization of motor activity.
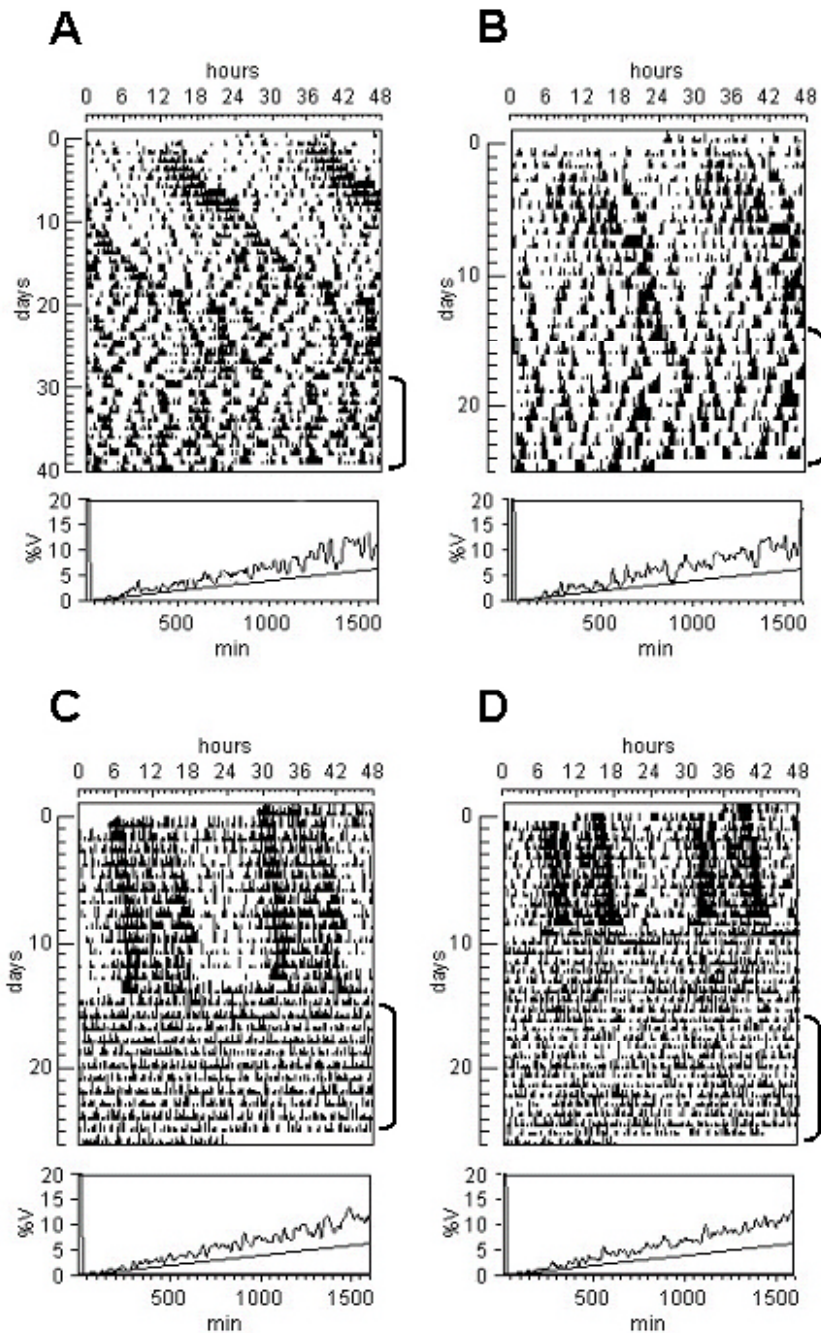
Figure 1. Representative data on actograms, double-plotted in 24 h format showing experimental progress towards arrhythmicity. Panels A and B corresponded to two individuals from the LL-exposed group, B and C, to the SCNx group. The square bracket on the right indicates the 10-day data segment used for the analysis. The white arrows marks the day which the animals received SCN lesions. Plots below actograms are χ^2 periodograms showing percentage of variance (% V) calculated from 0 to 1600 min, corresponding to the data selected for the study. A line depicts significance level (p=0.05) calculated for the spectra.
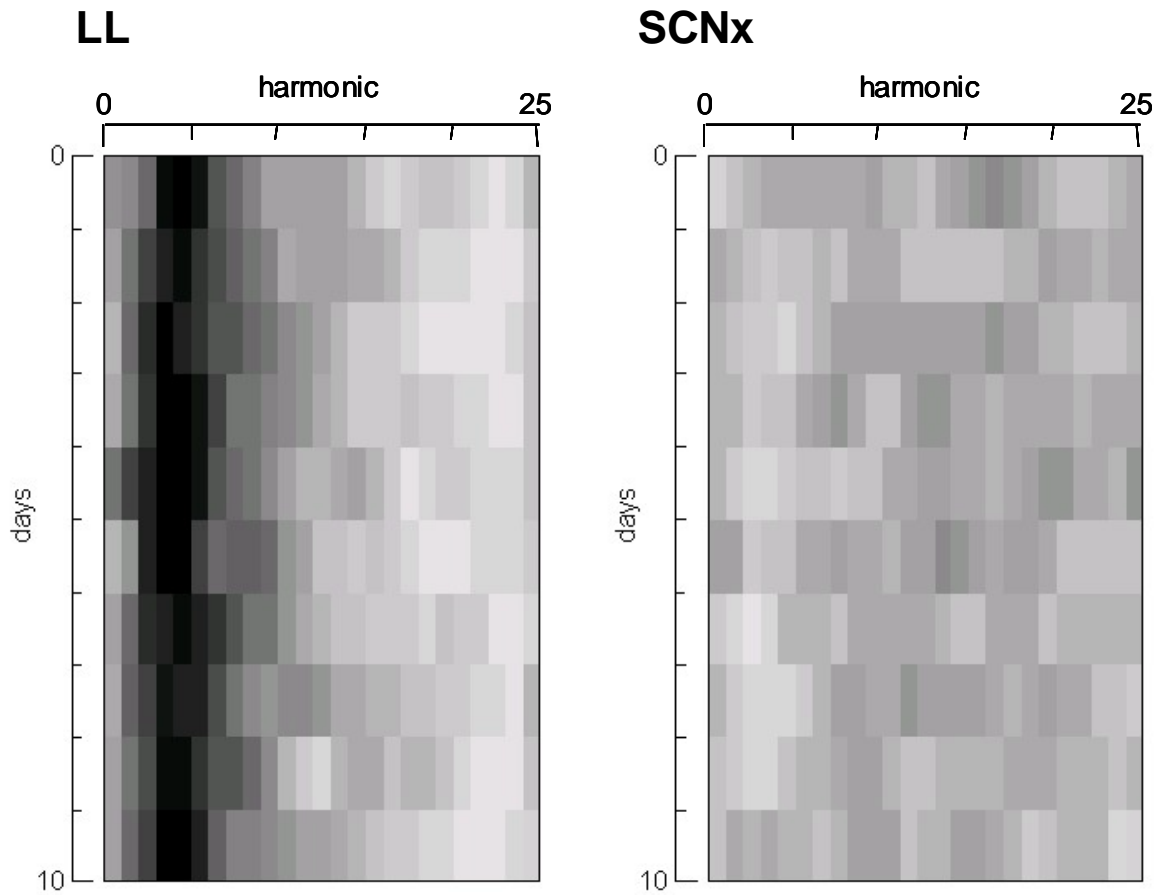
Figure 2. Plots are mean graphic matrixes obtained for each group from individual Fourier spectra. The columns represents PC values of sucessive 24 H_i submultiples of 24 h, that were calculated for each consecutive day at 10-day data segment. Values are represented on a grey scale from black as the highest ones. See text for additional explanations.
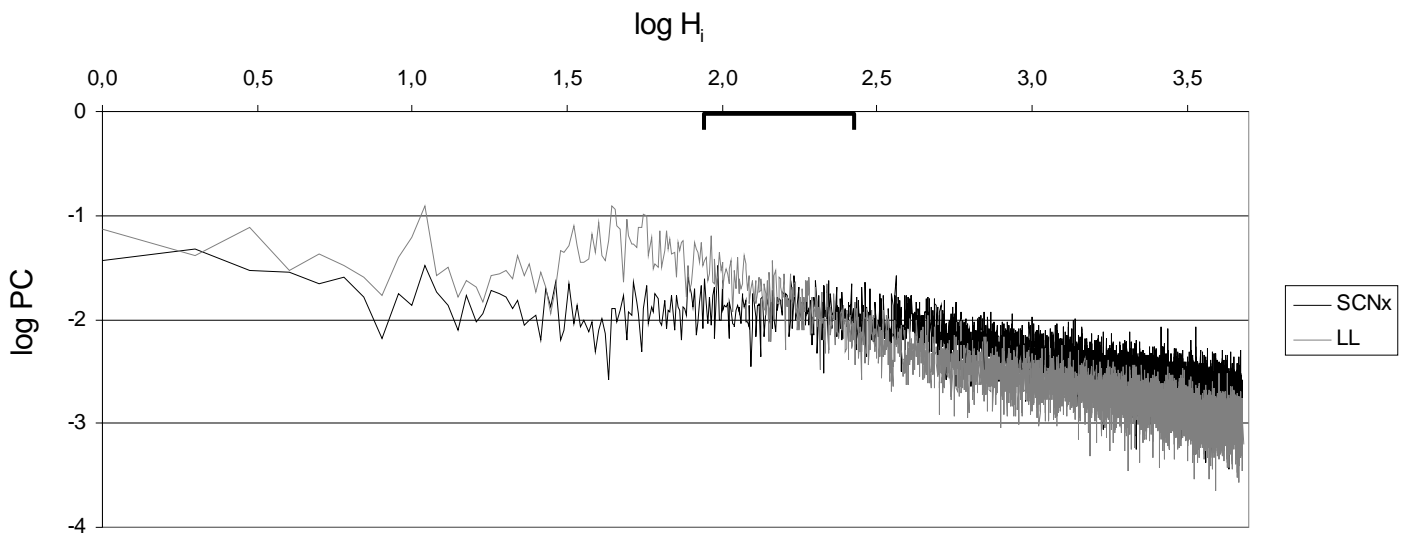
Figure3. PSD analysis obtained for the widest frequency range allowed by sampling rate, at the entire 10-day segment. The Y-axis represents the logarithm of PC values obtained for each H_i, whereas the X-axis is the logarithmic sucession of H_i from H_1 to H_{7200}. Mean values calculated for LL group are represented with a grey line, whereas the black line are mean values of the SCNx group. The frequency range from 3 to 1 h where β slope was calculated is indicated with a bracket.
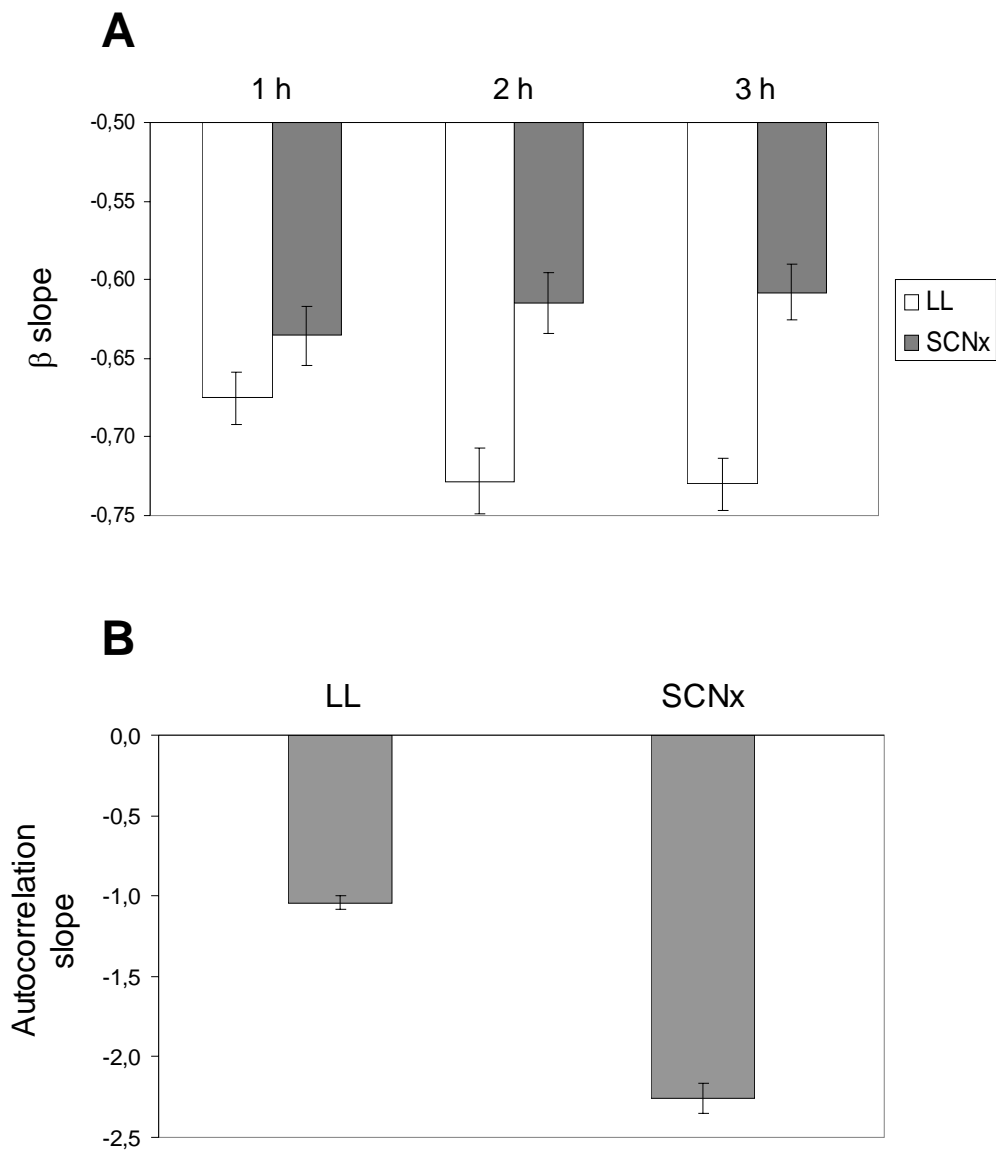
Figure 4. Fractal measures at high frequency variability characterising correlational structure of time series. A- Graph represents mean (± SD) *β* slope of PSD analysis calculated for both LL (white) and SCNx (grey) groups, obtained at each of three different ranges from 1, 2, and 3 h towards 2 min (1 h, 2 h, and 3 h respectively). B- Mean (± SD) slope obtained from autocorrelation analysis of time-series for each group. See text for additional explanations.

REFERENCES

Antle MC, Silver R (2005) Orchestrating time: arrangements of the brain circadian clock. Trends Neurosci 28(3):145-51.

Aschoff J (1981) Freerunning and entrained circadian rhythms. In: *Handbook of behavioural neurobiology: Biological rhythms*, J Aschoff, ed, pp 81-93, Plenum Press, New York.

Baker FC, Angara C, Szymusiak R, McGinty D(2005) Persistence of sleep-temperature coupling after suprachiasmatic nuclei lesions in rats. Am J Physiol Regul Integr Comp Physiol 289(3):R827-38.

Cassone VM (1992) The pineal gland influences rat circadian activity rhythms in constant light. J Biol Rhythms 7(1):27-40.

Depres-Brummer P, Levi F, Metzger G, Touitou Y (1995) Light-induced suppression of the rat circadian system. Am J Physiol Regul Integr Comp Physiol 268:R1111-6.

Eastman C, Rechtschaffen A (1983) Circadian temperature and wake rhythms of rats exposed to prolonged continuous illumination. Physiol Behav 31(4):417-27.

Eastman CI, Mistlberger RE, Rechtschaffen A (1984) Suprachiasmatic nuclei lesions eliminate circadian temperature and sleep rhythms in the rat. Physiol Behav 32(3):357-68.

Eke A, Herman P, Kocsis L, Kozak LR (2002) Fractal characterization of complexity in temporal physiological signals. Physiol Meas 23(1):R1-38.

Herzog ED, Takahashi JS, Block GD (1998) Clock controls circadian period in isolated suprachiasmatic nucleus neurons. Nat Neurosci 1(8):708-13.

Honma S, Honma K (1999) Light-induced uncoupling of multioscillatory circadian system in a diurnal rodent, Asian chipmunk. Am J Physiol Regul Integr Comp Physiol 276:R1390-6.

Honma S, Shirakawa T, Nakamura W, Honma K (2000) Synaptic communication of cellular oscillations in the rat suprachiasmatic neurons. Neurosci Lett 294(2):113-6.

Ibuka N, Inouye SI, Kawamura H (1977) Analysis of sleep-wakefulness rhythms in male rats after suprachiasmatic nucleus lesions and ocular enucleation. Brain Res 122(1):33-47.

Masubuchi S, Honma S, Abe H, Ishizaki K, Namihira M, Ikeda M, Honma K (2000) Clock genes outside the suprachiasmatic nucleus involved in manifestation of locomotor activity rhythm in rats. Eur J Neurosci 12(12):4206-14.

Ohta H, Yamazaki S, McMahon DG (2005) Constant light desynchronizes mammalian clock neurons. Nat Neurosci 8(3):267-9.

Patxinos G, Watson C. The rat brain in stereotaxic coordinates. Academic Press, 1998; USA.

Pittendrigh CS (1981a) Circadian systems: Entrainment. In: *Handbook of behavioural neurobiology: Biological rhythms*, J Aschoff, ed, pp 95-124, Plenum Press, New York.

Quintero JE, Kuhlman SJ, McMahon DG (2003) The biological clock nucleus: a multiphasic oscillator network regulated by light. J Neurosci 23(22):8070-6.

Ralph MR, Foster RG, Davis FC, Menaker M (1990) Transplanted suprachiasmatic nucleus determines circadian period. Science 247(4945):975-8.

Sokolove PG, Bushell WN (1978) A chi square periodogram: Its utility for the analysis of circadian rhythms. J Theor Biol 72:131-160.

Steinlechner S, Stieglitz A, Ruf T (2002) Djungarian hamsters: a species with a labile circadian pacemaker? Arrhythmicity under a light-dark cycle induced by short light pulses. J Biol Rhythms 17(3):248-58.

Stephan FK, Zucker I (1972) Circadian Rhythms in Drinking Behavior and Locomotor Activity of Rats Are Eliminated by Hypothalamic Lesions. Proc Natl Acad Sci USA 69(6):1583-1586.

Welsh DK, Logothetis DE, Meister M, Reppert SM (1995) Individual neurons dissociated from rat suprachiasmatic nucleus express independently phased circadian firing rhythms. Neuron 14(4):697-706.

Winfree AT (1971) Corkscrews and singularities in fruitflies: Resetting behavior of the circadian eclosion rhythm. En: Biochronometry, M Menaker, ed, pp 81-109, National Academy of Sciences, Washington DC.

Yamaguchi S, Isejima H, Matsuo T, Okura R, Yagita K, Kobayashi M, Okamura H (2003) Synchronization of cellular clocks in the suprachiasmatic nucleus. Science 302(5649):1408-12.

A method to obtain long-term motor activity records with high spatiotemporal resolution by means of a force-plate actometer.

Artículo pendiente de publicación.

A method to obtain long-term motor activity records with high spatiotemporal resolution by means of a force-plate actometer.

JUAN J. CHIESA[1], JOHN F. ARAUJO[2], AND ANTONI DÍEZ-NOGUERA[1]

[1]Departament de Fisiologia, Facultat de Farmacia, Universitat de Barcelona, 08028 Barcelona, Spain.

[2]Departamento de Fisiologia, Universidade Federal do Rio Grande do Norte, Natal-RN, Brazil.

RUNNING TITLE: high resolution motor activity recording

[1]CORRESPONDING AUTHOR: Juan J. Chiesa. Departament de Fisiologia, Facultat de Farmacia, Universitat de Barcelona. Av Joan XXIII s/n, 08028 Barcelona, Spain. Phone: (0034) 93 402 4505, Fax: (0034) 93 403 5901; e-mail 1: jchiesa@ub.edu, e-mail 2: adieznoguera@ub.edu

ABSTRACT

Motor activity rhythm is considered a marker of the circadian clock, with which period and phase can be reliable determined. Daily patterns of motor activity are commonly acquired both with infrared photobeams or with running wheels, characterising rhythm properties in chronobiological studies. Patterns of motor activity under circadian control may arise from a more complex mechanism than a single output. In spite of this, the qualitative aspects of motor output related to this functional activity are poorly described. The aim of this work was to develop a tool that would obtain a wide description of the motor activity in chronobiological studies. A method to make long-term and high temporal and spatial resolution registers for quantifying the dynamics of motor activity in rodents is described. The device is based on a horizontal square platform, which holds three force transducers supporting a load plate. Force transducers give an electrical output proportional to the intensity of the applied force, and related to the point of application on the load plate. Therefore, an XY plane was defined into which displacements of the center of force could be calculated, constituting a force-plate actometer. Strain data obtained from transducers were useful to estimate the locomotion of an animal in a 40-cm diameter arena, with less than 1 mm spatial, and 1 s temporal resolution. A computer program processed data providing an exhaustive analysis of motion in a qualitative fashion, e.g. length and velocity of displacements, lateralization, and time of permanence in quadrants. To test the method, high resolution analysis of daily motor activity was therefore obtained in normal rats exposed to light-dark cycles, constant darkness, and constant lighting conditions. Additionally motor activity of animals with permanent lesions of the hypothalamic suprachiasmatic nucleus (the circadian pacemaker in mammals) in constant darkness were also characterized. Hence, selective discrimination between different kinds of behavioral variables was afforded at a circadian scale. This analysis allowed to obtain among others, distinct temporal patterns of different behavioral rhythms, regional preference in rhythmic animals related to activity/rest cycle, and some intriguingly characteristics within daily activity patterns such as emergent rhythm of slow motions in animals that were arrhythmic for the rest of motor activity. The potential use of this method in chronobiological studies is discussed.

INTRODUCTION

All behavioral outputs executed by an organism can be reflected in motor activity. Briefly, motor regulation comprises a wide system distributed in premotor and motor areas, within the parietal and frontal cortex respectively. These strucutures encode and transmit neural activation patterns to medullar motoneurons, whereas flexible motor regulation may also involve other structures (Roitman et al., 2005). Motor activity is an outcome of motivated behavior that requires coordinated somatic, autonomic, and endocrine responses, where the proper motor act comprises initiation, procurement, and consummatory phases (Swanson et al., 1981). Obviously, such behavior may involve the entire central nervous system. Hypothalamic subsystems important for the execution of instinctive behaviors are mainly modulated by sensory (reflex), central control (e.g., circadian), and volitional (cortical) inputs. Hypothalamic output for motor regulation is characterized by descending projections to brainstem and spinal motor systems, and by direct or thalamus-relayed projections back to the cerebral cortex (Risold et al., 1997).

Behavioral motor performance and stereotypes are studied at short-term scales (testing sessions in minutes, or at least hours) to characterize, among others, learning (Mizuno et al., 2004; Roitman et al., 2005; Liu et al., 2005) and psychopharmacology of drugs (Creese and Iversen, 1972; Ali et al., 1995; Cabib et al., 2000; Wolansky et al., 2005). Both temporal and spatial characteristics of motion are necessary to study patterns of motor behavior. Indeed, that locomotor behavior is in fact structured and patterned was assumed with different approaches (Paulus et al., 1990; Paulus and Geyer, 1991; Brodkin and Nash, 1995), and the appropiate measures should reflect this structure. The most common method for measuring motor activity employs infrared photobeams emitter-detector pairs in a small test cage, with beam spacing and/or number according to specific research interests. For example, to detect subtle motions as during drug-induced tremor or to detect segmentation between lingering and displacements, some devices integrates dense arrays of beams (Kafkafi et al., 2001) or sophisticated devices combined by a photobeam arena with ultrasound phase-shift technique (Young et al., 2000) to enhance spatial (majorly vertical) resolution. However, most photobeam-based devices have limitations in horizontal resolution of space to detect both natural or drug-induced modes of motion in rodents. Several methods developed provide some improvement in spatial resolution, such as an

apparatus based on a joy-stick (Brodkin and Nash, 1995), open field using video tracking (e.g., http://www.med-associates.com/activity/openFieldVideo.htm), and a touch-pad transducer (Kao et al., 1995).

Chronobiology involves the systematic study of the temporal features of living things in all of its organization levels (Rotenberg et al., 1997). Biological rhythms are self-sustained oscillations expressed at the entire physiology of the organisms, that are driven by pacemakers synchronized with the temporal features of ecological niche by environmental cues (or zeitgebers). The light-dark transitions imposed by the daily revolution of the earth are the main zeitgeber, at least for epigeous organisms, that synchronizes rhythms with a period of approximately 24 h, the majorly expressed circadian ones (Aschoff, 1981). To assess daily rhythms at the behavioral level by means of long-term recordings is a hallmark in chronobiological studies, where the motor activity rhythm is commonly considered as a direct marker of pacemaker activity. It has been suggested that the circadian pacemaker of mammals, located at the hypothalamic suprachiasmatic nucleus (SCN), is a system comprised by multiple coupled oscillators (Winfree, 1967; Pittendrigh, 1981). In effect, the neural substrate for such individual oscillators has been identified later (Welsh et al., 1995). Lighting conditions appear to modulate the functional coupling among oscillators, in such a way that constant light may lead to both ultradian pattern or arrhythmicity of the motor activity (Vilaplana et al., 1997; Cambras et al., 1997). Although humoral factors are mainly involved in pacemaker output to regulate motor activity rhythm (Silver et al., 1996), the behavioral description of the components involved at these temporal reorganizations of activity pattern may provide information about other possible neural regulation at pacemaker output to motor systems.

The more extended devices used to acquire motor activity in chronobiological studies involve photobeam-based devices, or running wheel. This devices counts for beam interruptions or wheel revolutions respectively in relation to animal movements. Therefore, information obtained is generally the amount of bin-accumulated counts of beam interruptions or wheel revolutions, which are analysed to obtain rhythm parameters, such as period and phase, in the circadian scale. Wheel-running is a single volitive activity that is directly related to the motivational state of the animal (Janik and Mrosovsky, 1993). Measuring motor activity by infrared photobeams reflects the underlying notion that the variable is rather stochastic in nature. In this way,

underestimation of possible complex motor pattern arising on behavioral activity may occur, with consequent loss of information. Cage activity may comprise a wide set of rigid patterns of behavior, including stereotypes like exploration, rearing, grooming, climbing, drinking, etc, and also, flexible time and contextual-dependent motor responses from possible learning processes. This information is generally ignored in chronobiological studies, were only the temporal structure (distribution) and amount of activity are considered to assess circadian system output. However, whether distinct motor behaviors can be characterized at the circadian scale, has not been proposed to date. Also, rhythmic characterization of behavioral alterations in animals models, was claimed to improve knoweledge about clinical noncognitive symptomatology in neurological disorders such as Alzheimer disease (Vloeberghs et al., 2004). Therefore, the aim of this work is to investigate a tool that perform the acquisition of motor activity data of a freely moving small animal like rodents, with high spatiotemporal resolution, in the long-term studies as those necessary in chronobiological research.

MATERIAL AND METHODS

General description of the method

A force-plate actometer is a device constructed to measure the changes through time in the magnitude and position of any force applied over a rigid horizontal surface, such us the ones produced by a freely-moving animal. Hence, displacements are temporally and spatially resolved obtaining paths travelled with its spatiotemporal attributes. Motor activity of rats housed on the proper experimental arena was registered with force-plate actometer, during long-term sessions of several days, under different experimental conditions. Time-series of the center of force coordinates during consecutive days were obtained to analyze motion trajectories. Educed time-series of several motor variables were calculated to perform the chronobiological study of distinct features of behavioral patterns.

Force-plate actometer components

Mechanical support: a solid square aluminium base was used for supporting force transducers, that were mechanically fixed at the vertices of a triangle (side=30 cm). A rigid square metacrylate surface of 40x40 cm and about 1 kg that lean over the force transducers was placed as the load plate. A metacrylate cylinder of 40 cm diameter and 13 cm height, was used as enclosure for the animals isolation into the recording arena. Figure 1 shows a diagram of the device.

Force transducers: single-point load cells each one of 0,3 - 3 kg capacity (allowing a total charge of 9 kg over the load plate), with a precision of $\pm$ 0.0067 % of the rated output (0.9 $\pm$ 0.1 mV/V), were used as force transducers (model 1004, Vishay Transducers, USA, www.tedea-huntleigh.com). A force applied at a specific point of the cell produces deflections that change the input resistance of a Wheatstone bridge, to achieve the measurement of such small changes of the resistance related to the applied force.

Signal conditioning: electronic circuitry was constructed to condition electrical signal from each force transducer, obtaining appropriate range of variation for the force/signal relationship. This device allowed both gain and level control to obtain range and zero adjustment.

Analog/Digital interface: PCI-DAS 1000 computer board (Measurement Computing Corporation, USA, http://www.measurementcomputing.com) was used to receive and convert analog input signals transduced by the load cells to digital numeric values with a 12-bit resolution. Although input board allowed sample rate as high as 250 Khz, an interval sampling of 40 ms was considered enough for the temporal resolution necessary for rodent displacements. Data from three actometers used 9 input channels (one for each transducer), whose digitalized signals were monitored on-line and simultaneously recorded every second averaging 25 consecutive samples by a specific computer application (see below).

Basic operational principles

A moving object over a load plate that lean over force transducers at single-points, will produce a variable force at each point related to its position. Hence, variations in time of force values that result proportional to transducer signal can be obtained. The essential of the method is to track down the trajectory of such moving

object, which is analytically obtained by using force values to calculate the centre of force. To define a plane, three force transducers must be utilized in a manner that the total force (F) applied to the load plate, taking an ideal infinite surface rigidity, is the addition of the forces at each transducer (f_1, f_2 and f_3) located at fixed coordinates (x_i, y_i). A force applied at a single point on a rigid surface will produce a linear momentum at each lean point were transducers are located. Despite the fact that the momentum of the force at each x_i, y_i coordinates of transducers were annullated in between, it is possible to obtain the relationship between the coordinates of the force application point and the three forces sensed at the transducers, as:

$$x = (f_1\, x_1 + f_2\, x_2 + f_3\, x_3) / F$$
$$y = (f_1\, y_1 + f_2\, y_2 + f_3\, y_3) / F$$

where f_i are values from transducers, and $F = f_1 + f_2 + f_3$ is the total applied force. Therefore, the force application point in the plane can be calculated by using the value of the force measured at each transducer.

Calculations

From daily time-series of force at transducers, the position of the animal at the circular arena was estimated by the calculation of the centre of force coordinates. The temporal changes in this point became the trajectories, and the basis for calculation of displacement, velocity (e.g., quiescence or vigorous motion), area swept by displacement, time of presence in certain regions of the arena, etc. This set of variables is included generically in a "motion analysis". Hence, all the variables were calculated from time-series of *xy* coordinates of the force center (P_i), obtained with a sample rate of 1 s. A graphic explanation of each variable calculation is drawn in Figure 2. Panel A represents a given displacement (D) calculated as the difference between two consecutive P_i (P_1 and P_2 at figure). A third consecutive point (P_3) was necessary to estimate lateralization, by assigning positive values to displacements to the left (D_L) and negative values to displacements to the right (D_R). Furthermore, lateral displacement (latD) was calculated as the side of the right triangle defined with the projection of P_1 - P_2 line and P_3, and the area enclosed estimates the area swept by displacements (A).

Paths enclosing areas to the left (A_L) were positive area values, whereas the ones to the right (A_R) were negative. Spatial patterning was also estimated with the polygonal area (AP) enclosed by any path as it is shown at Panel B in Figure 2. Additionally, five regions were geometrically differentiated at the circular arena to study the animal leaning to rest (T_i) or to move (D_i) at a given place. Panel C in Figure 2 shows how regions were defined: the four delimited by two perpendicular lines intersected at the centre of the circular arena (regions from 1 to 4), and a square of 20x20 cm centered at this point delimited a 0 region superposed to the other four. Animal access to food pellets and water bottle was located at regions 1 and 2 of the arena. Also, the quiescence of the animal, or the more vigorous activity, were studied as the number of slow (NsM), intermediate (NiM), or rapid motions (NrM) within a bin. Given that samples are taken at regular time intervals of 1 s, D can be used as a measure of velocity. A Heavyside function (h) was utilized to discriminate the velocity of displacements into the three excluding categories, according to a corresponding defined treshold (U):

$$NM = \sum_{i=1}^{n} h(D - U) \qquad\qquad h(z) = \begin{cases} 1 & \text{if } z > 0 \\ 0 & \text{if } z < 0 \end{cases}$$

where n are seconds within a bin. U_s=0.5 cm was defined as the threshold for slow (NsM), U_i=5 cm for intermediate (NiM), and U_r=10 cm for rapid motions. These thresholds were adequate for the aims of this study according to empirical observations, because rhythmic patterns of NsM were strongly distinguishable from that of NiM and NrM. However, no consistent differences were encountered between NiM and NrM by varying U_i and U_r along a plausible range.

Lateralization was calculated as the sum between right and left-sided variables: D, latD, A, and velocity of motion (NxM). Calculated values for all the variables were compiled into 15-min bin, and hence time-series of each variable were obtained which were studied as described below. A list of the total variables included in motion analysis is shown at Table 1.

variable	abreviation	feature measured
displacement	D	distance travelled between P_i and P_{i-1}
displacement to the left	D_L	distance travelled to the left, with respect to the direction established by P_{i-2} and P_{i-1}
displacement to the right	D_R	distance travelled to the right
sum of displacement	D_S	$D_L - D_R$
lateral displacement	latD	(see explanation at Figure 2)
lateral displacement to the left	$latD_L$	lateral displacement calculated by considering D_L
lateral displacement to the right	$latD_R$	lateral displacement to the right
sum of lateral displacement	$latD_S$	$latD_L - latD_R$
area to the left	A_L	area calculated by considering D_L
area to the right	A_R	area to the right
sum of area	A_S	$A_L - A_R$
poligonal area	AP	(see explanation at Figure 2)
number of slow motion	NsM	tendency to quiescence (see explanation at text)
number of slow motion to the left	NsM_L	tendency to quiescence calculated by considering D_L
number of slow motion to the right	NsM_R	tendency to quiescence to the right
sum of number of slow motion	NsM_S	$NsM_L - NsM_R$
number of intermediate motion	NiM	tendency to activity
number of intermediate motion to the left	NiM_L	tendency to activity calculated by considering D_L
number of intermediate motion to the right	NiM_R	tendency to activity to the right
sum of intermediate motion	NiM_S	$NiM_L - NiM_S$
number of rapid motion	NrM	tendency to vigorous activity
number of rapid motion to the left	NrM_L	tendency to vigorous activity calculated by considering D_L
number of rapid motion to the right	NrM_R	tendency to vigorous activity to the right
sum of rapid motion	NrM_S	$NrM_L - NrM_S$
time in region i	T_i	time of presence in region i of the arena
displacement in region i	D_i	distance travelled in region i of the arena
"agitation" in region i	G_i	D_i / T_i

Table 1. The set of variables calculated from trajectories to obtain motion analysis. Time-series of the variables were studied to obtain a chronobiological description of the distinct behavioral rhythms.

Software

Two specific computer applications were used to record and analyze data: one for data recording and on-line processing of the signal, and the other for decoding, calibration, calculation of the force centre, and to obtain variables motion analysis. The data acquisition software served to: 1) define board channels for each transducer, 2) control sampling process of computer board by setting voltage resolution (2.5 V for appropriate scaling range with a moving rat) and sampling interval (25 samples each 40 ms, nearly 1 data/seg), 3) real-time viewing of data acquisition in graphic and numeric format, and 4) record raw data matrix from digital output channels in ASCII format on hard disk. A second computer application was used to: 1) decode raw data files from ASCII to integer numeric format, 2) obtain coefficients from linear regression which calibrate the transducer response, hence obtaining real values of detected force due to animal weight, 3) compute positional coordinates of the force center from tranducers data, and 4) calculate motion analysis from trajectories obtained from change in time of the position of the force centre.

Calibration procedure

Calibration was made to calculate straight lines for the relationship between force and digital readings from transducers, obtaining numerical values in force units from digital output. First of all, immobile weight of $\approx$ 3 kg constituted by load plate, circular cage together with wood chips bed, and plastic cover with a metal grid containing food pellets with water bottle, was disposed to distribute similar load at each transducer. Signal gain and zero point were adjusted to hang-up for this static weight. A standard weight of 400 g was located over the cover at transducers location in a manner that $\approx$ 3,75 units/g were obtained. This value was based on empirical experience, with a practical compromise between sensitivity and range. Calibration of each transducer was performed by means of the slope and the ordinate from linear regression for the relationship between the obtained signal and the standard weight at fixed positions. To do so, the standard weight was registered at four different positions over the cover. After this, the animal was placed inside the cage and data recording began. This procedure was performed at least each two days to compensate the loss of mass due to

water and urine evaporation. On further calculations, data obtained were multiplied by slope and summed to ordinate obtained from calibration line. Thus, daily time-series of force values for each transducer were obtained.

Experimental sessions

Motor activity of four groups of rats were studied with the force-plate actometer in long-term records. The groups were: 1) animals exposed to 12 h light:12 h dark cycles (LD, n=4), 2) animals exposed to constant darkness (DD, n=4), 3) suprachiasmatic nucleus lesioned animals (SCNx) exposed to DD (n=8), 4) animals exposed to prolonged constant light (LL, n=11). Hence, animales were studied in two environments that favour circadian rhythmicity, LD and DD. Also the arrhythmicity of motor activity was induced in other two groups by prolonged exposure to LL, or by SCN lesion. In this way, motor variables were characterized under or in the absence of the circadian system regulation. To assess rhythmicity, general motor activity was monitored with infrared activity-meter prior to conduct force-plate records, which lasted between 3 and 5 days.

Animals and housing

Male rats of four-month age (Charles River Laboratories, Les Oncins, France) and approximately 350-450 gr. weight, were used as subjects for data acquisition in the force-plate actometer. Animals were isolated into transparent metacrylate cages of 25x25x12 cm with food pellets (Panlab® A04) and tap water *ad libitum*, and housed in sound-proof, temperature and humidity conditioned chambers (room temperature ~ 20-22 ºC, and humidity ~ 50-80 %) with time-adjustable light regimes. Lighting was supplied by two 36 W Mazdafluor fluorescent tubes, producing ~ 300 lux of reflected cool white light at cage level during the light phase, and a dim red light of ~ 0.1 lux during the dark phase (Gossen Metrawatt Camille Bauer, Mavolux 5032B digital luxmeter). General motor activity of the animals was monitored with infrared activity-meter provided with two perpendicular photobeams crossing the cage at 7 cm over de floor, coupled to an electronic circuitry. A sample rate of 1 min generated time-series that served to other studies, and that were compiled into 15 min bin for the present

study. When the appearance of arrhythmic patterns occurred the animals were moved to a chamber where corresponding lighting condition was maintained, provided with three force-plate actometers that were used in parallel during recording sessions. Animals registered in DD were temporally removed from the chamber to perform calibration.

SCN lesion was made by surgery performed under Ketamine ($\approx$ 0.12 g/kg) and Xylazine ($\approx$ 0.01 g/kg) anesthesia. Animals were placed at a stereotaxic instrument (David Kopf®, model 900) to guide an electrode that supplied a radio-frequency from an electronic device (lesion generator system Radionics®, model RFG-4A), producing heat at tissue. A trepan was made in the skull with a crown drill at bregma point, allowing electrode pass nearly centered at SCN coordinates (-1.3 mm posterior to bregma; 9.2 mm down from the skull surface) that were obtained with the stereotaxical atlas (Patxinos and Watson, 1998). Stimulation interval was 1-min, registering $\approx$ 90 ºC temperature at the tissue level.

Time-series analysis

Time-series compiled into 15-min bins of general motor activity were examined in all animals by means of graphic methods, i.e. histograms of activity counts double-plotted on columns of successive 24-h data sections (actogram), and educed activity profiles (waveforms) from averaged consecutive data sections of 24 h that represents the average daily profile. Also, the χ^2 periodogram analysis (Sokolove and Bushell, 1978) was conducted to assess significant periodicities in general motor activity. 15-min bin series of each variable obtained from motion analysis were studied with the same graphic methods to characterize behavioral patterns in both rhythmic and arrhythmic animals. A regressive periodogram analysis was adequate for periodicity characterization in such time-series. To calculate significant period, this method employs a less-square fitting of data to a cosenoidal function obtaining a regression line with the daily estimated acrophases (Klemfuss and Clopton, 1993). Fourier analysis was conducted to obtain power spectra of D and NsM time-series of rhythmic animals. The power content (PC) calculated the presence of a given harmonic in the time-series at the frequency domain. Nine entire submultiples of the 24-h harmonic were calculated, the sum of corresponding PCs assess an ultradian band. All graph and calculations were

made using the integrated package for time-series analysis in chronobiology, "El Temps" (©Antoni Díez-Noguera, University of Barcelona, Spain, 1998-2005, http://www.ub.es/dpfisiv/soft/ElTems).

RESULTS

Rhythms in rhythmic animals

The behavioral characteristics of activity were studied on a daily basis by means of the different variables after motion analysis. First of all, both rhythms driven by environmental ligh-dark cycle (LD) and spontaneous ones in constant darkness (DD) were analysed, attempting to characterize possible inner behavioral patterns within general motor activity. Clear circadian rhythms were found for most of the variables, except for all those that quantify lateral differences in motion (e.g., D_S, A_S, NrM_S). This indicates that no clear motor lateralization was encountered associated with any behavioral rhythm. Although photobeam-detected general motor activity was not recorded simultaneously with force-plate, little or no differences detectable with the graphic methods employed were observed among rhythmic pattern of D compared with animal's previous pattern of photobeam data (data not shown). Also latD appeared with the same rhythmic pattern as D, and with a lesser daily mean value according to the geometrical calculation of the variable (latD and D as the cathetus and hypotenuse of a right triangle, respectively, see Figure 2). Moreover, measures of the area covered by motion (A) showed a rhythmic pattern temporally similar as the one in D, but with peaks of higher amplitude with respect to the daily mean (data not shown). Again, this is as expected because any linear increment in D produces a quadratic one of the derived A. Additionally, the area enclosed within paths, AP, resulted in arrhythmic or unclear patterns for all individuals. Again, this indicates that no motor lateralization is evident at the circadian scale since AP values were cancelled in between because lateral tendencies in motion are similar throughout the day.

However, distinct behavioral rhythms appeared with a different temporal structure, when considering some dynamic attributes of the travelled path as the velocity of motion. Figure 3 exhibits the 24-h rhythm of D (panel A) covered by an

animal in LD, as well as the rhythm in NsM (panel B). When comparing these two behavioral rhythms, it can be seen primarily at waveform a clear ultradian component within the circadian encircling of the rhythm in D, whereas a circadian rhythm in NsM appeared with a reduced ultradian component. The power spectra obtained with Fourier analysis show these differences in the rhythmic patterns. Spectra of D rhythm in this animal showed a major amplitude related to the first 24-h harmonic (PC=17%). An ultradian band comprised by the sum of the 9 submultiple harmonics produced a PC=16%. On the other hand, Fourier decomposition of NsM time-serie presented most of the amplitude related to the 24-h harmonic with a PC=25%, whereas ultradian harmonics had a PC=11%. These differences between D and NsM in the frequency structure of time-series appeared in most LD submitted animals. Behavioral rhythms of animals under DD condition appeared with less differences in the frequency structure, as it can be seen at Figure 3. Although waveform exhibits more ultradian components for the rhythm in D (panel C) respect to the NsM one (panel D), Fourier analysis does not reflect such difference, generating similar power spectra among time-series.

Most rodents reserve an area of the cage for nesting and rest. It was found that generally, the time spent by the animals at the different regions of the experimental arena (T_i) exhibited noticeable circadian rhythms. This differential place-preference was clearly related to the activity/rest rhythm, as it can be seen at Figure 4. Panel A shows the rhythm in T_1, whose "active" phase (the time when the variable exceeded the daily mean) appeared confined to the light phase of the LD cycle, that is, when the animal should be resting. The rhythm detected in T_1 was nearly similar to the one in T_0 (data not shown) revealing that the resting area of the arena comprised mainly region 1, together with region 0. The marked squareness of waveform of T_1 rhythm acquiring a stable maximum value near 15 min (maximum time accumulated within a bin) also featured this behavioral pattern, since lingering in a place to rest involved sustained quiescence and thus total time spent within 15 min bin. Preferred places for displacements within the arena were also detected, because T_2 exhibited a rhythm that was locked to the dark phase of the LD cycle (figure 4, panel B). Rhythm in T_2 appeared similar to that in T_3, whereas in T_4 becomes more unclear, and these patterns correlates with the ones in D_i at corresponding regions (data not shown). Thus, this indicates that the time spent at both regions 2 and 3 is likely related to the activity performed by the animal within these regions at the arena. However, T_1 rhythm

waveform (figure 4, panel A) also shows that region 1 is not excluding only for resting, because some time spent by the animal (values under the daily mean) was related to the dark phase of the LD cycle due to motions within that region. Generally, the same description is adequate for the animals in constant darkness that also presented clear rhythmic patterns of placing related to the endogenous activity/rest rhythm. Panel C of figure 4 represents the rhythm in the T_1 variable, that was also nearly similar to T_0 and thus, both region 1 and 0 comprised the area selected by the animal to rest. T_1 rhythm was presented in anti-phase with respect to the T_3 rhythm (figure 4, panel D). Region 3 was primarily selected by the animal to perform activity as well as region 4, because T_3 and T_4 rhythms appeared with a nearly similar pattern when compared with D_3 and D_4 (data not shown).

Rhythms in arrhythmic animals

Arrhythmicity in the activity pattern was induced both by submitting the animals to prolonged LL or by carrying out permanent SCNx. Arrhythmicity was checked with χ_2 periodogram before force-plate recording by using time-series of general motor activity (MA) detected by conventional photobeam activity-meter. The effect of the SCNx on the activity rhythm was manifested almost immediately, whereas LL produced a gradual disrupting effect until no discernible rhythmic pattern was detected both in actograms and periodograms. Once arrhythmicity was observed, the animals were moved to force-plate actometers to record behavioral patterns maintaining the same prior environmental condition (LL for intact animals, DD for SCNx ones). Figure 5 shows data describing the activity patterns of three studied animals, one that undergoes SCNx, and two that were exposed under LL (LL_1 and LL_2). For each animal, data at the left side of the figure correspond to MA (upper actogram) and D (lower actogram and waveform below) variables. Data at the right side are plotted both at actogram and waveform corresponding to T_0 for SCNx animal, NsM for LL_1 and T_3 for LL_2. Actograms displaying MA data on previous three days before force-plate recording evidence arrhythmicity in the three animals. Pattern of D that are visible both in actograms and waveforms, quite correlates with the one of MA. Moreover, most of the motion analysis variables also evidenced the arrhythmicity state.

However, the emergence of circadian rhythms was detected in some specific variables in these three animals. In the SCNx, a rhythm in T_0 is clearly observed both at actogram and waveform (periodogram analysis, $p<0.0001$). Actogram shows that the active phase (when values are above the daily mean) began at similar times among the three days, but it extended for more time during the 3rd day. The rhythm featured a similar pattern compared with T_i rhythms related to the rest phase in both LD and DD intact animals. Mean daily profile produced a square waveform with stable maximum values close to 15 min above the mean, but also a non-sustained drop below the mean appeared at waveform revealing temporally instable rhythmicity. Also rhythms in behavioral variables were observed in two animals exposed to LL that appeared arrhythmic in MA and D. First, a 24-h rhythmic profile can be observed at actogram in the LL$_1$ animal for the NsM variable (periodogram analysis, $p<0.0001$). An instable daily amplitude is manifested with a major oscillation during the first day. Indeed, its waveform shows sinusoidal rhythmic variation with a low amplitude related to the average of this variable daily amplitude. Also a rhythm could be observed in another animal exposed to LL (LL$_2$ animal) in the time of permanence in an specific quadrant, T_3 (periodogram analysis, $p<0.005$). First of all, it can be seen at actogram that the active phase showed stable daily onsets but it extended for more time during the 2nd day. Hence, although at waveform the rhythm presented a marked active phase onset it also exhibited fragmentation and unclear offset of active phase due to a great instability in its duration.

DISCUSSION

This paper describes the use of the force-plate actometer as a powerful new instrument for recording motor activity in long-term studies as those used in chronobiology. Successful detection of behavioral patterns at the circadian scale, improved the description of general motor activity rhythm usually obtained with conventional photobeam and running wheel devices. Data from the presented examples are illustrations on possible scopes of this method, instead of being constitutive to develop general inferences. Generally, rhythmic pattern of D features nearly the same as photobeam-detected activity revealing that spatial description of motion, in terms of

total distance, is equally acquired with both methods when a long-term study is conducted. However, some dynamic characteristics of travelled path, such us velocity of motion, suggest a possible distinct regulation of the different behavioral rhythms. Indeed, the characteristics of its temporal structure varied according with the type of behavioral activity. Ultradian pattern appeared when considering rapid motions, but the slower ones mainly presented a circadian one. Also, a clear lingering at the place to rest was encountered associated to the activity/rest cycle. Selecting a place to rest, a behavior frequently observed in most rodents, appeared with a marked rhythm in all intact animals submitted to LD and DD. As should be expected, the animals separate regions to perform activity that were not strictly defined as the one preferred to rest. However, the behavior of lingering in a place to rest could indicate possible alterations due to change in the nesting environment (i.e., when a cage cleaning occurred), because strong effects on the phase of circadian activity rhythm can occur after a cage change (Mrosovsky et al., 1989). Also, while in some cases photobeam-based devices may fail to estimate the onset and offset of the activity/rest rhythm, determining resting place as well as the time spent to rest can be useful to accurately obtain those phase marks hence becoming an important methodological tool for rhythm analysis.

The induction of arrhythmicity by both SCN lesion or by prolonged constant lighting in the present work was observed in most of the behavioral variables studied, but some of them showed intriguing rhythmic patterns that were observed in some of the animals. These illustrations suggest that studies of motor behavioral patterns with the use of force-plate, could reveal other underlying rhythms when an arrhythmic state is apparently at work. As the data presented are too scant, it was not the aim of this study to provide a physiological framework concerning this phenomenon. Nevertheless, extending analysis on population-based analysis could provide hints to describe distinct regulations in the interface between circadian pacemaker and motor output, as for instance in studies of circadian regulation of motor lateralization. Also, long-term studies with force-plate will be a helpful tool to assess whether other learning processes participate in the temporal organization of the circadian rhythms, such us during entrainment of peripheral oscillators to restricted feeding access (Stephan, 2002). For example, characterization of such oscillators is done by the presence of food anticipatory activity (FAA), which is determined by an increase in activity level or in time spent in front of the feeder. On the other hand, ¿is the FAA rather an active motor

response that was conditioned associated to the expectancy of the repetitive reinforcement, more than a passive motor output coupled to a peripheral oscillation? To obtain the behavioral structure of FAA rhythm this method may provide hints into these questions.

Disruption of normal sleep/wake pattern and other circadian abnormalities occurred in humans suffering Alzheimer disease (AD) (Satlin et al., 1995). Circadian rhythm disturbances may underlie the "sundowning" syndrome, frequently observed among AD patients (Volicer et al., 2001). Sundowning is poorly defined, as the appearance of behavioral disturbances (exacerbation of "agitation"), or behavioral symptoms in general, associated with the afternoon and/or evening hours (Volicer et al., 2001). Studying disturbances within the daily activity profile in transgenic models was suggested to improve the knowledge of that noncognitive symptomatology (Vloeberghs et al., 2004; Wisor et al., 2005). The assessment of disturbances in such transgenic models, involved principally the characterization of the modal daily distribution of photobeam counts and wheel running activity. However, such a behavioral description does not supply a complete framework to the aim of enhance the clinical knowledge of AD. Hence, to study behavioral rhythms in animal models of AD with the support of high resolution force-plate will improve this knoweledge, nearly obtaining an appropriate framework to characterize circadian alterations related to AD.

A high spatiotemporal resolution method for quantifying rodent behaviors based on a force-plate actometer, was reported previously by Fowler et al. (2001). Also, the advantages of measuring motor patterns with force-plate, compared to other methods, were extensively described. The aim of this method was claimed to improve behavioral measurements in psychopharmacological models, such as the study of drug-induced tremor and depression of locomotor activity (Wang and Fowler, 2001), rotation and spatial patterning (Fowler et al., 2001), spatially-focused stereotypes (Chen et al., 2003), and varying limb reaction force to ground in small rodents (Handley et al., 1998). Also, force-plate devices are widely used to study alterations of locomotor behavior such us in Parkinson disease (Muir and Whishaw, 1999; Adkin et al., 2003), and to assess motor performance in studies with humans (Slobounov et al., 2005; Laffaye et al., 2005). Generally, the common features of these methods are: 1) the high spatial resolution to study displacements, 2) the high vertical (signal) resolution to detect subtle variations in the operating forces, 3) the high horizontal (temporal)

resolution to both accurately estimate travelled path, and to sample high-frequency motions such as the ones occurring during tremor.

The aim of the present work was not only to provide a tool with such precission, but to develop a method that widely characterize behavioral patterns at long-term recordings, for instance those in the context of biological rhythm's studies. Furthermore, the main contribution of this method does not rely solely in the detection technique. Specially, a powerful method including calculation and data analysis of trajectories provided the calculation of time-series in a great number of behavioral variables. Moreover, the importance of achieve a description of rhythms related to the different kind of behavioral variables included in the general motor activity, which is commonly considered as the expression of a somewhat homogeneous an stochastic phenomenon, was discussed. It should be noted that the principal negative aspect of recording high spatiotemporal resolution data of motor activity on long-termed studies, has limitations both in the management of the great amount of data required, and also calibration. The general methods used at chronobiological laboratory permitted both automation and easy detection of general motor activity, and are widely validated for characterising the circadian pacemaker activity. However, specific research problems as the aforementioned ones, may determine the need of more "fine-grained" behavioral information further than the obtained with the general motor activity.
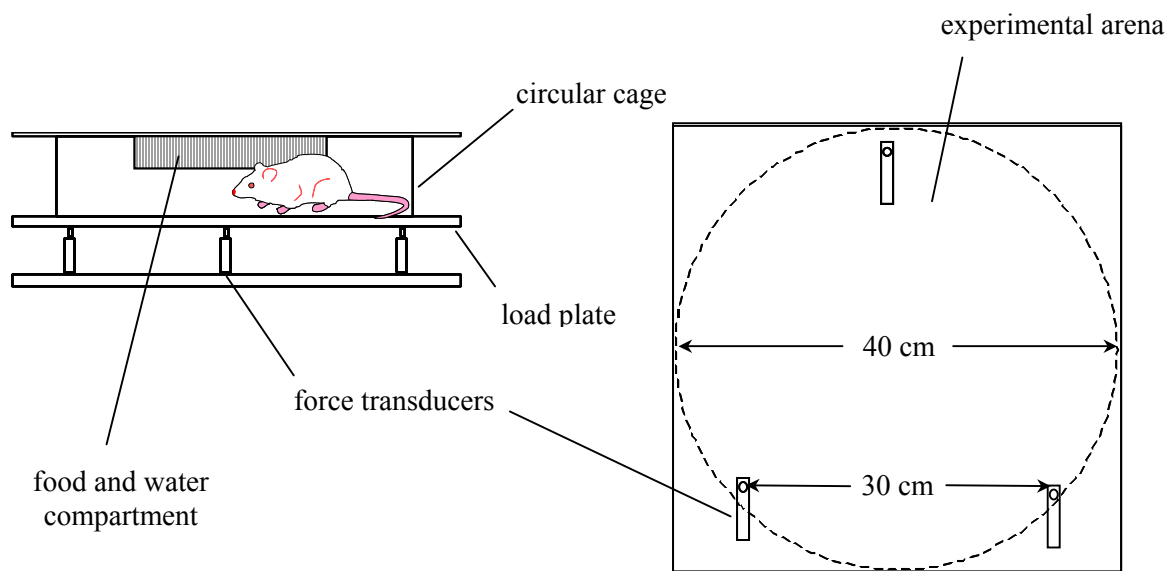
ACKNOWLEDGMENTS

Figure 1. A schematic representation of the force-plate actometer. The left diagram represents a lateral view of the device. A solid aluminium base holds three force transducers attached. They served as points to support a load plate over which a circular cage confined the animal. In this way, a circular experimental arena of 40 cm diameter was defined for the recording of behavioral activity (right diagram).
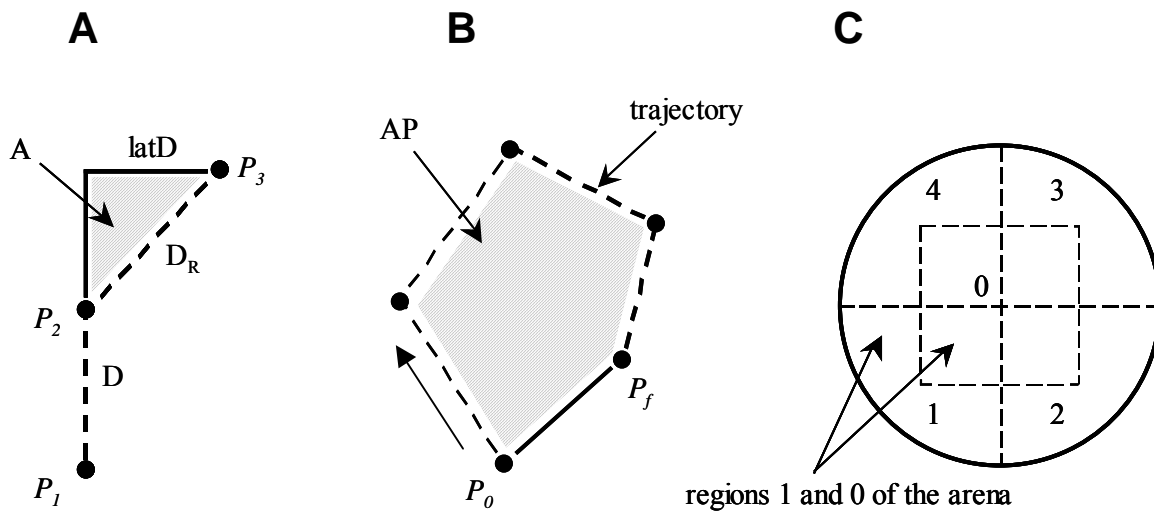
Figure 2. Graphic explanation of the calculation methods. A- P_i are *xy* coordinates of the center of force at the load plate surface, obtained at a sample rate of 1 s, where P_1, P_2 and P_3 are three successive points of a given trajectory. Initial distance travelled from P_1 to P_2 defines a displacement (D), that can be used to calculate displacement to the right (D_R) from P_2 to P_3. Lateral displacement (latD) can be obtained as the side of the resultant right triangle, and the area of the triangle constitutes the sweep area (A, grey lines). B- Calculation of the polygonal area (AP, grey lines) enclosed by a trajectory from an initial P_0 to a final P_f. Panel C represents the circular arena divided into five regions from 0 to 4, where the time of presence at region i (T_i) and the D_i were measured. Access for the animal to food pellets and water bottle was located at regions 1 and 2 of the arena.
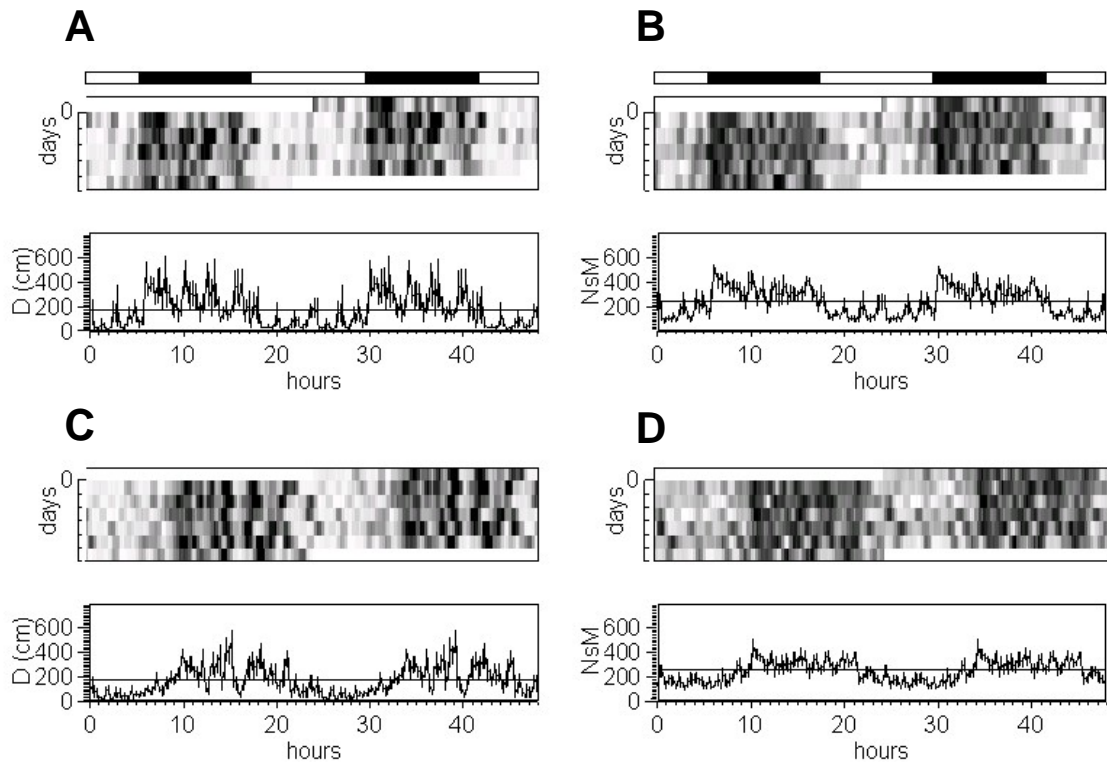
Figure 3. Actograms with corresponding waveforms below, double-plotted at 24 h showing data of the distance travelled (D, panels at left side) and of the number of slow motions (NsM, panels at right side) during five consecutive days. Panels A and B shows D and NsM rhythms of a representative animals submitted to LD, whereas panels C and D corresponds to the same rhythms of another submitted to DD. Black and white bar on top represents the presence of the dark and light phases of the LD cycle. Data records on actograms were smoothed (15 min step) and represented in a grey scale. At waveforms, the mean value of the daily average profile is represented by a line, and time-scale in hours also corresponds to actograms. The rhythm of D appeared with a major ultradian component when compared with the one of NsM, specially in the animals submitted to LD.
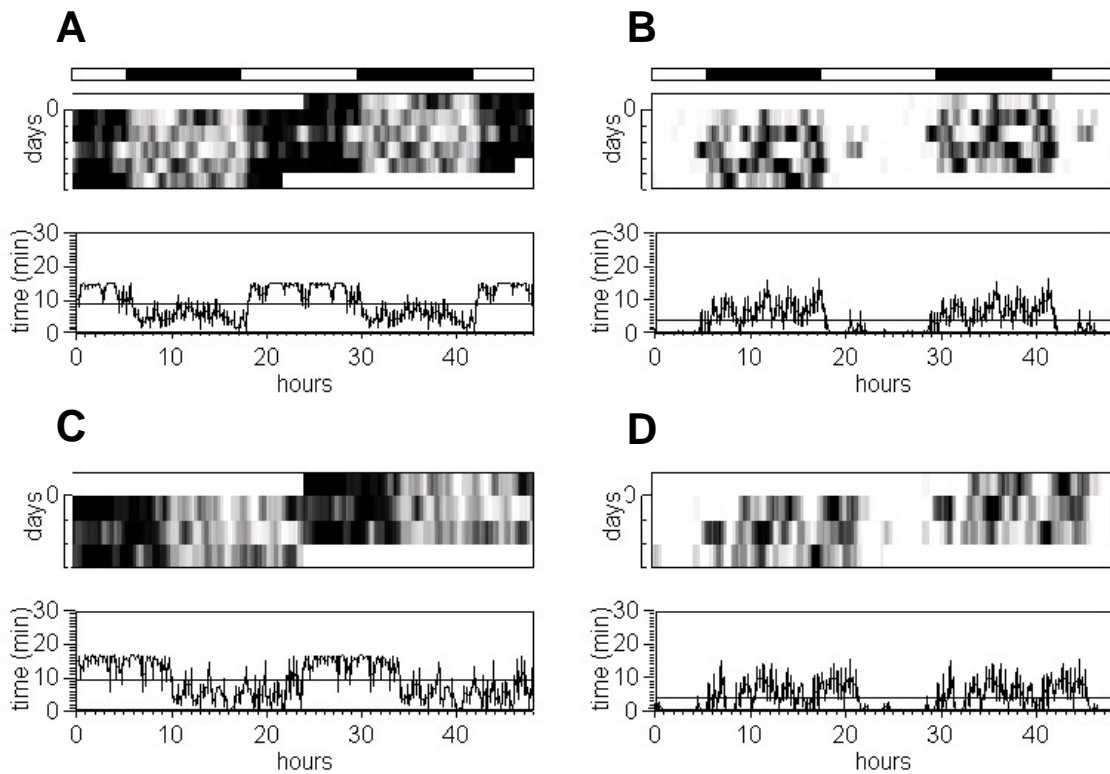
Figure 4. Actograms and waveforms showing data of the time spent by the animals at different regions within the arena. Panels A and B: a representative individual submitted to LD, panels C and D, an individual submitted to DD. Placing behavior within the arena is clearly related to the activity/rest pattern. Animal submitted to LD shows a rhythm of T_1 (panel A) revealing that the resting area of the arena comprised mainly region 1. Panel B shows a conspicuous rhythm in T_2 locked to dark phase, that was similar with the one of displacements in such region (D_2) suggests preferred region 2 for activity. The same description accounts for rhythms in T_1 (panel C) that measured placing to rest at region 1, and in T_3 (panel D) that is temporally related to activity phase. Time-series length is five days for LD and three for DD. Explanation for actogram and waveform graphs is the same as in Figure 3.
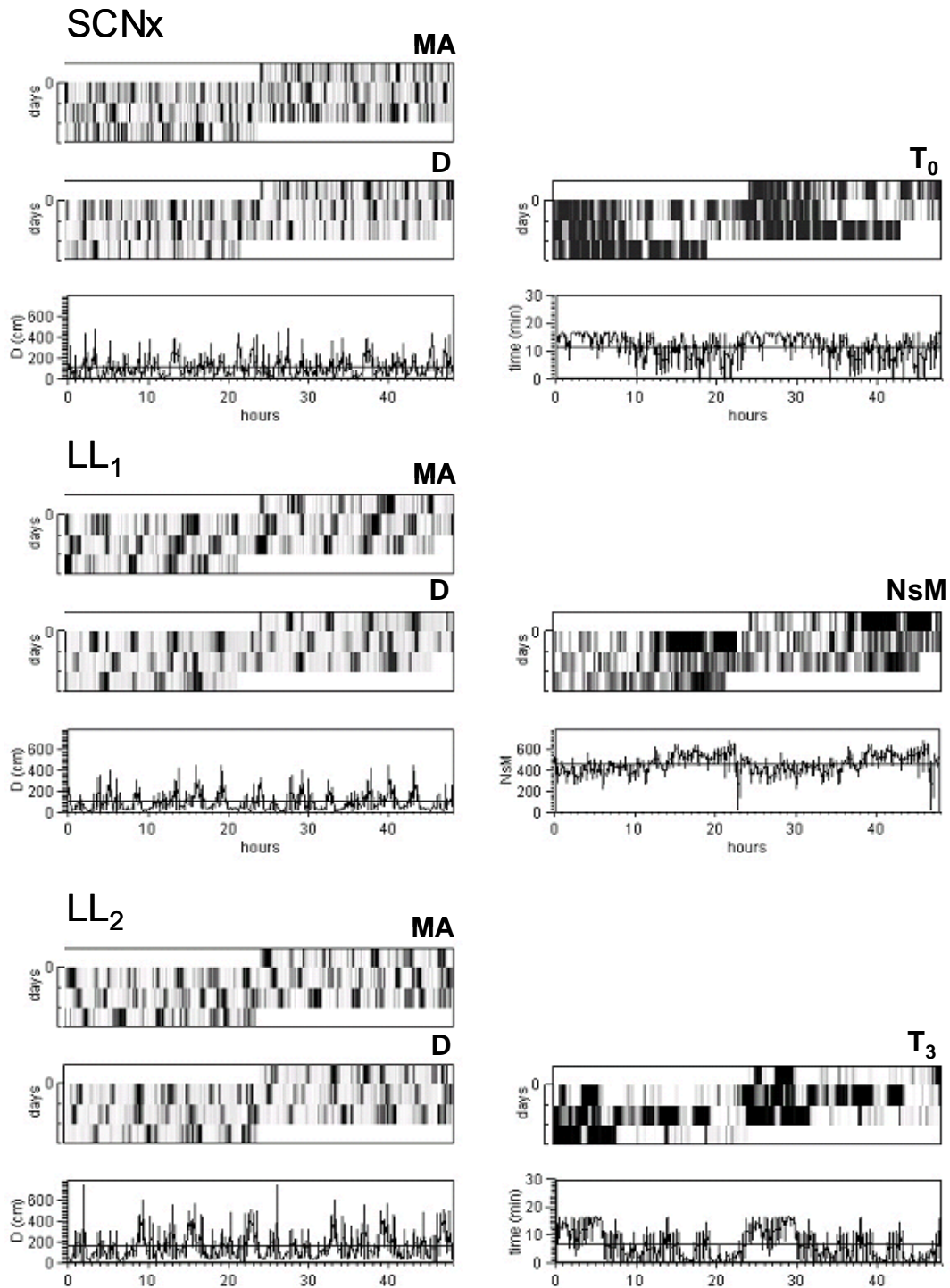
Figure 5. Actograms and waveforms with data records of an animal with a permanent SCN lesion (SCNx), together with two of the LL-submitted ones (LL$_1$ and LL$_2$). Actograms displays records of the general motor activity pattern (MA) detected by photobeams during the three days prior to force-plate session, showing arrhythmicity. Session at force-plate actometer record similar behavioral patterns in the most of the analysed variables. Pattern of D that are visible both in actograms and waveforms, quite correlates with the one of MA. The appearance of circadian rhythms was observed when considering other variables: in the SCNx animal, a rhythm in T$_0$ is observed both at actogram and waveform (periodogram analysis, p<0.0001). Also, a rhythm of NsM appeared in the LL$_1$ animal (periodogram analysis, p<0.0001), and another of T$_3$ (periodogram analysis, p<0.005) in the LL$_2$.

REFERENCES

Adkin AL, Frank JS, Jog MS. Fear of falling and postural control in Parkinson's disease. Mov Disord 2003; 18(5):496-502.

Ali SF, Kordsmeier KJ, Gough B (1995) Drug-induced circling preference in rats. Correlation with monoamine levels. Mol Neurobiol, 11(1-3):145-54.

Aschoff J (1981) Freerunning and entrained circadian rhythms. In: Handbook of behavioural neurobiology: Biological rhythms, J Aschoff, ed, pp 81-93, Plenum Press, New York.

Brodkin J, Nash JF. A novel apparatus for measuring rat locomotor behavior. J Neurosci Methods 1995; (2):171-6.

Cabib S, Orsini C, Le Moal M, Piazza PV (2000) Abolition and reversal of strain differences in behavioral responses to drugs of abuse after a brief experience. Science, 289(5478):463-5.

Cambras T, Canal MM, Torres A, Vilaplana J, Díez-Noguera A. Manifestation of circadian rhythm under constant light depends on lighting conditions during lactation. Am J Physiol 1997; 272(4 Pt 2):R1039-46.

Chen R, Osterhaus G, McKerchar T, Fowler SC. The role of exogenous testosterone in cocaine-induced behavioral sensitization and plasmalemmal or vesicular dopamine uptake in castrated rats. Neurosci Lett 2003; 351(3):161-4.

Creese I, Iversen SD (1972) Amphetamine response in rat after dopamine neurone destruction. Nat New Biol, 238(86):247-8.

Fowler SC, Birkestrand BR, Chen R, Moss SJ, Vorontsova E, Wang G, Zarcone TJ (2001) A force-plate actometer for quantitating rodent behaviors: illustrative data on

locomotion, rotation, spatial patterning, stereotypies, and tremor. J Neurosci Methods, 107(1-2):107-24.

Handley DE, Ross JF, Carr GJ. A force plate system for measuring low-magnitude reaction forces in small laboratory animals. Physiol Behav 1998; 64(5):661-9.

Janik D, Mrosovsky N (1993) Nonphotically induced phase shifts of circadian rhythms in the golden hamster: activity-response curves at different ambient temperatures. Physiol Behav, 53(3):431-6.

Kafkafi N, Mayo C, Drai D, Golani I, Elmer G. Natural segmentation of the locomotor behavior of drug-induced rats in a photobeam cage. J Neurosci Methods 2001; 109(2):111-21.

Kao SD, Shaw FZ, Young MS, Jan GJ. A new automated method for detection and recording of animal moving path. J Neurosci Methods 1995; 63(1-2):205-9.

Klemfuss H, Clopton P (1993) Seeking tau: a comparison of six methods. J Interdiscipl Cycle Res 24(1): 1-16.

Laffaye G, Bardy BG, Durey A. Leg stiffness and expertise in men jumping. Med Sci Sports Exerc 2005; 37(4):536-43.

Liu GT, Ferguson AR, Crown ED, Bopp AC, Miranda RC, Grau JW. Instrumental learning within the rat spinal cord: localization of the essential neural circuit. Behav Neurosci 2005; 119(2):538-47.

Mizuno M, Malta RS Jr, Nagano T, Nawa H (2004) Conditioned place preference and locomotor sensitization after repeated administration of cocaine or methamphetamine in rats treated with epidermal growth factor during the neonatal period. Ann N Y Acad Sci, 1025:612-8.

Mrosovsky N, Reebs SG, Honrado GI, Salmon PA. Behavioural entrainment of circadian rhythms. Experientia 1989; 45:696-702.

Muir GD, Whishaw IQ. Ground reaction forces in locomoting hemi-parkinsonian rats: a definitive test for impairments and compensations. Exp Brain Res 1999; 126(3):307-14.

Patxinos G, Watson C. The rat brain in stereotaxic coordinates. Academic Press, 1998; USA.

Paulus MP, Geyer MA. A temporal and spatial scaling hypothesis for the behavioral effects of psychostimulants. Psychopharmacology (Berl) 1991;104(1):6-16.

Paulus MP, Geyer MA, Gold LH, Mandell AJ. Application of entropy measures derived from the ergodic theory of dynamical systems to rat locomotor behavior. Proc Natl Acad Sci USA 1990; 87(2):723-7.

Pittendrigh CS. Circadian Systems: General Perspective. In: Handbook of behavioral neurobiology: Biological rhythms, edited by Aschoff J. New York: Plenum Press, 1981, p. 57-80.

Risold PY, Thompson RH, Swanson LW (1997) The structural organization of connections between hypothalamus and cerebral cortex. Brain Res Brain Res Rev, 24(2-3):197-254.

Roitman MF, Wheeler RA, Carelli RM. Nucleus accumbens neurons are innately tuned for rewarding and aversive taste stimuli, encode their predictors, and are linked to motor output. Neuron 2005; 45(4):587-97.

Rotenberg L, Marques N, Menna-Barreto L. Desarrollo de la Cronobiología. In: Cronobiología. Principios y aplicaciones. Marques N, Menna-Barreto L, Golombek DA (eds.). Editorial Universitaria de Buenos Aires 1997; pp 33-56.

Satlin A, Volicer L, Stopa EG, Harper D. Circadian locomotor activity and core-body temperature rhythms in Alzheimer's disease. Neurobiol Aging 1995; 16(5):765-71.

Silver R, LeSauter J, Tresco PA, Lehman MN. A diffusible coupling signal from the transplanted suprachiasmatic nucleus controlling circadian locomotor rhythms. Nature 1996; 382(6594):810-3.

Slobounov S, Hallett M, Stanhope S, Shibasaki H. Role of cerebral cortex in human postural control: an EEG study. Clin Neurophysiol 2005; 116(2):315-23.

Stephan FK. The "other" circadian system: food as a Zeitgeber. J Biol Rhythms 2002; 17(4):284-92.

Swanson LW, Mogenson GJ. Neural mechanisms for the functional coupling of autonomic, endocrine and somatomotor responses in adaptative behavior, Brain Res Rev 1981; 3:1-34.

Tate B, Aboody-Guterman KS, Morris AM, Walcott EC, Majocha RE, Marotta CA. Disruption of circadian regulation by brain grafts that overexpress Alzheimer beta/A4 amyloid. Proc Natl Acad Sci USA 1992; 89(15):7090-4.

Vilaplana J, Cambras T, Díez-Noguera A. Dissociation of motor activity circadian rhythm in rats after exposure to LD cycles of 4-h period. Am J Physiol 1997; 272(1 Pt 2):R95-102.

Volicer L, Harper DG, Manning BC, Goldstein R, Satlin A. Sundowning and circadian rhythms in Alzheimer's disease. Am J Psychiatry 2001;158(5):704-11.

Wang G, Fowler SC. Concurrent quantification of tremor and depression of locomotor activity induced in rats by harmaline and physostigmine. Psychopharmacology (Berl) 2001; 158(3):273-80.

Welsh DK, Logothetis DE, Meister M, Reppert SM. Individual neurons dissociated from rat suprachiasmatic nucleus express independently phased circadian firing rhythms. Neuron 14 1995; 697-706.

Winfree A. Biological rhythms and the behavior of populations of coupled oscillators. J Theor Biol 1967; 16: 15-42.

Wisor JP, Edgar DM, Yesavage J, Ryan HS, McCormick CM, Lapustea N, Murphy GM Jr. Sleep and circadian abnormalities in a transgenic mouse model of Alzheimer's disease: a role for cholinergic transmission. Neuroscience 2005; 131(2):375-85.

Wolansky MJ, Azcurra JM. Permanent motor activity and learning disorders induced by exposure to phenytoin during gestation and early infancy in the rat. Neurotoxicol Teratol 2005; 27(2):299-310.